THE EFFECT OF TEMPERATURE ON WEST NILE VIRUS TRANSMISSION DYNAMICS

DON YU

A DISSERTATION SUBMITTED TO
THE FACULTY OF GRADUATE STUDIES
IN PARTIAL FULFILMENT OF THE REQUIREMENTS
FOR THE DEGREE OF
DOCTOR OF PHILOSPHY

GRADUATE PROGRAM IN MATHEMATICS AND STATISTICS
YORK UNIVERSITY
TORONTO, ONTARIO

January 2018

Abstract

West Nile virus (WNV) is a vector-borne disease that first appeared in New York in 1999, then in Southern Ontario, Canada in 2002. Since its arrival, WNV has rapidly spread across the North American continent to establish itself as a seasonal endemic infection. Among other environmental variables, temperature is the primary determinant of WNV transmission dynamics. In this dissertation, the relationship between temperature and WNV transmission dynamics is investigated and a single-season predictive model that explicitly accounts for temperature in various biological and epidemiological processes is proposed. First, we develop a mosquito abundance model where temperature is the driving force behind mosquito development, survival, and diapause. Then, the model is extended to include the WNV transmission cycle between mosquitoes and birds. Under simplifying assumptions, we derive an expression for the basic reproduction number and analyze its dependence on temperature. The transmission model was applied to the Peel Region in Southern Ontario for validation. Numerical results demonstrate the capacity of the model to capture the within-season trends of mosquito- and WNV- surveillance data. The proposed model can potentially be used as a real-time predictive tool to inform public health policy.

For

mltw, meli, & mickey

Pyong San & Ki Suk Yu

Acknowledgements

It is difficult to put in words how sincerely grateful I am to Professor Huaiping Zhu and Professor Neal Madras for the opportunity to pursue one of my lifelong goals of obtaining my Ph.D. in applied mathematics. It is only because of their unwavering commitment to guide, mentor, and encourage me throughout my studies that I was able to complete my Ph.D. research. I am truly honored to have been able to work with them.

I would also like to thank my supervisory- and oral exam- committee members Professor Xin Gao, Professor Beate Sander, Professor Zijiang Yang, Professor Richard Bello, and Professor Robert Smith? for their instrumental involvement in the completion of my dissertation. Thank you so much for your support and constructive advice on my research.

To my wife, Kathleen Yu, I could easily double the number of pages in this dissertation to thank you for all the things you've done to support and encourage me through this journey. I don't even know how to begin repaying you for the sacrifices you've made so that I could pursue this endeavor. Thank you mltw. I love you. ~birdie.

To my parents, Pyong San and Ki Suk Yu, thank you for your unceasing prayers. I hope I've made you proud.

Table of Contents

List of Tables

List of Figures

1 Introduction

Vector-borne diseases account for more than 17% of all infectious diseases and affect hundreds of millions of people worldwide (World Health Organization 2017). Mosquitoes are not only the deadliest of the disease vectors, but they are one of the deadliest animals in the world and are responsible for over a million deaths every year globally (Caraballo and King 2014, World Health Organization 2017). Mosquito-borne diseases are a constant threat to human populations due to their aerial mobility and the availability of breeding sites near human settlements. Of the six major mosquito-borne diseases (Chikungunya, Dengue, Malaria, West Nile virus (WNV), Yellow fever, and Zika virus), WNV and Zika virus pose a current threat to public health across the North American continent. In Canada, as of the date of this study, only WNV has confirmed cases of the virus being transmitted by mosquitoes while there have been no reported cases of Zika virus (Public Health Canada 2017).

WNV is a mosquito-borne disease that was first discovered in Africa in 1937. Since the first appearance of West Nile virus (WNV) in New York in 1999 (Centers for Disease Control and Prevention 1999a, 1999b), the mosquito-borne disease has rapidly spread across the North American continent establishing itself as a seasonal endemic infection (Sejvar 2003, Reisen 2013). By 2004, WNV had been detected in all states in the continental US; in 2002, the first WNV human infection in Canada was reported in southern Ontario and has since been detected in all provinces except Prince Edward Island and Newfoundland (Infection Prevention and Control Canada 2017).

The majority of people (70–80%) who become infected with WNV are asymptomatic. Approximately 10% of infected people will develop flu-like symptoms such as headache, body aches, joint pains, vomiting, diarrhea, or rash. Most people with this form of the disease will recover completely; however, fatigue and weakness may last from several weeks to several months post-recovery. In rare instances (less than 1%), infected individuals will develop serious neurological illness such as encephalitis or meningitis. About 10% of those who develop neurological infection due to WNV will die from the disease (Centers for Disease Control and Prevention 2014). Currently, there is no vaccine or specific treatment for people infected with WNV.

Unlike the other mosquito-borne diseases that are transmitted between mosquitoes and humans, WNV has the added complexity of involving birds, which act as amplifying reservoirs in the disease transmission cycle. The transmission cycle between mosquitoes and birds is heavily dependent on environmental conditions such as ambient temperature, precipitation, humidity, and wind. Among them, ambient temperature has been shown to be an important determinant of transmission dynamics (Kunkel et al. 2006, Hartley et al. 2012, Paz 2015). A considerable number of laboratory and entomological field studies have been conducted to assess the influence of temperature on mosquito biology (Eldridge et al. 1976, Spielman 2001, Shelton 1973, Madder et al. 1983, Rueda et al. 1990, Ruiz et al. 2010, Lounibos et al. 2002, Loetti et al. 2011, Ciota et al. 2014, Jetten and Takken 1994, Bayoh and Lindsay 2003, Denlinger and Armbruster 2014, Reisen et al. 2006). These studies showed that temperature affects almost every aspect of their life cycle including oviposition, development, survival, biting rates, host-seeking activity, life-history traits,

overwintering behavior, and the extrinsic incubation period (EIP), all of which have some influence on transmission dynamics.

Understanding the relationship between temperature and its broad spectrum of influence on disease transmission is imperative for public health prevention in the fight against disease outbreaks. The continued risk to the human population prompted the establishment of annual surveillance programs to monitor virus infection in mosquito populations. In regions where mosquito-borne diseases are prevalent, the primary means of decreasing the risk of infection in humans is the implementation of mosquito control programs (e.g., elimination of breeding sites, larvaciding, and adulticiding) and personal protection measures (e.g., wearing appropriate clothing, insect repellant, and avoiding sites with high mosquito activity). For mosquito control to be effective, it is important to understand what factors affect their population abundance.

A substantial number of mathematical and statistical models have been developed to assess the influence of climate variables, such as temperature and precipitation, on the population dynamics and behavior of various mosquito species (Ahumada et al. 2004, Cailly et al. 2012, Cochran and Xu 2012, Ezanno et al. 2015, Gong et al. 2011, Gu and Novak 2006, Otero et al. 2006, Shaman et al. 2006, Tachiiri et al. 2006, Tran et al. 2013, Wang et al. 2011, Yoo et al. 2016). Most of these models were developed for a specific vector species in a specific geographical context (Ahumada et al. 2004, Tachiiri 2006, Otero et al. 2006, Yoo et al. 2016), while other studies sought to develop more generalized models that could be adapted to various vector species in different areas (Cailly et al. 2012, Gong et al. 2011). Tachiiri et al., (2006) created a raster-based mosquito abundance map for two species, *Culex (Cx.) tarsalis* and *Cx. pipiens*, which allowed them to identify areas of greatest potential risk of WNV in British Columbia, Canada. Cailly et al. (2012) developed a generic climate-driven mosquito abundance model that could be run over several years. Their

model identified several potential control points in the biological system of mosquitoes that could be used to reduce the risk of mosquito-borne disease outbreak. Otero et al. (2006) developed a temperature-driven stochastic population model for the species *Aedes aegypti* and identified temperature and environmental conditions that are needed for the survival of a local population of mosquitoes in a temperate climate. Spatio-temporal dynamics of mosquito host-seeking behavior were examined in the study by Cummins et al. (2012), where they developed an agent-based/continuum model to explore the effect of behavioral decisions and spatial heterogeneity on the contact rate between mosquito vectors and bird hosts. The study by Gunaratne et al. (2016), used agent-based modelling to describe the population dynamics of Zika vector *Aedes aegypti* subjected to spatial and climatic constraints. Wang et al. (2011) developed a predictive statistical model for mosquito abundance which defined threshold criteria for temperature and precipitation conditions for the population growth of WNV vector species *Cx. pipiens* and *Cx. restuans*. The model developed by Yoo et al. (2016), used harmonic analysis and kernel density estimation as a means of examining the associations with major landscape predictors—including land-use type, population density, and elevation—on the spatial patterns of mosquito abundance.

In the studies that account for temperature, various approaches have been used to model the effect of temperature on the mosquito life cycle. For example, some dynamical models use temperature-dependent development functions (Abiodun et al. 2016, Cailly et al. 2012, Lana et al. 2011) to determine the instantaneous rate of development at each time step. Gu and Novak (2006) developed a stochastic phenological model, which calculated probabilities of individuals residing in larval, pupal, and emerging adult stages as a function of temperature. A drawback of using instantaneous rate functions to model mosquito development is their limitation in capturing certain

population dynamics, such as sudden population increases caused by weather patterns that allow for the simultaneous eclosion of multiple generations.

Some studies also include a temperature-dependent mortality function, which calculate daily mortality rates based on the temperature experienced by developing mosquitoes on a single day (Ewing et al. 2016, Shaman et al. 2006, Otero et al. 2006, Tachiiri et al. 2006); however, in a natural environment, immature mosquitoes can survive exposure to high temperatures for short periods of time without significant impact on their mortality (Bayoh and Lindsay 2004). Thus, mortality rates can potentially be overestimated in temperate climates that experience a wide range of diurnal temperature fluctuations. Furthermore, these studies used temperature-dependent mortality functions with a Gaussian shape. Although it is a common practice to model temperature-dependent mortality rates in this way, it can lead to an overestimation of daily mortality rates at lower temperatures; it has been shown that colder temperatures act more as an inhibitor to development rather than causing higher mortality (Bayoh and Lindsay 2003). Models that use constant mortality rates are also subject to diminished model performance when applied to areas that experience large fluctuations in seasonal temperatures.

An often neglected but critical factor in mosquito population dynamics is the diapause phenomenon. Environmental conditions trigger a physiological and behavioral response in developing mosquitoes, which enable them to survive harsh winter conditions in a form of metabolic dormancy until more favorable conditions induce their emergence in the following season (Eldridge 1966, Spielman 2001, Zhang and Denlinger 2011). Models that exclude this phenomenon may experience an overestimation of the active mosquito population in numerical simulations during the middle and later months of the mosquito season when diapause-destined mosquitoes begin seeking shelter for the upcoming winter months. Some of the models that do

account for diapause consider photoperiod alone to determine the fraction of diapausing mosquitoes (Gong et al. 2011, Cailly et al., 2012); however, there is evidence that temperature influences the proportion of mosquitoes destined for diapause at a given photoperiod (Eldridge 1966, Madder et al. 1983, Spielman 2001).

Developing mathematical models describing the disease transmission cycle allows for the analysis of the mechanisms that influence transmission dynamics as well as the effectiveness of control methods (Abdelrazec 2014b). Several modelling initiatives on WNV have given valuable insight into various aspects of WNV transmission dynamics (Wonham et al. 2004, Bowman et al. 2005, Cruz-Pacheco et al. 2005, Blayneh et al. 2010, Abdelrazec 2014a). Some of these models do not include the effect of temperature on disease transmission. The well-known and heavily cited study by Wonham et al. (2004) proposed that the primary driver of WNV outbreaks is the ratio of initial susceptible mosquitoes to birds. However, analysis of transmission dynamics excluding the environmental context in which it is being assessed inhibits the practical application of their model as a tool that can be used to inform real-time public health policy in the assessment of infection risk.

Many of the models that consider the effect of temperature make simplifying biological assumptions on the vital dynamics of mosquitoes that limit their capacity to capture certain phenomena observed in surveillance data. The study by Laperriere et al. (2011) developed an SEIR-type model simulating the seasonal cycles of bird, equine, and human WNV cases. While the model included a temperature-dependent oviposition rate function, the rate of adult eclosions was assumed to be a proportion of the daily oviposition rate at a given temperature. This assumption ignores an important aspect of mosquito population dynamics where certain

temperature patterns can cause sudden and dramatic increases in the population, which consequently affects transmission dynamics.

In addition, temperature has been shown to have a strong influence on vector competence and the extrinsic incubation period (EIP) (Anderson et al. 2010, Dohm et al. 2002, Reisen et al. 2006, Kilpatrick et al. 2008). The EIP is the time it takes for the virus to replicate itself within a host before it becomes infectious. The EIP for mosquitoes plays a critical role in the appearance of WNV in surveillance data as well as the severity of outbreaks, should they occur. Depending on temperature, the EIP can range from a week to a month (Goddard et al. 2003, Reisen et al. 2006, Bolling et al. 2009). Shortening the EIP means that an exposed mosquito becomes infectious in a shorter amount of time and can transmit the virus for a longer proportion of its lifetime as an adult. Some studies that include the effect of EIP on transmission dynamics assume either a constant rate of transition or use a rate that is a function of temperature for the progression from exposed (asymptomatic) to infectious compartments (Thomas and Urena 2001). Although the EIP is accounted for in their models, the assumption of a constant or functional rate of transition that is applied per unit time reduces model performance with respect to capturing important temperature-dependent dynamics such as the timing and magnitude of peaks of WNV surveillance data.

Based on our current understanding of WNV transmission and its continued persistence across North America, it is unlikely the disease can be fully eradicated. Nevertheless, the continued threat to public health warrants further research to gain a better understanding of the factors that affect transmission dynamics to develop more effective risk reduction strategies. To this end, this dissertation focuses on improving our understanding of the relationship between temperature and the WNV transmission cycle through the formulation of realistic mathematical models that enable us to qualitatively assess the mechanisms that drive transmission dynamics. Insights gained from

this study reinforce our current understanding of the relationship between temperature and infection dynamics as well as highlight issues that warrant more attention when developing model frameworks intended to assess the risk level of disease outbreaks.

1.1 Mosquito biology and related factors

The mosquito life cycle consists of three successive aquatic juvenile phases (egg, larvae, and pupae) and one terrestrial adult stage (Figure 1.1). Depending on the surface water temperature, it usually takes 1–3 weeks from the time the egg is laid until emergence to the adult stage (Madder et al. 1983, Rueda et al. 1990, Shelton 1973, Spielman 2001). Adult female mosquitoes generally mate within the first few hours of emergence and then seek a blood meal to provide a protein source for their eggs. After feeding, the female seeks out a sheltered place to rest for a few days while her eggs develop. Once the eggs are fully developed, the female oviposits her eggs on a raft of 150–350 eggs on the surface of standing water (Madder et al. 1983). The adult female then proceeds to find another blood meal and repeat the gonotrophic cycle (United States Environmental Protection Agency 2017). During winter months, nulliparous inseminated female mosquitoes can enter a state of diapause for the duration of the winter until climate conditions are conducive for their re-emergence in the spring. The induction of diapause begins during the mosquito season and depends on the number of daylight hours and temperature experienced by mosquitoes in the fourth larval instar and pupal stages of development (Denlinger and Armbruster 2014).

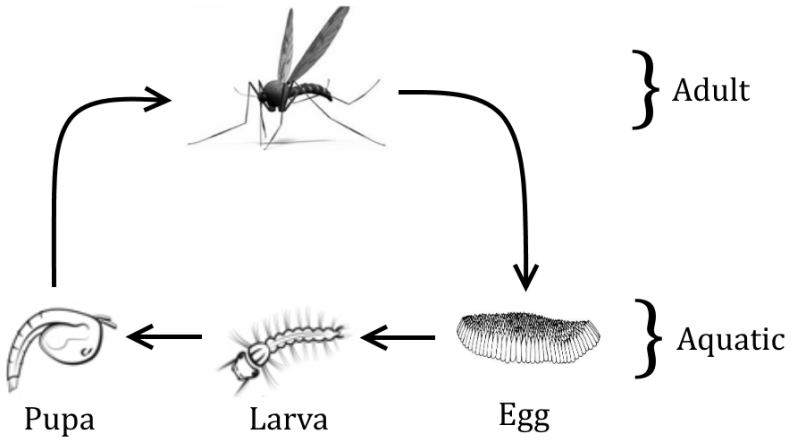

Figure 1.1: The mosquito life cycle

1.2 WNV transmission cycle

The transmission cycle of WNV involves mosquitoes (vector) and birds (amplifying hosts). A susceptible mosquito can contract the virus by biting an infected bird, defined as a bird that has developed high enough levels of the virus in its bloodstream. Only certain species of birds act as virus amplifying reservoirs. Some of these species, such as crows and jays, have been shown to have a high mortality rate due to infection. The virus will then incubate within the bloodstream of an infected mosquito until it reaches sufficient levels to become infectious (Reisen et al. 2006, Chen et al. 2013, Centers for Disease Control and Prevention 2014). Depending on temperature, the incubation period of the virus can vary from days to weeks. Infectious mosquitoes can then transmit the virus back to a susceptible bird or to other incidental hosts such as horses or humans (dead-end hosts). Incidental hosts do not develop high enough levels of WNV in their bloodstream to transmit the virus to other biting mosquitoes (Hayes 1988, (Paz and Semenza 2013, Centers for Disease Control and Prevention 2014). Mosquitoes can also transmit the virus vertically, which is the primary mechanism enabling the disease to persist in regions that experience harsh winter conditions (Goddard et al. 2003, Anderson and Main 2006).

1.3 Mosquito surveillance program and data

1.3.1 Study area (Peel Region, Southern Ontario)

The Regional Municipality of Peel (also known as Peel Region) is a regional municipality in Southern Ontario, Canada, residing on the north shore of Lake Ontario with a total population of 1,296,814 and a total area of 1,246.89 km^2 (Statistics Canada 2011). It consists of three municipalities to the west and northwest of Toronto: the cities of Brampton and Mississauga, and the town of Caledon, as well as portions of the Oak Ridges Moraine and the Niagara Escarpment, 3,270 ha of wetland (2.6% of land area), and 41,329 ha of farmland (33% of land area) (Wang et al. 2011). The four seasons in the region are clearly distinguished. Spring and autumn are transitional seasons with generally mild or cool temperatures with alternating dry and wet periods. Summer runs from June until mid-September with an average monthly temperature of 20°C for the warmest months of July and August. Temperatures during summer can occasionally surpass 32°C.

1.3.2 Mosquito surveillance program

Mosquito surveillance in Southern Ontario was started in 2001 by the Ministry of Health and Long-Term Care (MOHLTC). The Peel Region Health Unit used the Centers for Disease Control miniature light trap (Service 1993) with both CO_2 and light to attract host-seeking adult female mosquitoes. Adult mosquitoes were trapped weekly from mid-June to early October (usually weeks 24–39), and the continuous observation for each trap started in 2004 (Wang et al. 2011). Traps are set up on one day each week and allowed to collect mosquitoes overnight until the traps

are collected the next day. Trapped mosquitoes were identified to species and counted, except for *Cx. pipiens* and *Cx. restuans*, which were combined into one group and counted due to the difficulty in distinguishing the species. Except for year 2002, mosquito abundance in 2003–2016 was measured during a period of active larval control in catch basins and surface water sites. During each mosquito season, there were four rounds of larval mosquito control in non-surveillance-based catch basins. Larviciding in surface water sites was surveillance based. Larviciding was not done in 2002 (Wang et al. 2011).

As was done in Wang et al. (2011), we used the average mosquito counts from the 30 trap locations to represent the mosquito population at the regional level. For each trap, the original count was smoothed over preceding and succeeding weeks: $W_j = \frac{w_{j-1}+w_j+w_{j+1}}{3}$, where w_j is the original mosquito count in week j and W_j is its smoothed value for the week that reduces random effects such as moonlight or wind on capture probabilities (Service 1993). Year to year variability exhibited in mosquito trap counts over the same area is likely due to the seasonal fluctuations of temperature and precipitation in the region as well as other environmental factors. Furthermore, during some weeks within a given year, certain traps are observed to capture a disproportionate number of mosquitoes relative to other traps in the area. This presents a challenge to modelling population dynamics of mosquitoes for this region and will be considered in the analysis of model performance.

1.3.3 Temperature data

Mean daily temperature data for the Peel Region were obtained from Canada's National Climate Archive (www.climate.weatheroffice.gc.ca). Among the three weather stations in Peel Region having temperature records available (Pearson International Airport, Georgetown, and

Orangeville), we used the data collected from Pearson International Airport to represent the temperature conditions for the Peel Region as they had no missing data for years 2004–2016 (Wang et al. 2011).

1.4 Parameters and functions (Tables 1 & 2)

Table 1: Model parameters

Par.	Description	Value (Range)	Dimension	Source
t	Time	$[t_0, t_{end}]$	day	
k	The day of oviposition used to indicate discrete cohorts	$[t_0, t_{end}]$	day	
i	The day of exposure to virus	$[t_0, t_{end}]$	day	
μ_{op}	Aquatic mortality rate at optimal temperature of development T_{op}	0.015	day^{-1}	[1–4], [6–9]
ω	Lifespan of adult mosquito	28	day	[5]
m_{14}	Slope of diapause function γ_k for 14 daylight hours	0.0375	-	
$m_{14.75}$	Slope of diapause function γ_k for 14.75 daylight hours	0.05625	-	
j	Scale factor for $\mu_l(T(t))$	$1/25{,}000$	-	
q	Scale factor for $\mu_l(T(t))$	$3/1{,}000$	-	
T_e	Minimum temperature at which larva can develop	9	°C	[12]
T_{op}	Optimal temperature for aquatic development	25	°C	[1], [4], [6], [7], [9]
T_{DDe}	Total number of degree-days required to complete aquatic stage of development	149	°C	[3], [6–8]
T_a	Lower temperature threshold below which temperature is not accumulated toward the completion of the EIP	14	°C	[11]
T_{DDa}	Total number of degree-days required to complete the EIP	139	°C	[11]
β	Per capita oviposition rate	0.125 (0–1)	day^{-1}	[5]
a	Per capita biting rate of mosquitoes on birds	(0.03–0.16)	day^{-1}	[5]
σ	Per capita recovery rate of infected birds	(0–0.2)	day^{-1}	[5]
μ_b	Per capita mortality rate of birds due to WNV infection	(0.02–0.3)	day^{-1}	[5]
c_v	Probability of vertical transmission in mosquitoes	(0–1)		[5]
c_b	Probability of transmission from mosquito to bird	(0.80–1.00)	-	[5]
c_m	Probability of transmission from bird to mosquito	(0.02–0.24)	-	[5]

Sources: [1] Madder et al. 1983 [2] Tachiiri et al. 2006 [3] Jetten and Takken 1994 [4] Rueda et al. 1990 [5] Wonham et al. 2004 [6] Bayoh and Lindsay 2004 [7] Loetti et al. 2011 [8] Gong et al. 2011 [9] Ciota et al. 2014 [10] Komar et al. 2003 [11] Reisen et al. 2006 [12] Wang et al. 2011

Table 2: Model functions

Var.	Description	(Range)	Dimension	Source
$DD_e(t)$	Amount of degree-days accumulated towards development on day t	Variable	°C	
$df_k(t)$	Proportion of T_{DD_e} accumulated on day t by a cohort born on day k.	Variable (0–1)	-	[7]
$f_k(t)$	Cumulative development time of a cohort born on day k up to time t.	Variable	-	[7]
t_k	The day of eclosion for a cohort born on day k i.e. $t_k = t$ when $f_k(t) \geq 1 > f_k(t-1)$	Variable	day	
τ_k	Total number of days to complete development for a cohort born on day k.	Variable	day	
P_k	Photoperiod of the day 4th larval instar begins for a cohort born on day k (4th larval instar assumed to begin when 80% of aquatic development is complete).	Variable (8.93–15.44)	hours	[1], [10], [12], [13]
T_k	Mean daily temperature while in 4th larval instar and pupal stages of development for a cohort born on day k (4th larval instar assumed to begin when 80% of aquatic development is complete).	Variable	°C	[1], [10], [12], [13]
$\gamma_k(T_k, P_k)$	Proportion of non-diapausing adult female mosquitoes at time of eclosion	Variable (0–1)	-	[1], [10], [12], [13]
T_l	Two-day mean temperature of days t and $t-1$ for calculating temperature-dependent aquatic mortality rate on day t.	Variable	°C	[11]
$\mu_l(T_l(t))$	Temperature-dependent mortality rate for adult mosquitoes (continuous time); per capita survival rate for difference equations given by $e^{-\mu_l(T_l(t))}$ (discrete time)	Variable	day^{-1}	[1–4], [5], [6], [8], [9]
$\mu_m(T_l(t))$	Temperature-dependent mortality rate for adult mosquitoes (continuous time); per capita survival rate for difference equations given by $e^{-\mu_m(T_l(t))}$ (discrete time)	Variable	day^{-1}	[14]
$DD_a(t)$	Amount of DDs accumulated towards completion of the EIP on day t.	Variable	°C	
$d\delta_{k,i}(t)$	Proportion of T_{DD_a} accumulated on day t by a mosquito in cohort k that was exposed to virus on day i.	Variable	-	[15]
$\delta_{k,i}(t)$	Cumulative time of completion of the EIP of a mosquito in cohort k that was exposed to virus on day i.	Variable	-	[15]
$\overline{\delta}(T(t))$	Instantaneous rate of transition from asymptomatic to infectious compartment.	Variable	day^{-1}	[15]

Sources: [1] Madder et al. 1983 [2] Tachiiri et al. 2006 [3] Jetten and Takken 1994 [4] Rueda et al. 1990 [5] Bayoh and Lindsay 2004 [6] Loetti et al. 2011 [7] Craig et al. 1999 [8] Gong et al. 2011 [9] Ciota et al. 2014 [10] Eldrige 1966 [11] Canada's National Climate Archive [12] Spielman 2001 [13] Edillo et al. 2009 [14] Cailly et al. 2012 [15] Reisen et al. 2006

1.5 Summary of dissertation

The primary objective of this dissertation is to gain a better understanding of how mosquito biology and WNV transmission is influenced by temperature to develop reliable predictive models to forecast mosquito population abundance and WNV infection risk in the Peel Region, Southern Ontario. We aim to identify and assess temperature-dependent mechanisms involved in WNV transmission dynamics. To accomplish our objectives, we began by developing a temperature-driven mosquito abundance model based on data obtained from laboratory studies on the effect of temperature on mosquito biology (Ch. 2). Under simplifying assumptions, the abundance model is transformed into an age-structured population model where we explore the existence and stability of equilibria. The model is then extended to describe the WNV transmission cycle of mosquitoes and birds (Ch. 3). Under simplifying assumptions, we formulate an expression for the basic reproduction number R_0. The effect of temperature on R_0 is then investigated. To test the model's capacity to predict the risk of infection to humans, we compare numerical results of our simulated minimum infection rate (SMIR) with observed minimum infection rate (MIR) surveillance data for validation. Finally, we illustrate how the model can use the local temperature forecast as input to predict mosquito abundance and WNV infection risk within the forecasted timeframe.

2 Temperature-driven mosquito abundance model

2.1 Introduction

The aim of this chapter was to develop a temperature-driven abundance model simulating Cx. *pipiens* and Cx. *restuans* population dynamics over a single-season. We developed temperature-dependent response functions for mosquito development, mortality, and diapause based on data available in published field and laboratory studies. The model was then applied to the Peel Region, Southern Ontario, using mosquito surveillance data from 2004–2016. Simulation results showed the model could capture the general trend of observed mosquito population dynamics for each mosquito season. The proposed model demonstrates it has potential to be used as a real-time mosquito abundance forecasting tool and would have direct application in mosquito control programs.

2.2 Model formulation

We developed a model composed of ODEs, evaluated at discrete time steps, to study the impact of temperature on the temporal dynamics of the mosquito population in the Peel Region, Southern Ontario. The model was designed to encompass both immature and adult stages of mosquitoes by separating the life cycle into two distinct stages: aquatic stage (eggs, larvae, and pupae) and adult stage. Only female mosquitoes will be modelled, as male mosquitoes do not take blood meals and are not carriers of WNV. Following the method of Shaman et al. (2006), we assume the mosquito

life cycle will proceed continuously. Eggs are deposited directly on breeding waters and immediately proceed through development. The total amount of eggs oviposited in a single day is determined by the total number of adult mosquitoes across all cohorts multiplied by the oviposition rate β. All eggs oviposited on the same day are grouped into the same cohort, which are identified and labelled by the day of oviposition, denoted k. Once a cohort of eggs is oviposited, there is no other recruitment into that cohort population. Aquatic mosquito populations are diminished by a temperature-dependent mortality rate and by eclosion. Adult mosquitoes are assumed to live a maximum of ω days after eclosion and are diminished with a temperature-dependent mortality rate $\mu_m(T)$. Time is assumed to be integer-valued, with a time step of 1 day. We assume that mortality occurs at the beginning of each time step and reproduction occurs at the end of each time step. Hence, on the day adult mosquitoes reach their maximum lifespan, they die without reproducing.

The notation $N_{s,k}(t)$ is used to identify both aquatic and adult mosquito populations at time *t* and by cohort born on day k. The subscript *s* indicates the life cycle stage (*l* = aquatic stage and *m* = adult stage). The time ranges from the first to last day of the study period $t \in [t_0, t_{end}]$ based on an annual interval of 365 days. Similarly, the discrete cohort index *k* also ranges from the first to last day of the study period $k \in [t_0, t_{end}]$. Each mosquito cohort is tracked throughout its lifetime through both aquatic and adult stages from oviposition to death; i.e., $N_{m,k}$ represents the female mosquitoes that have eclosed from the corresponding aquatic cohort $N_{l,k}$. A model diagram of the mosquito life cycle is depicted in Figure 2.1.

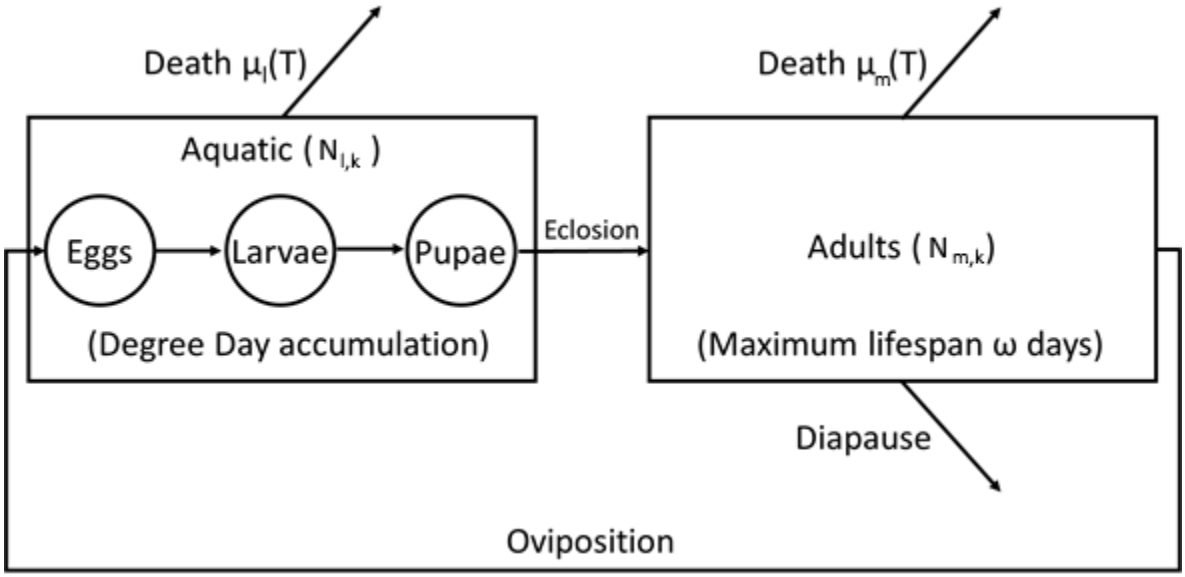

Figure 2.1: Model diagram describing the *Cx. pipiens* and *Cx. restuans* life cycle. The number of eggs oviposited into a cohort $N_{l,k}$ on any day is the total number of adult mosquitoes multiplied by the daily oviposition rate. Once a cohort accumulates enough DDs to complete development, all members of that cohort will simultaneously eclose into adults. Adults lay eggs daily until they die ω days after eclosion**.**

Temperature-dependent response functions describing the relationship between temperature and aquatic development (Sec. 2.2.1), mortality (Sec. 2.2.2), and diapause (Sec. 2.2.3) were developed a priori and locally tuned for Cx. *pipiens* and Cx. *restuans* mosquitoes in the study area. Model parameters were based on the most relevant data from existing literature. Definition, value, and dimension of model parameters and variables are given in Tables 1 and 2, respectively. Model equations describing mosquito survival and critical events (boundary conditions) are detailed in Section 2.2.4.

2.2.1 Aquatic development

There are several commonly used functions to fit development rate data obtained from laboratory studies; e.g., Logan, Holling, Briere, Lactin, Sharpe de Michelle, and Degree Days. Based on the results of laboratory studies on aquatic development at constant temperatures, we employed the

concept of degree-days (DD) to track the physiological age of developing mosquitoes as it provides a straightforward, accessible method of estimating development rates. This method of tracking temperature-dependent development has been applied in a variety of ways in existing models (Craig et al. 1999, Jetten and Takken 1994, Tachiiri et al. 2006). Although the linear model may tend to underestimate development rates at low temperatures and overestimate development rates at high temperatures, the mean daily temperatures in the Peel Region over the study period (June-September) generally range from 17°C–22°C which is well within the temperature range (15°C–30°C) in which the linear approximation is valid for the *Cx. pipiens* and *Cx. restuans* species (Canada's National Climate Archive).

Degree days are calculated by measuring the accumulated thermal units above a zero-development threshold temperature.

$$DD_e(t) = \begin{cases} 0, & T(t) \leq T_e \\ T(t) - T_e, & T(t) > T_e \end{cases} \tag{2.2.1}$$

where $T(t)$ is the mean temperature °C on day t. The parameter T_e is the minimum temperature threshold below which development is halted. The total number of DDs required for a cohort of larva to be fully developed into adults is denoted by T_{DDe}. Empirical functions that describe the relationship of temperature and development time generally take the following form (Craig et al. 1999):

$$df_k(t) = \frac{\max(0, T(t) - T_e)}{T_{DDe}} = \frac{DD_e(t)}{T_{DDe}} \tag{2.2.2}$$

where $df_k(t)$ is the proportion of T_{DDe} accumulated on day t by a cohort born on day k. The function $f_k(t) = \sum_{n=k}^{t} df_k(n)$ tracks the cumulative development of each cohort. Once a cohort

accumulates enough DDs, it will eclose into adults. The day of eclosion, denoted t_k, for a cohort born on day k is given by $t_k = t$ when $f_k(t) \geq 1 > f_k(t-1)$.

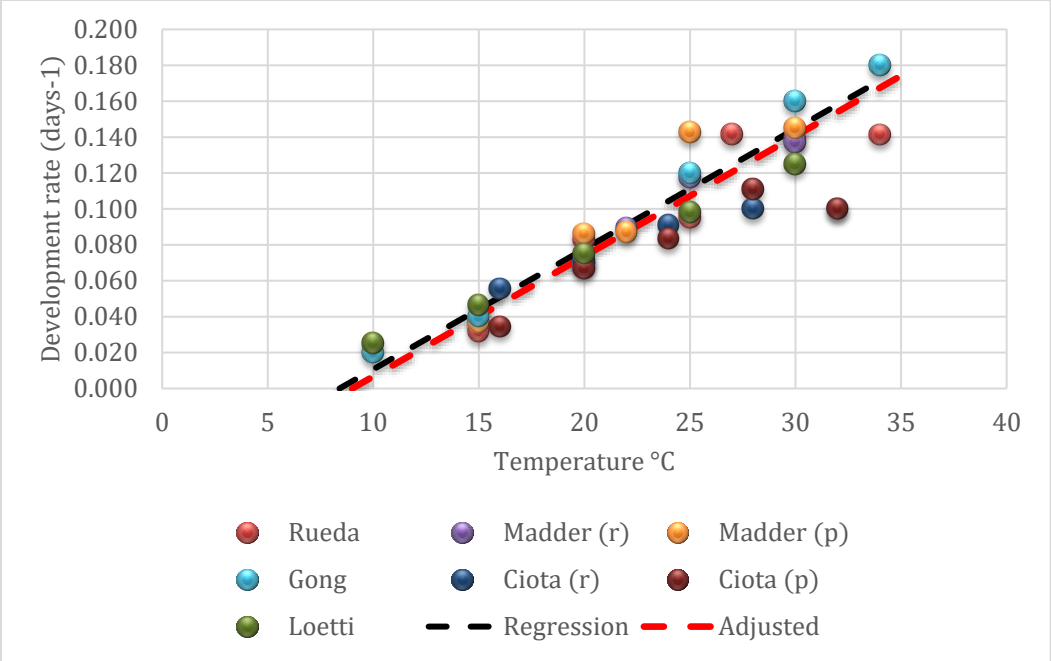

Figure 2.2: Comparison of temperature-dependent development rates obtained from laboratory studies. The black dashed line represents the linear regression of the collective development rates. The red dashed line represents the adjusted regression line that was locally tuned for the Peel Region, Ontario.

Figure 2.2 displays the results of multiple laboratory and field studies for *Cx. pipiens* and *Cx. restuans* aquatic development at constant temperatures (Madder et al. 1983, Rueda et al. 1990, Loetti et al. 2011, Gong et al. 2011, Ciota et al. 2014). A linear regression through the data points from all the studies was used to estimate parameters T_e and T_{DDe}. The linear regression estimated a minimum threshold temperature of $T_e = 8.4$°C and a total number of degree-days to emergence, $T_{DDe} = 144$°C. Previous studies specific to Southern Ontario (Wang et al. 2011) have used a minimum threshold temperature of 9°C. Adjusting the original estimate of the fitted regression

line to reflect a minimum threshold temperature of $T_e = 9°C$ yields a total number of degree-days to emergence of $T_{DDe} = 149°C$.

2.2.2 Mortality

Within an optimum range, larval mortality is not significantly affected by temperature fluctuations. The effect of temperature on larval mortality is primarily observed at higher temperatures where high development rates are accompanied by high mortality rates (Madder et al. 1983, Jetten and Takken 1994, Rueda et al. 1990, Bayoh and Lindsay 2004, Loetti et al. 2011, Meillon et al. 1967). In addition, when developing at high temperatures, mosquitoes that do survive until adulthood experience adverse effects on their biological development that decrease the likelihood of survival and successful reproduction; e.g., wing length, follicle length, and adult mass. In contrast, colder temperatures closer to the lower development threshold act more as an inhibitor to larval development rather than causing high mortality (Bayoh and Lindsay 2003). Furthermore, larval mortality is not significantly affected when exposed to high temperatures for no more than a few hours during the day (Bayoh and Lindsay 2004). Thus, in our model, daily mortality rates are calculated based on a two-day average temperature to reduce the effect of daily temperature fluctuations on developing mosquito mortality. These studies also show that the optimal temperature for mosquito development ranges between 24–26°C, where a high rate of development corresponds with a low mortality rate (Madder et al. 1983, Loetti et al. 2011; Rueda et al. 1990, Shelton 1973).

Some existing models that utilize a temperature-dependent mortality function do not account for both the development time and the proportion of individuals surviving the development period. They also assume mortality increases as temperature decreases and hence the shapes of the

functions they use resemble Gaussian or parabolic functions. Figure 2.3 shows several functions used in different studies to describe the functional relationship between temperature and daily mortality rates for developing mosquitoes.

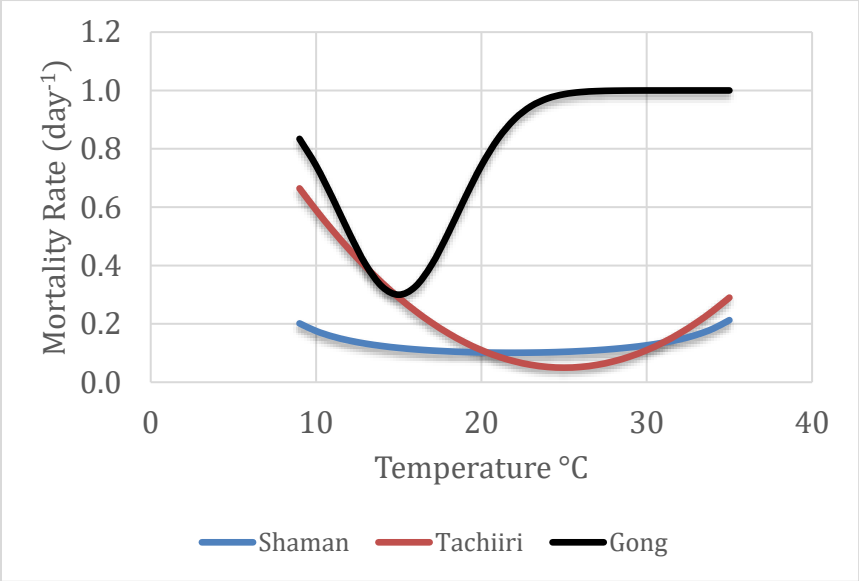

Figure 2.3: Comparison of temperature-dependent mortality rate functions used in existing studies: Shaman et al., (2006): $\mu = (-4.4 + 1.31T - 0.03T^2)^{-1}$, Tachiiri et al., (2006): $\mu = (0.24(T - 25)^2 + 5)$ %, Gong et al., (2011): $\mu = 1 - 0.7e^{-(\frac{T-15}{5})^2}$.

We develop a temperature-dependent mortality function based on data obtained from laboratory and field studies. Mortality rates obtained from these studies were not originally presented as daily mortality rates. They measured the fraction of individuals that survived the aquatic stage of development when reared at various constant temperatures. Converting these survival percentages to daily mortality rates for each temperature was done using the exponential model for population dynamics shown below:

$$\frac{dL}{dt} = -\mu L, \qquad with\ solution: \qquad L(t) = L_0 e^{-\mu t}$$

Solving for daily mortality rate μ yields:

$$\mu(t) = -\frac{1}{t}\ln\left(\frac{L(t)}{L_0}\right) \tag{2.2.3}$$

where L_0 is the initial number of larvae at the beginning of the experiment and $L(t)$ is the number of larvae that survived the aquatic development period up to time t. The resulting mortality rates from each study as well as the mortality function we formulated based on the results of these studies are depicted in Figure 2.4.

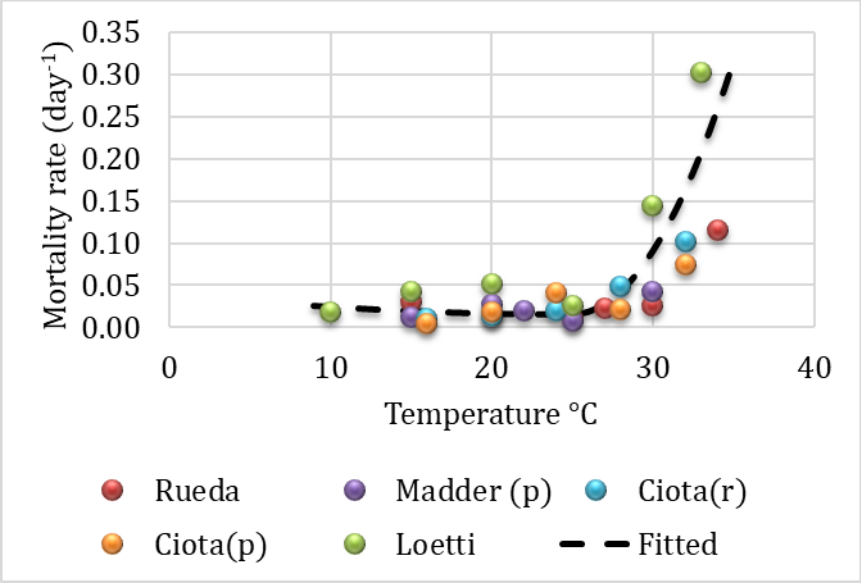

Figure 2.4**:** Comparison of temperature-dependent mortality rates (day^{-1}) based on data obtained from available literature. The function $\mu_l(T_l(t))$, defined in equation (2.2.4), used to fit the data points is represented by the black dashed line.

Instead of a function with a Gaussian shape, we formulated a piecewise parabolic function to fit the data for temperatures above and below the optimal temperature of development.

$$\mu_l(T_l(t)) = \begin{cases} j(T - T_{op})^2 + \mu_{op}, & if\ \ T(t) < T_{op}, \\ q(T - T_{op})^2 + \mu_{op}, & if\ \ T(t) \geq T_{op}. \end{cases} \quad (2.2.4)$$

where j and q are scale factors, T_{op} is the optimal temperature of aquatic mosquito development, and μ_{op} is the corresponding mortality rate at the optimal temperature. Aquatic mortality rates are calculated based on a two-day average daily temperature, denoted $T_l(t)$, to reduce the impact of daily temperature fluctuations on the survival of developing mosquitoes.

2.2.3 Diapause

To survive unfavorable environmental conditions over winter, many mosquito species undergo a hibernal dormancy called diapause. Depending on species, most mosquitoes can diapause in only one life cycle stage: egg, larval, or adult. Photoperiod (number of day light hours), is the primary environmental signal responsible for the induction of diapause. Once the number of daylight hours decrease below a photosensitive threshold, a proportion of developing mosquitoes will undergo physiological changes that better prepare them to survive the winter as an adult (Zhang and Denlinger 2011, Spielman 2001, Eldridge 1966). While photoperiod is responsible for determining the induction of diapause, it has also been shown that temperature enhances the photoperiodic response generating a higher incidence of diapause the lower the temperature (Eldridge 1966, Madder et al. 1983, Denlinger and Armbruster 2014). In these studies, experiments were conducted at constant temperatures. At each temperature, developing mosquitoes were subjected to a range of photoperiods. For *Cx. pipiens* and *Cx. restuans* mosquitoes, the photosensitive stages where the initiation of diapause occurs have been shown to be the fourth larval instar and pupal stages of development. Adult females that are destined for diapause do so soon after eclosion prior to taking

a blood meal and after mating. Our model only considers the non-diapausing adult female mosquito population, as they are still actively seeking blood meals and are thus susceptible to WNV infection.

Many existing mosquito abundance studies do not include the diapause phenomenon in their models (Shaman et al. 2006, Ruiz et al. 2010, Wonham et al. 2004). Most of the studies that do account for diapause primarily consider the proportion of diapausing mosquitoes as a function of photoperiod only (Gong et al. 2011, Cailly et al. 2012, Tachiiri et al. 2006). Figure 2.5 shows results from a study by Spielman (2001) where the percentage of mosquitoes destined for diapause increases as photoperiod length decreases when reared at a constant temperature of 18°C. To improve on existing methods of modelling the diapause phenomenon, we develop a response function that includes the effect of temperature based on the results of several field and laboratory studies.

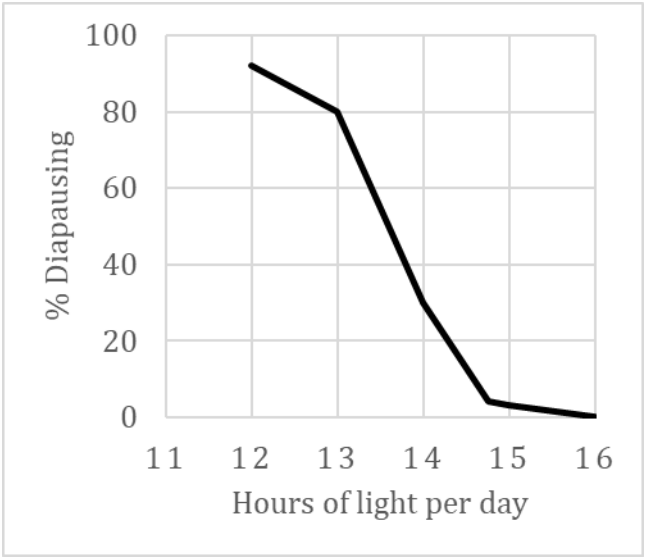

Figure 2.5: Effect of photoperiod on the proportion of diapause-destined blood-fed female mosquitoes reared at a constant 18°C (Spielman, 2001).

Based on data obtained from published laboratory and field studies on mosquito diapause, we define a linear function to describe the relationship between temperature and the proportion of non-diapausing females at different photoperiods. The photoperiodic threshold of 14.75 daylight hours for the induction of diapause was derived from these studies and corresponds with the end of July in the study area. The maximum photoperiod in the study area in any given year is approximately 15.5 daylight hours which occurs in late June, while the photoperiod corresponding to the disappearance of mosquitoes is approximately 12 daylight hours at the end of September. For photoperiods of 12 hours and below, all mosquitoes will enter diapause upon eclosion.

Parameters P_k and T_k represent the photoperiod and mean temperature experienced during the photosensitive fourth larval instar and pupal stages of development, respectively (4th larval instar assumed to begin when 80% of aquatic development has completed). The photoperiod for each cohort born on day k is selected from a table containing the observed number of daylight hours for each day in the city of Toronto, ON, for each year from 2004–2016. For each cohort, the photoperiod P_k used for diapause induction is assumed to be the number of daylight hours on the day the cohort completes 80% of its aquatic development. The mean temperature T_k for the days spanning the last 20% of aquatic development is then used to determine the incidence of emerging non-diapausing adult mosquitoes. For consistency with the function for degree-days, we assumed a base temperature of 9°C. The function $\gamma_k(T_k, P_k)$ is given by equation (2.2.5) and depicted in Figure 2.6.

$$\gamma_k(T_k, P_k) = \begin{cases} 1 & if\ 14.75 < P_k \\ \left[m_{14} + (m_{14.75} - m_{14})\dfrac{P_k - 14}{0.75}\right](T_k - T_e) & if\ 14 < P_k \leq 14.75 \\ \left[m_{14}\dfrac{P_k}{14}\right](T_k - T_e) & if\ 12 < P_k \leq 14, \end{cases} \quad (2.2.5)$$

where m_p is the slope of the function $\gamma_n(T_n, p)$ for the photoperiod indicated by the subscript p.

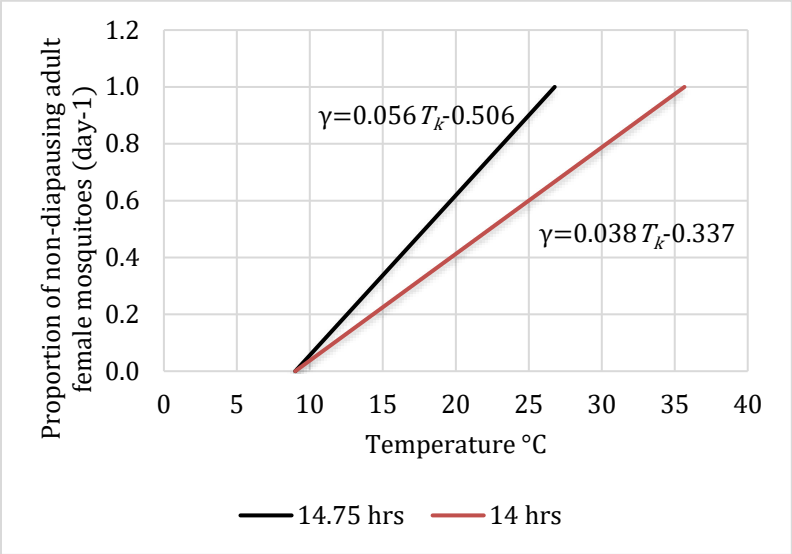

Figure 2.6: Temperature and photoperiod-dependent functions for two key photoperiods defined in (2.2.5).

Year-to-year variation in photoperiod for the same day is assumed to be negligible. Thus, we use a periodic sine function to estimate the number of daylight hours each day.

$$P_k = 3.257\sin\big(0.017(k + 0.8\tau_k - 81)\big) + 12.186, \qquad k = t_0, \ \ldots, t_{end} \tag{2.2.6}$$

The function was formulated based on average photoperiodic values obtained from a table containing the observed number of daylight hours for each day in the city of Toronto, Ontario for years 2004–2016 (United States Naval Observatory 2017).

2.2.4 Model equations

The model is composed of a system of multiple paired ODEs to track the survival of population cohorts through their lifetime in the aquatic and adult stages of development. The ODE system for governing the survival of each cohort is given by:

$$\frac{dN_{l,k}(s)}{ds} = -\mu_l\big(T_l(t)\big)N_{l,k}(s), \qquad f_k(t) < 1 \; and \; t+1 > s > t, \tag{2.2.7}$$

$$\frac{dN_{m,k}(s)}{ds} = -\mu_m\big(T(t)\big)N_{m,k}(s), \qquad f_k(t) > 1 \; and \; t+1 > s \geq t, \tag{2.2.8}$$

where $\mu_l\big(T_l(t)\big)$ is the temperature-dependent aquatic mortality rate. Aquatic mortality rates are calculated based on a two-day average daily temperature, denoted $T_l(t)$, to reduce the impact of daily temperature fluctuations on the survival of developing mosquitoes.

Boundary conditions defining critical events such as oviposition, eclosion, and maximum adult lifespan are defined by the following.

Oviposition:

The number of eggs oviposited on any day t equals the total number of adults that are at least one day old since eclosion multiplied by the oviposition rate β. Adults that reach their maximum lifespan die on that day before reproducing. The number of eggs oviposited on day t is

$$N_{l,k=t}(t) = \beta \sum_{k=t_0}^{t-2} N_{m,k}(t) \tag{2.2.9}$$

Eclosion:

Upon eclosion, the variable tracking a cohort of aquatic mosquitoes will equal zero and the active host-seeking proportion of emerging adults will be initiated.

$$N_{l,k}(t) = 0, \qquad f_k(t) \geq 1 > f_k(t-1) \tag{2.2.10}$$

$$N_{m,k}(t) = e^{-\mu_l}\gamma_k(T_k, P_k)N_{l,k}(t-1), \qquad f_k(t) \geq 1 > f_k(t-1) \tag{2.2.11}$$

where the function $\gamma_k(T_k, P_k)$ represents the proportion of non-diapausing emerging adult female mosquitoes (2.2.5).

Adult Lifespan:

All remaining adults in a cohort die before reproducing ω days after eclosion:

$$N_{m,k}(t) = 0, \qquad if\ t = t_k + \omega. \tag{2.2.12}$$

2.3 Simplified model at constant temperature

The model developed in this study was designed to adhere to the basic and well-understood characteristics of mosquito biology. It was formulated in a manner that inhibits unbounded growth of the mosquito population over a single-season due to the inclusion of the diapause phenomenon. Furthermore, model equations (2.2.7) and (2.2.8) will never have negative solutions for aquatic and adult populations. Remaining consistent with mosquito biology at extreme temperatures, our model restricts mosquito development outside the range of temperatures shown to be conducive to mosquito development.

In the following sections, we investigate the existence and stability of equilibrium solutions of our model under simplifying assumptions. Although the model was developed with an objective to accurately describe the vital dynamics of the mosquito life cycle, the assumptions in this section may over simplify certain biological processes. Nevertheless, these assumptions must be made in order to linearize the model equations to study the existence and stability of equilibria. Analytical results obtained from our simplified model are intended to draw attention to the relationship

between temperature and mosquito population dynamics as well as highlight some important mechanisms that drive population abundance. To begin, we define the model system to be in a state of equilibrium when the population structure does not change with time. For positive equilibrium solutions to exist in our model, temperature must be held constant and the effect of photoperiod must be ignored. At constant temperatures, the aquatic mortality rate μ_l and larval development time τ become constant. Consequently, the model will be composed of $\tau + \omega$ paired equations tracking cohorts of developing mosquitoes that are 1 to τ days old and after they become adults that are 1 to ω days old relative to the day of eclosion. Hence, the model equations (2.2.7) and (2.2.8) can be simplified as

$$\begin{aligned} &\frac{dN_{l,k}(t)}{dt} = -\mu_l N_{l,k}(t), \\ &N_{l,k}(t) = N_{l,k}(k)e^{-\mu_l(t-k)}, \qquad 0 < (t-k) < \tau \end{aligned} \tag{2.3.13}$$

$$\begin{aligned} &\frac{dN_{m,k}(t)}{dt} = -\mu_m N_{m,k}(t), \\ &N_{m,k}(t) = N_{m,k}(k+\tau)e^{-\mu_m(t-k-\tau)}, \qquad \tau < (t-k) < \omega, \end{aligned} \tag{2.3.14}$$

where τ is the total aquatic development time (days) for each cohort and is calculated by

$$\tau = \left\lceil \frac{T_{DDe}}{T - T_e} \right\rceil. \tag{2.3.15}$$

Since the development time τ for each cohort is now constant, we observe that the term, $N_{m,k}(k+\tau)e^{-\mu_l(t-k-\tau)}$ in the solution for adult mosquitoes (2.3.14) can be expressed in terms of its initial population in the aquatic stage. The solution for the adult equation can be rewritten as:

$$N_{m,k}(t) = N_{l,k}(k)e^{-\mu_l\tau}e^{-\mu_m(t-k-\tau)}, \qquad if\ \tau \le (t-k) < \omega. \tag{2.3.16}$$

The boundary conditions defined for oviposition, eclosion, and maximum adult lifespan can also be simplified and are given below.

Oviposition:

The total number of eggs oviposited at time t is found by solving the system of equations for each cohort of mosquitoes in terms of their initial populations in the aquatic stage.

$$N_{l,k}(t) = \beta\big[N_{l,t-\tau-\omega+1}(t-\tau-\omega+1)e^{-\mu_l\tau}e^{-\mu_m(\omega-1)} + N_{l,t-\tau-\omega+2}(t-\tau-\omega+2)e^{-\mu_l\tau}e^{-\mu_m(\omega-2)} + \cdots + N_{l,t-\tau-1}(t-\tau-1)e^{-\mu_l\tau}e^{-\mu_m}\big]$$

$$= \beta e^{-\mu_l\tau}\sum_{k=t-\tau-\omega+1}^{t-\tau-1} N_{l,k}(k)\, e^{-\mu_m(t-\tau-k)}. \tag{2.3.17}$$

Eclosion of cohort born on day k:

$$N_{l,k}(k+\tau) = 0,$$

$$N_{m,k}(t) = 0, \qquad t < (k+\tau), \tag{2.3.18}$$

$$N_{m,k}(k+\tau) = N_{l,k}(k)e^{-\mu_l\tau}.$$

Maximum Lifespan (ω days after eclosion):

$$N_{m,k}(k+\tau+\omega) = 0. \tag{2.3.19}$$

2.4 Age-structured population model (Leslie matrix)

Under the conditions that temperature is held constant and the effect of diapause is ignored, the resulting model system defined by equations (2.3.13) through (2.3.19) can be transformed into an autonomous time-discrete linear age-structured population model of the form

$$x(t+1) = Ax(t), \qquad x(t_0) \geq 0 \quad and \quad t = t_0, \qquad t_0 + 1, \ldots \tag{2.4.20}$$

The vector is the age class population distribution at time t and is defined

$$x(t) = \begin{bmatrix} x_0(t) \\ x_1(t) \\ . \\ . \\ . \\ x_{\tau-1}(t) \\ x_\tau(t) \\ . \\ . \\ . \\ x_{\tau+\omega-1}(t) \end{bmatrix} = \begin{bmatrix} N_{l,t}(t) \\ N_{l,t-1}(t) \\ . \\ . \\ . \\ N_{l,t-(\tau-1)}(t) \\ N_{m,t-\tau}(t) \\ . \\ . \\ . \\ N_{m,t-(\tau+\omega-1)}(t) \end{bmatrix} \tag{2.4.21}$$

where $x_i(t)$ is the number of females in the i^{th} age class at time t. Newly oviposited mosquito eggs are in the $x_0(t)$ age class. The model is constructed such that oviposition occurs after mortality takes place and then population census at time t is taken. Thus, the $x_{\tau+\omega}$ age class is not directly modelled since all mosquitoes in age class $x_{\tau+\omega-1}$ at time $t-1$ will die at the beginning of the following day t before the census.

The coefficient matrix A is referred to as a Leslie projection matrix (Leslie 1945) that classifies individuals into $\tau + \omega$ age classes and is written as

$$A = F + P \geq 0. \tag{2.4.22}$$

where the matrix F is referred to as the "fertility" matrix containing per capita oviposition rates and is given by

$$F = \begin{bmatrix} f_1 & f_2 & . & . & . & f_{\tau+\omega} \\ 0 & 0 & . & . & . & 0 \\ . & . & & & & . \\ . & . & & & & . \\ . & . & & & & . \\ 0 & 0 & . & . & . & 0 \end{bmatrix} \geq 0, \qquad f_i \geq 0, \qquad i = 1,2,\dots,\tau+\omega, \qquad \sum_{i=1}^{\tau+\omega} f_i \neq 0. \tag{2.4.23}$$

The "transition" matrix P contains the age class survival probabilities and is given by

$$P = \begin{bmatrix} 0 & 0 & . & . & . & . & 0 \\ p_1 & 0 & . & . & . & . & 0 \\ 0 & p_2. & . & . & . & . & 0 \\ . & . & & & & & . \\ . & . & & & & & . \\ . & . & & & & & . \\ 0 & 0 & . & . & . & p_{\tau+\omega-1} & 0 \end{bmatrix} \geq 0, \qquad 0 < p_i < 1, \qquad i = 1,2,\dots,\tau+\omega-1. \tag{2.4.24}$$

The Leslie matrix A of this linear system is

$$A = F + P = \begin{bmatrix} f_1 & f_2 & f_3 & . & . & . & f_{\tau+\omega-1} & f_{\tau+\omega} \\ p_1 & 0 & 0 & . & . & . & 0 & 0 \\ 0 & p_2 & 0 & . & . & . & 0 & 0 \\ . & . & . & & & & . & . \\ . & . & . & & & & . & . \\ . & . & . & & & & . & . \\ 0 & 0 & 0 & . & . & . & p_{\tau+\omega-1} & 0 \end{bmatrix} \geq 0, \tag{2.4.25}$$

which is a non-negative, square matrix of order $\tau + \omega$ with all elements strictly zero except those that are in the first row and in the sub-diagonal immediately below the principal diagonal. Based on model equations defined by (2.3.13) through (2.3.19), the nonzero entries in the $(\tau + \omega) \times (\tau + \omega)$ fertility and transition matrices F and P are

$$f_i = \beta e^{-\mu_m}, \qquad i = \tau+1, \tau+2, \dots, \tau+\omega-1 \tag{2.4.26}$$

$$p_i = \begin{cases} e^{-\mu_l}, & i = 1, 2, \dots, \tau \\ e^{-\mu_m}, & i = \tau + 1, \dots, \tau + \omega - 1. \end{cases} \tag{2.4.27}$$

The entries f_i in the first row of the fertility matrix $F = (f_i)$ are the number of eggs oviposited by an adult mosquito in the i^{th} age class that survive one unit time. The entry p_i in the transition matrix $P = (p_i)$ is the probability of individuals in the i^{th} age class surviving one unit time. Thus, the total number of eggs produced by mosquitoes in age class i in one time step is calculated by multiplying f_{i+1} by the number of females in age class i at time $t - 1$. The sum of all these values gives the total number of offspring produced at any given time.

$$x_0(t) = f_1 x_0(t-1) + f_2 x_1(t-1) + \cdots + f_{\tau+\omega} x_{\tau+\omega-1}(t-1). \tag{2.4.28}$$

The mosquitoes in the second age class at time t are those mosquitoes in the first age class at time $t - 1$ who are still alive at time t. In general, the mosquitoes in the i^{th} age class at time t are those individuals in age class $i - 1$ at time $t - 1$ who are still alive at time t. More precisely we have

$$x_i(t) = p_i x_{i-1}(t-1). \tag{2.4.29}$$

Equations (2.4.28) and (2.4.29) can be expressed more compactly;

$$x(t) = Ax(t-1), \qquad t = t_0, t_0 + 1, \dots \tag{2.4.30}$$

By simple induction, it can be shown that given an initial age class distribution $x(t_0)$ we can obtain

$$x(t) = A^{(t-t_0)} x(t_0), \qquad t = t_0, t_0 + 1, \dots \tag{2.4.31}$$

Thus, we can determine the age distribution of adult female mosquitoes at any time t if we given an initial condition $x(t_0)$ and the Leslie matrix A.

2.5 Limiting behavior

From equation (2.4.31) we can determine the age distribution of the mosquito population at any given time; however, the general dynamics of the growth process is not immediately given by this equation alone. To study the asymptotic dynamics of the model, we need to investigate the eigenvalues and corresponding eigenvectors of the Leslie matrix A. Of interest are the properties of the eigenvector, denoted v_1, corresponding to the dominant eigenvalue, denoted λ_1.

2.5.1 Eigensystem: growth rate and stable age distribution

If a Leslie matrix is non-negative, irreducible, and primitive the Perron–Frobenius theorem, proved by Oskar Perron (1907) and Georg Frobenius (1912), guarantees that the Leslie matrix will have a real and simple root with multiplicity one that is greater in modulus than all other eigenvalues and its associated eigenvector will be strictly positive. A square matrix A of order n is said to be primitive if, for some integer p, A^p has only positive (non-zero) entries. Due to the post-reproductive age class in our model, the matrix A is reducible and does not immediately satisfy the conditions to apply the Perron–Frobenius theorem, since its associated graph is not strongly connected; i.e., contains a path from every node to every other node. However, in our model, partitioning the matrix A into submatrices such that,

$$A = \begin{bmatrix} B & 0 \\ C & 0 \end{bmatrix} \tag{2.5.32}$$

allows for the application of the Perron–Frobenius theorem to the submatrix B, which is a square matrix of order $(\tau + \omega - 1)$ consisting of reproductive age classes. The matrix B is either irreducible or it can be further divided to eventually yield a series of irreducible diagonal blocks

(Gantmacher 1959). Submatrix C is a $1 \times (\tau + \omega - 1)$ matrix consisting of all zero entries except for the last element, which is the probability of surviving to the following time step. It can be verified that the submatrix B in our model is irreducible because its associated graph is strongly connected. A sufficient condition for primitivity of an irreducible age-classified matrix is the existence of any two adjacent age classes with positive fertility (Caswell 2001). The submatrix B clearly satisfies this condition by equations (2.4.26) and (2.4.27) and thus is primitive. When studying the long-term behavior of reducible Leslie matrices of the form in (2.5.32), it is sufficient to analyze the smaller submatrix B that consists of the reproductive age classes as it alone determines the growth rate of the entire system and is unaffected by post-reproductive age classes (Caswell 2001).

The eigenvalues of the matrix B are the roots of its characteristic equation which is found by solving $\det(\lambda I - B) = 0$, where λ is an eigenvalue of the matrix B.

$$\det(\lambda I - B) = \lambda^{(\tau+\omega-1)} - f_1\lambda^{(\tau+\omega-2)} - f_2 p_1\lambda^{(\tau+\omega-3)} - \cdots - f_{\tau+\omega-1}p_1 p_2 \ldots p_{\tau+\omega-2} = 0 \quad (2.5.33)$$

Substituting model parameter values into the characteristic equation and using summation notation yields

$$\lambda^{(\tau+\omega-1)} - \beta e^{-\mu_l \tau} \sum_{j=1}^{\omega-1} e^{-\mu_m j} \lambda^{(\omega-j-1)} = 0. \quad (2.5.34)$$

As we are interested in studying the asymptotic dynamics of the model, we need to be able to say something in general about the roots of the characteristic equation. For convenience of analysis we first divide (2.5.34) by $\lambda^{(\tau+\omega-1)}$ and rearrange the terms to yield

$$\beta e^{-\mu_l \tau} \sum_{j=1}^{\omega-1} e^{-\mu_m j} \lambda^{-(\tau+j)} = 1. \tag{2.5.35}$$

Equation (2.5.35) is known as the discrete form of the Lotka-Euler equation. We then define a function $\psi(\lambda)$ to be the terms on the left-hand side of equation (2.5.35),

$$\psi(\lambda) = \beta e^{-\mu_l \tau} \sum_{j=1}^{\omega-1} e^{-\mu_m j} \lambda^{-(\tau+j)} \tag{2.5.36}$$

so that it becomes

$$\psi(\lambda) = 1, \qquad \lambda \neq 0. \tag{2.5.37}$$

Since all the coefficients of $\psi(\lambda)$ are non-negative, we see that

$$\lim_{\lambda \to 0} \psi(\lambda) = \infty,$$

$$\lim_{\lambda \to \infty} \psi(\lambda) = 0. \tag{2.5.38}$$

Furthermore, $\psi(\lambda)$ is strictly decreasing

$$\frac{d\psi(\lambda)}{d\lambda} = -\beta e^{-\mu_l \tau} \sum_{j=1}^{\omega-1} (\tau + j) e^{-\mu_m j} \lambda^{-(\tau+j+1)} < 0. \tag{2.5.39}$$

Since $\psi(\lambda)$ is continuous, the Intermediate Value Theorem tells us it will cross the horizontal line $\psi(\lambda) = 1$. In addition, since $\psi(\lambda)$ is strictly decreasing, it will cross the line $\psi(\lambda) = 1$ exactly once. Therefore, $\psi(\lambda) = 1$ has only one positive real solution $\lambda = \lambda_1$ with multiplicity 1. All other roots λ_i are either complex or negative.

Our next objective is to find the eigenvector v_1 corresponding to the dominant eigenvalue λ_1 such that

$$Bv_1 = \lambda_1 v_1 \tag{2.5.40}$$

A nonzero vector solution of (2.5.40) exists only if the matrix $(\lambda I - B)$ is singular; i.e., if $\det(\lambda I - B) = 0$. If such an eigenvector exists, then

$$x(t) = {\lambda_1}^{(t-t_0)} v_1, \qquad t = t_0, t_0 + 1, t_0 + 2, \ldots \tag{2.5.41}$$

is a solution to the model equation (2.4.20) with $x(t_0) = v_1$ since $x(t+1) = \lambda^{(t-t_0+1)} v = \lambda^{(t-t_0)} \lambda v = \lambda^{(t-t_0)} Av = A(\lambda^{(t-t_0)} v) = Ax(t)$. Note that if v_1 is an eigenvector and c is a scalar, then cv_1 is also an eigenvector. For the eigenvector corresponding to the dominant eigenvalue, we choose a scalar c such that $c = {v_{1,1}}^{-1}$, where $v_{1,1}$ is the first element in the eigenvector associated with the dominant eigenvalue λ_1. It should be noted that since the eigenvector v_1 is strictly positive, by the Perron–Frobenius Theorem, the first element $v_{1,1} > 0$. Choosing a scalar c in this way gives us a normalized eigenvector v_1 with the first entry equal to one.

$$v_1 = {v_{1,1}}^{-1} \begin{bmatrix} v_{1,1} \\ v_{1,2} \\ . \\ . \\ . \\ v_{1,\tau+\omega-1} \end{bmatrix} = \begin{bmatrix} 1 \\ v_{1,2} \\ . \\ . \\ . \\ v_{1,\tau+\omega-1} \end{bmatrix} \tag{2.5.42}$$

We then compute $Bv_1 = \lambda_1 v_1$ to get

$$Bv_1 = \begin{bmatrix} f_1 + f_2 v_{1,2} + \cdots + f_{\tau+\omega-1} v_{1,\tau+\omega-1} \\ p_1 \\ p_2 v_{1,2} \\ . \\ . \\ p_{\tau+\omega-2} v_{1,\tau+\omega-2} \end{bmatrix} = \lambda_1 v_1 = \begin{bmatrix} \lambda_1 \\ \lambda_1 v_{1,2} \\ \lambda_1 v_{1,3} \\ . \\ . \\ \lambda_1 v_{1,\tau+\omega-1} \end{bmatrix}. \quad (2.5.43)$$

Solving successively for $v_{1,2}$ through $v_{1,\tau+\omega-1}$ we have

$$v_{1,2} = {\lambda_1}^{-1} p_1, \quad v_{1,3} = {\lambda_1}^{-2} p_1 p_2, \qquad \ldots, v_{1,\tau+\omega-1} = {\lambda_1}^{-(\tau+\omega-2)} p_1 p_2 \ldots p_{\tau+\omega-2} \quad (2.5.44)$$

Substituting these values back into (2.5.42) gives

$$Bv_1 = \begin{bmatrix} f_1 + f_2 {\lambda_1}^{-1} p_1 + \cdots + f_{\tau+\omega} {\lambda_1}^{-(\tau+\omega-2)} p_1 p_2 \ldots p_{\tau+\omega-2} \\ p_1 \\ {\lambda_1}^{-1} p_1 p_2 \\ . \\ . \\ . \\ {\lambda_1}^{-(\tau+\omega-3)} p_1 p_2 \ldots p_{\tau+\omega-2} \end{bmatrix} = \lambda_1 v_1 = \begin{bmatrix} \lambda_1 \\ p_1 \\ {\lambda_1}^{-1} p_1 p_2 \\ . \\ . \\ . \\ {\lambda_1}^{-(\tau+\omega-3)} p_1 p_2 \ldots p_{\tau+\omega-2} \end{bmatrix} \quad (2.5.45)$$

For v_1 to be an eigenvector, the first entries agree. That is

$$f_1 + f_2 {\lambda_1}^{-1} p_1 + \cdots + f_{\tau+\omega-1} {\lambda_1}^{-(\tau+\omega-2)} p_1 p_2 \ldots p_{\tau+\omega-2} = \lambda_1. \quad (2.5.46)$$

After substituting parameter values into equation (2.5.43) and simplifying, we obtain the familiar Lotka–Euler equation derived in equation (2.5.35), which we know has exactly one positive root, and this positive root is the dominant eigenvalue of the matrix B. The normalized age class distribution vector is

$$v_1 = \begin{bmatrix} 1 \\ {\lambda_1}^{-1} p_1 \\ {\lambda_1}^{-2} p_1 p_2 \\ . \\ . \\ {\lambda_1}^{-(\tau+\omega-2)} p_1 p_2 \dots p_{\tau+\omega-2} \end{bmatrix} \tag{2.5.47}$$

Using what we know about the properties of the eigenvalues and associated eigenvectors of the matrix B we can determine the long-term behavior of the population structure. We employ the use of a theorem by Sykes (1969):

THEOREM 1. *Let B be a primitive population projection matrix with maximal eigenvalue* λ_1 *and associated positive eigenvector* v_1. *Then* $\lim_{t\to\infty} \frac{B^{t-t_0}}{{\lambda_1}^{t-t_0}} = H$ *exists, where* H *is a matrix whose columns are positive multiples of* v_1.

By the Perron–Frobenius theorem, we know the submatrix B in our model has a strictly dominant eigenvalue and associated positive eigenvector that satisfies the conditions for Theorem 1. Hence, we can write

$$\lim_{t\to\infty} \frac{x(t)}{{\lambda_1}^{t-t_0}} = \lim_{t\to\infty} \left(\frac{B^{t-t_0}}{{\lambda_1}^{t-t_0}}\right) x(t_0)$$

$$= Hx(t_0) = c_1 v_1, \tag{2.5.48}$$

where the coefficient c_1 is a positive constant depending only on the initial age class distribution vector $x(t_0)$. Theorem 1 tells us that if a Leslie matrix is primitive, the long-term dynamics of the population are determined by the population growth rate λ_1 and the stable age class population

distribution v_1. The age structure of the population will converge to a fixed (time-invariant) age structure that is independent of the initial population distribution $x(t_0)$. For large t, we can approximate $x(t)$ by

$$x(t) \simeq c_1 {\lambda_1}^{(t-t_0)} v_1, \tag{2.5.49}$$

If the analysis is extended to cover the entire matrix A, then the Perron–Frobenius theorem cannot be applied in this case since the matrix A is reducible and hence not primitive. However, reducibility of this system, due to the post-reproductive age class, still allows us to solve for the long-run outcome. The last entry $v_{1,\tau+\omega}$ of the limiting distribution $v_1 = \{v_{1,1}, \dots, v_{1,\tau+\omega}\}^{\mathrm{T}}$ for the matrix A can be solved using the equation

$$\lambda_1 v_{1,\tau+\omega} = p_{\tau+\omega-1} v_{1,\tau+\omega-1}. \tag{2.5.50}$$

This last entry in the limiting distribution represents the proportion of the population associated with the post-reproductive age class. In general, if the age classes of a Leslie matrix are written as $\{1, \dots, m, \dots, n\}$ where m is the highest age class with positive fertility, then having obtained the entry $v_{1,m+t}$, the distribution for successive post reproductive age classes can be solved using the equation

$$\lambda_1 v_{1,m+t+1} = p_{m+t} v_{1,m+t} \tag{2.5.51}$$

to ultimately obtain the entire limiting distribution $v_1 = \{v_{1,1}, \dots, v_{1,\tau+\omega}\}^{T}$.

The eigenvalues of A can be found by solving $\det(\lambda I - A) = 0$, where λ is an eigenvalue of the matrix A.

$$\det(\lambda I - A) = \lambda^{(\tau+\omega)} - f_1\lambda^{(\tau+\omega-1)} - f_2 p_1\lambda^{(\tau+\omega-2)} - \cdots - \lambda f_{\tau+\omega-1}p_1 p_2 \ldots p_{\tau+\omega-2} = 0. \quad (2.5.52)$$

Factoring out a λ from the characteristic equation we arrive at

$$\lambda\left(\lambda^{(\tau+\omega-1)} - f_1\lambda^{(\tau+\omega-2)} - f_2 p_1\lambda^{(\tau+\omega-3)} - \cdots - f_{\tau+\omega-1}p_1 p_2 \ldots p_{\tau+\omega-2}\right) = 0. \quad (2.5.53)$$

From (2.5.50) we see that $\lambda = 0$ is a root of the characteristic equation with an associated right eigenvector $v = \{0,0,\ldots,1\}^T$. The remaining $\tau + \omega - 1$ eigenvalues of the matrix A are identical to that of submatrix B derived from (2.5.33). Thus, the dominant eigenvalue λ_1 for the submatrix B is also the dominant eigenvalue for the larger matrix A. Furthermore, the associated eigenvector, denoted $v_1\hat{}$,

$$v_1\hat{} = \begin{bmatrix} v_{1,1} \\ . \\ . \\ . \\ v_{1,\tau+\omega-1} \\ v_{1,\tau+\omega}\hat{} \end{bmatrix} \quad (2.5.54)$$

will be strictly positive. Note, the first $\tau + \omega - 1$ entries of $v_1\hat{} = v_1$ and the last term $v_{1,\tau+\omega}\hat{}$ are positive and are found by using equation (2.5.51). The last term $v_{1,\tau+\omega}\hat{}$ represents the individuals in the age class that will die before reproducing at the next time step. Having a strictly dominant eigenvalue with associated positive eigenvector for the matrix A, we can now analyze the long-term behavior of the reducible system. It must be noted that for the following analysis to hold, the initial population distribution $x(t_0)$ cannot solely consist of individuals in the post-reproductive age class associated with the entry $x_{\tau+\omega-1}(t)$. From equation (2.4.31), we know that, beginning with an initial population distribution $x(t_0)$, we can determine the population distribution $x(t)$ at

any time t by taking matrix powers of $A^{(t-t_0)}$ and applying the resulting matrix to the initial population distribution $x(t_0)$. The matrix $A^{(t-t_0)}$will then take the form

$$A^{(t-t_0)} = \begin{bmatrix} B^{(t-t_0)} & 0 \\ f(B,C,0) & 0 \end{bmatrix} \tag{2.5.55}$$

where $f(B,C,0) > 0$. If we write (2.4.31) in matrix notation we have

$$\begin{bmatrix} x_0(t) \\ x_1(t) \\ . \\ . \\ x_{\tau+\omega-1}(t) \end{bmatrix} = \begin{bmatrix} B^{(t-t_0)} & 0 \\ f(B,C,0) & 0 \end{bmatrix} \begin{bmatrix} x_0(t_0) \\ x_1(t_0). \\ . \\ . \\ x_{\tau+\omega-1}(t_0) \end{bmatrix} = \begin{bmatrix} B^{(t-t_0)}x(t_0) \\ - - - - - - - - - - \\ f(B,C,0)x(t_0) \end{bmatrix}$$

$$= \begin{bmatrix} B^{(t-t_0)}x(t_0) \\ - - - - - - - - - - \\ p_{\tau+\omega-1}\left[B^{(t-1-t_0)}x(t_0)\right]_{\tau+\omega-2} \end{bmatrix}, \qquad t > t_0. \tag{2.5.56}$$

The last term in the resulting distribution vector $x(t)$ in (2.5.56) is always a constant multiple $p_{\tau+\omega-1}$ of the previous age class at time $t-1$, which is consistent with (2.5.50). From (2.5.48), we know the population distribution for the first $\tau+\omega-1$ reproductive age classes converge to v_1. Equation (2.5.56) implies that the population distribution for all $\tau+\omega$ age classes will converge to ${v_1}^{\wedge}$ for t large enough. This can be shown by using equation (2.5.41) with respect to the matrix A.

$$x(t) = A^{(t-t_0)}x(t_0) = {\lambda_1}^{(t-t_0)}{v_1}^{\wedge}, \tag{2.5.57}$$

where $x(t_0) = {v_1}^{\wedge}$. We deduce that the limit

$$\lim_{t\to\infty} \frac{A^{t-t_0}}{{\lambda_1}^{t-t_0}} = H^{\wedge} \text{ exists,} \tag{2.5.58}$$

where $H^{\wedge} = [c_1 {v_1}^{\wedge}, c_2 {v_1}^{\wedge}, \dots, c_{\tau+\omega-1} {v_1}^{\wedge}]$ is a matrix whose columns are positive multiples of ${v_1}^{\wedge}$. In the same fashion as (2.5.48), we can see for large t the population will converge to a positive multiple of ${v_1}^{\wedge}$.

$$\lim_{t\to\infty} \frac{x(t)}{{\lambda_1}^{t-t_0}} = \lim_{t\to\infty} \left(\frac{A^{t-t_0}}{{\lambda_1}^{t-t_0}} \right) x(t_0)$$

$$= H^{\wedge} x(t_0) = c {v_1}^{\wedge}, \qquad x_{1,\dots,\tau+\omega-1}(t_0) \geq 0 \tag{2.5.59}$$

where the coefficient c is a positive constant depending only on the initial age class distribution vector $x(t_0)$. We must note that convergence to the stable age distribution for the reducible matrix A now depends on $x(t_0)$ where previously in the irreducible case of the matrix B, convergence was independent of the initial population distribution. For example, if $x(t_0)$ consisted solely of post reproductive individuals then

$$Hx(t_0) = 0 \neq c {v_1}^{\wedge}, \tag{2.5.60}$$

since individuals in the post reproductive age class do not reproduce, causing the entire population to go extinct after one unit time.

2.5.2 Existence and stability of equilibria

In general, the asymptotic dynamics of linear population models and stability of equilibria are determined by the dominant eigenvalue of the Leslie matrix; however, formulas for the dominant

eigenvalue are not readily available for higher dimensional systems. The alternate method used with Leslie matrices involves the calculation of the net reproductive value *r* and can be applied to matrices of arbitrary dimension. In biological terms, the net reproductive value can be interpreted as the expected number of offspring per individual over its lifetime. Given a Leslie matrix of the form defined in equations (2.4.23) to (2.4.25), the net reproductive value is defined as

$$r = \sum_{i=1}^{\tau+\omega} f_i \prod_{j=0}^{i} p_j > 0 \tag{2.5.61}$$

where, for notational convenience, $p_0 = 1$ (Cushing and Yicang 1994). Substituting model parameter values for f_i and p_j the net reproductive value for our model is

$$r = \beta e^{-\mu_l \tau}\left(e^{-\mu_m} + e^{-2\mu_m} + \cdots + e^{-(\omega-1)\mu_m}\right) \tag{2.5.62}$$

Having a formula for the net reproductive value in terms of parameters that comprise the matrices F and T allows us to study how the net reproductive value is affected by changes in any of these parameters, particularly temperature.

The following lemma defines the relationship between the net reproductive value r and the asymptotic dynamics of the system (2.4.20) under the conditions of (2.4.23) to (2.4.25) (Cushing and Yicang 1994).

LEMMA 1. *For any initial distribution consisting of reproductive individuals such that* $x(t_0) > 0$:

(i) $\quad r < 1 \;\; implies \;\; \lim_{t\to\infty} x_i(t) = 0 \qquad \forall\, i = [1,\ (\tau + \omega - 1)]$

(ii) $\quad r > 1 \;\; implies \;\; \lim_{t\to\infty} x_i(t) = +\infty \quad \forall\, i = [1,\ (\tau + \omega - 1)].$

The biological interpretation of Lemma 1 for $r < 1$ means that individual mosquitoes are unable to fully replace themselves over the course of their lifetime and will eventually become extinct. The case when $r > 1$, implies the mosquito population will continue to grow unbounded with time.

The following theorem defines an explicit relationship between the net reproductive value and the dominant eigenvalue of general structured population models which also applies to the more specific age-structured population model we use in this study (Cushing and Yicang 1994).

THEOREM 2. *If an* $n \times n$ *Leslie matrix* A (2.4.25) *is primitive, where* F *and* P *satisfy* (2.4.23) *and* (2.4.24), *respectively, then*

(i) $\lambda_1 < 1$ *if and only if* $r < 1$,

(ii) $\lambda_1 > 1$ *if and only if* $r > 1$,

(iii) $\lambda_1 = 1$ *if and only if* $r = 1$.

Stability of the trivial equilibrium is determined by the dominant eigenvalue, denoted λ_1, of the projection matrix A; however, as previously mentioned, in age-structured population models the net reproductive value is a more practical method to determine the stability of the trivial equilibrium. Under the conditions of Theorem 2, the trivial solution $x = 0$ of (2.4.20) is exponentially asymptotically stable if $r < 1$ and unstable when $r > 1$. When $r = \lambda_1 = 1$, then non-trivial equilibria exist. The critical value of $r = 1$ represents a bifurcation when a branch of non-trivial equilibria intersects with the trivial equilibrium solution $x = 0$. At this bifurcation value, the asymptotic dynamics of the system changes from eventual extinction to unbounded population growth.

To find temperatures such that positive equilibria exist, we know that net reproductive value must equal $r = 1$. From equation (2.5.35) we have

$$1 = \beta e^{-\mu_l \tau}\left(e^{-\mu_m} + e^{-2\mu_m} + \cdots + e^{-(\omega-1)\mu_m}\right). \tag{2.5.63}$$

Solving for the temperature-dependent terms, μ_l and τ, then rearranging the equation yields

$$e^{-\mu_l \tau} = \frac{1}{\beta(e^{-\mu_m} + e^{-2\mu_m} + \cdots + e^{-(\omega-1)\mu_m})} \tag{2.5.64}$$

$$\mu_l \tau = \ln\left(\beta\left(e^{-\mu_m} + e^{-2\mu_m} + \cdots + e^{-(\omega-1)\mu_m}\right)\right). \tag{2.5.65}$$

From (2.5.63), we observe that if the oviposition rate

$$\beta \leq \frac{1}{(e^{-\mu_m} + e^{-2\mu_m} + \cdots + e^{-(\omega-1)\mu_m})}, \tag{2.5.66}$$

then no equilibrium solutions can exist, since the term $\mu_l \tau$ on the left-hand side of (2.5.65) is always positive. For oviposition rates above this value, equilibrium solutions exist for temperatures that satisfy (2.5.63). Substituting the functions $\tau = \left\lceil \frac{TDD_e}{T - T_e} \right\rceil$ and μ_l into (2.5.65) we have

$$\left[x\left(T - T_{op}\right)^2 + \mu_{op}\right]\left\lceil \frac{TDD_e}{T - T_e} \right\rceil = \ln\left(\beta\left(e^{-\mu_m} + e^{-2\mu_m} + \cdots + e^{-(\omega-1)\mu_m}\right)\right), \tag{2.5.67}$$

where, x takes the value of parameters j or q if the temperature is below or above $T_e = 25°C$, respectively. Since the development time τ is a temperature-dependent step function that contains discontinuities and the aquatic mortality rate μ_l is defined by a temperature-dependent piecewise function, solving (2.5.65) explicitly for temperature becomes tedious; however, we can simplify the calculation by removing the ceiling function from the term $\left\lceil \frac{TDD_e}{T - T_e} \right\rceil$ and then solving the resulting

equation for temperature T, accounting for the error ε introduced by removing the ceiling function. For simplicity, we set the right-hand side of (2.5.67) to a constant K.

$$K = \ln\left(\beta\left(e^{-\mu_m} + e^{-2\mu_m} + \cdots + e^{-(\omega-1)\mu_m}\right)\right) \tag{2.5.68}$$

$$\left[x\left(T - T_{op}\right)^2 + \mu_{op}\right]\left(\frac{TDD_e}{T - T_e}\right) = K. \tag{2.5.69}$$

After some algebra, we get a quadratic equation in terms of temperature T:

$$x\, TDD_e T^2 - \left(K + 2xT_{op}\, TDD_e\right)T + \, TDD_e\left(x{T_{op}}^2 + \mu_{op}\right) + KT_e = 0. \tag{2.5.70}$$

Solving for the roots of the quadratic equation in (2.5.70), we arrive at

$$T = T_{op} + \frac{K \pm \sqrt{K^2 + 4x(\, TDD_e(T_{op} - T_e)K - \mu_{op}\, {TDD_e}^2)}}{2x\, TDD_e}. \tag{2.5.71}$$

Thus, the two positive equilibrium temperature solutions are:

$$T_1 = T_{op} + \frac{K - \sqrt{K^2 + 4j\, TDD_e(T_{op} - T_e)K - 4j\mu_{op}\, {TDD_e}^2}}{2j\, TDD_e} + \varepsilon, \qquad T < 25, \tag{2.5.72}$$

$$T_2 = T_{op} + \frac{K + \sqrt{K^2 + 4q\, TDD_e(T_{op} - T_e)K - 4q\mu_{op}\, {TDD_e}^2}}{2q\, TDD_e} + \varepsilon, \qquad T \geq 25, \tag{2.5.73}$$

where ε denotes the error due to the ceiling function in (2.3.15).

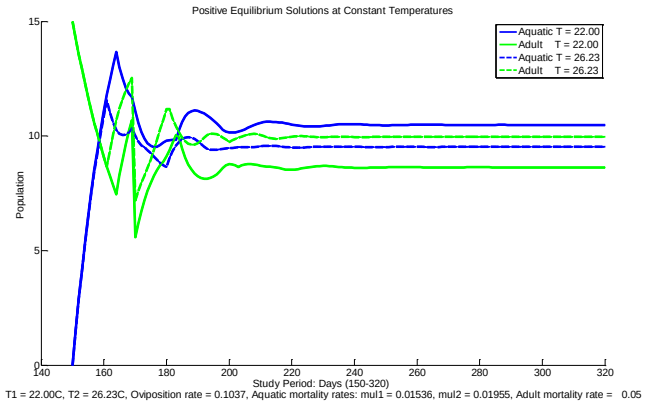

Figure 2.7**:** Model simulations where the net reproductive value is $r = 1$ at two temperatures $T_1 = 22°C$ (solid lines) and $T_2 = 26.23°C$ (dashed lines) for aquatic (blue) and adult (green) mosquitoes.

Numerical methods, such as the Chebfun function in Matlab 9.2.0 (R2017a), can easily find the solutions of (2.5.65). The critical temperatures T_1 and T_2 are bifurcation values in the sense that when temperature passes through one of these critical temperature values there is a drastic change in the population's asymptotic dynamics from unbounded growth to extinction, corresponding to $r > 1$ and $r < 1$, respectively. When the temperature is equal to T_1 or T_2, a family of non-trivial positive equilibrium solutions bifurcates from the trivial equilibrium $x = 0$ as depicted in Figure 2.7. After the initial transient state, both aquatic and adult populations remain constant with time for each temperature. The age class distribution vectors for both simulations were verified (not shown) to be consistent with (2.5.47).

2.6 Numerical simulations

Gaining a better understanding of how mosquito population dynamics are driven by environmental factors plays a key role in the study of vector-borne diseases. The results from numerical simulations in the following sections may help to elucidate this relationship under certain temperature scenarios and thereby allow us to better explain the variability observed in mosquito

populations. The model was designed so that temperature is the primary driving force behind mosquito population dynamics. Simulations are based on specified temperature scenarios and observed temperature data as model input. As constructed, the model is deterministic, and there is no stochasticity in model output.

To study the underlying cause behind certain population dynamics observed in surveillance data (low/high mortality and population spikes), we test the model under controlled temperature scenarios. In the first scenario (Figure 2.8), we illustrate the effect of diapause on mosquito populations. Next, we run the model at three constant temperatures to see how prolonged exposure to temperatures near the lower and upper temperature thresholds affect the mosquito population compared with the model when run at the optimal temperature for development $T_{op} = 25°C$ (Figure 2.9). Then we illustrate how observed surveillance data often exhibits sharp increases in trap counts from one week to the next. We present one possible temperature pattern that replicates this type of behavior (Figure 2.10). Finally, we apply the model to the Peel Region in Southern Ontario using observed temperature data for years 2004–2016 (Figure 2.11). Each run consisted of simulated immature and adult mosquito populations over a single-season. Since quantitative data for the total population of mosquitoes is unobtainable, model performance was assessed based on the correlation between simulation results and mosquito surveillance data for the Peel Region, Southern Ontario. Simulations were run on Matlab R2017a (9.2.0.538062).

2.6.1 Temperature scenarios

The effect of Diapause

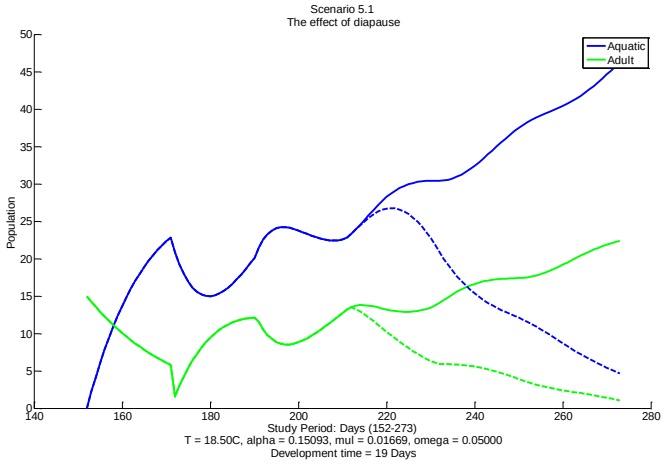

Figure 2.8: Time series from a 120-day run of the model with (dashed lines) and without (solid lines) the effect of diapause at a constant temperature of $T = 18.5°C$.

The results illustrated in Figure 2.8 show the effect of diapause on the mosquito population which begins in the middle of the season. When the effect of diapause is ignored, the model does not capture the decline in the adult mosquito population typically observed in nature between the middle and end of the season. This is due to the induction of diapause caused by a decrease in photoperiod experienced by mosquitoes in the last stages of aquatic development. Although a temperature of 18.5°C is conducive for an increasing mosquito population during the first part of the season, once the effect of diapause is introduced (dashed line) only a proportion of mosquitoes will continue their gonotropic cycle of host seeking and reproduction upon eclosion. Day 212, which corresponded to the first day photoperiod falls below 14.75 hours of daylight, is when we begin to observe the divergence of adult mosquito populations due to the effect of diapause. Since temperature is held constant, the incidence of non-diapausing mosquitoes is determined by the photoperiod. As time progresses, the number of daylight hours continues to decrease and thus the

proportion of non-diapausing mosquitoes upon eclosion also decreases in a linear fashion. Some existing models that ignore the effect of diapause tend to observe peaks towards the end of the mosquito season and attribute this behavior primarily to the exclusion of diapause, among other factors, from their models (Shaman et al. 2006, Gong and DeGaetano 2010).

Temperature-dependent development and mortality

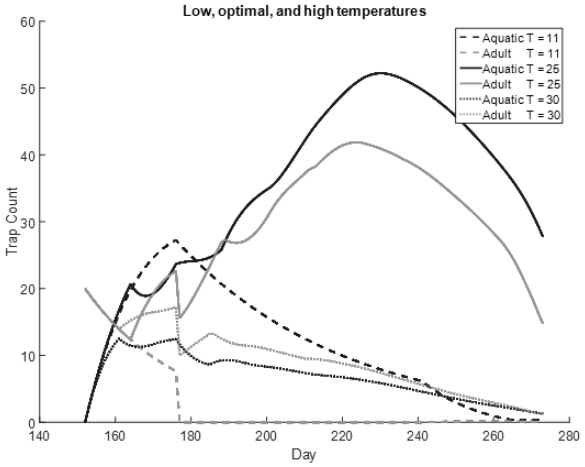

Figure 2.9: Time series from a 120-day run of the model at constant temperatures of *T*=11°C, *T*=25°C, and *T*=30°C.

Development and mortality rates of aquatic stage mosquitoes are dependent upon the temperature experienced during the aquatic stage. As previously mentioned, lower temperatures act more as an inhibitor to development and do not significantly affect mortality while temperatures near the upper temperature threshold cause a higher rate of mortality offsetting a higher rate of development. Figure 2.9 depicts simulation results of the model run at three constant temperatures: 11°C, 25°C, and 30°C. For simulation runs at low and high temperatures of 11°C and 30°C, the model performs as expected. At $T = 11$°C, cohorts in the aquatic stage (black dashed lines) are unable to accumulate enough DDs to complete development before the end of the simulation. Consequently, the adult population steadily declines towards extinction after the initial

transient period (grey dashed lines). At $T = 30°C$, a considerably shorter development time of 9 days is offset by a higher mortality rate for developing mosquitoes. Thus, both aquatic (black dotted lines) and adult populations (grey dotted lines) gradually decline until the end of the season. At the optimal temperature of development ($T = 25°C$), the mosquito population achieves a maximum on day 230 (mid-August), after which the population begins to decline due to the effect of diapause.

Peaks in the mosquito population

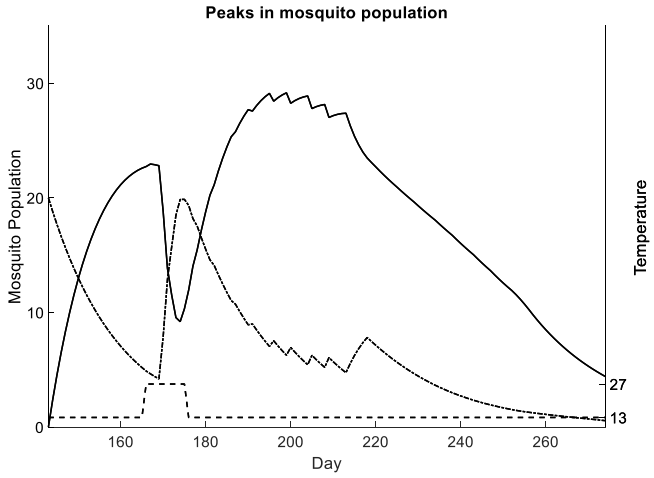

Figure 2.10: Temperature pattern (dashed line, right axis) causing a peak in the adult mosquito population (dot-dashed line, left axis). Aquatic population depicted by the solid line on the left axis.

While a variety of weather conditions may cause these sudden increases in the mosquito population, we present one plausible scenario that demonstrates how certain temperature patterns can produce a sudden increase in the mosquito population (Figure 2.10). In this scenario, a period of cooler daily temperatures followed by a sudden and significant rise in temperature for several days causes multiple cohorts of larvae to eclose in rapid succession over a short period of time. Cohorts oviposited during the cooler period prior to the sudden rise in temperature accumulate

small amounts of DDs each day. A sudden rise in temperature lasting for several days essentially synchronizes the time of eclosion of multiple cohorts that were oviposited during the period of cooler temperatures, causing a sharp increase in the mosquito population on day 176.

2.6.2 Observed temperatures

Due to a lack of data on the overwintering process and number of mosquitoes that emerge in the beginning of each mosquito season, initial conditions for the start date and number of adult female mosquitoes for each year had to be estimated. Shelton (1973) studied the temperature-dependent development of eight species of mosquitoes. He found the lower threshold temperature for eclosion from pupa to adult occurred between temperatures of 12–15°C. We assume that a seven-day average daily temperature above 14°C is sufficient to break hibernation and initiate the gonotrophic cycle of overwintering adult female mosquitoes. Based on these criteria the start times for simulations began as early as Day 112 (first week of May) to Day 150 (last week of May). All simulations were ended on Day 274 (approximately September 30th) corresponding with the disappearance of mosquitoes in the study area. Once the start date was determined, initial values for adult mosquitoes were then estimated by running simulations for a given year with an initial value of $N_{m,t_0}(t_0) = 1$ starting on the day determined in the previous step. The initial number of mosquitoes was then incremented by 1 and the simulation was repeated. For each simulation, the root mean squared error (RMSE) of simulation vs observed trap counts for the first three weeks was recorded. The initial value was then selected from the simulation run that yielded the lowest RMSE for the first 3 weeks of the study period.

Model simulations were run separately for each year from 2004–2016 (Figure 2.11) using observed temperature data obtained from the Pearson International Airport located in the Peel

Region. Since quantitative data for the total population of mosquitoes is unobtainable, model performance was assessed based on the correlation between model outputs and mosquito surveillance data for the Peel Region, Southern Ontario.

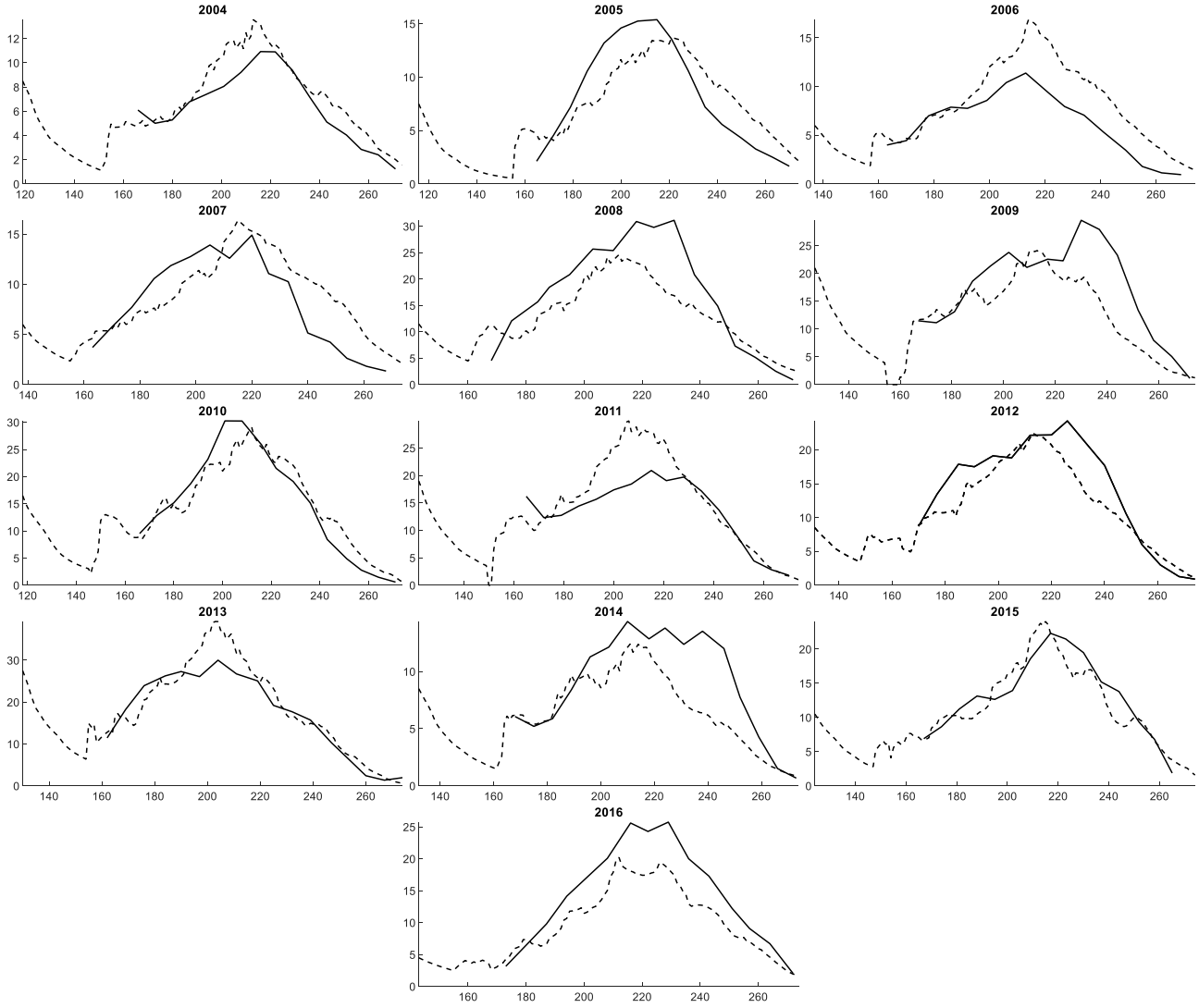

Figure 2.11: Comparison of simulated mosquito abundance (dashed line) and trap data (solid line) for years 2004–2016.

The model adequately simulated the observed trend in the mosquito trap counts and the timing of population peaks for most years except for 2008, 2009, and 2014 were the model underestimated

the observed trap counts. The model overestimated trap counts in 2011 and 2013. As previously mentioned, the differences between model output and observed data may be due to the skewness in the surveillance data caused by a small number of traps capturing a disproportionately large number of mosquitoes relative to other traps in the area during certain weeks. To determine the cause of the disparity in capture amounts among traps requires further investigation and is planned for future modelling initiatives.

Model performance during these years may also be due to factors other than temperature—such as precipitation, landscape, and wind, that may have a strong influence on mosquito population dynamics and capture rates. For example, in 2008 there was above-average rainfall during the mosquito season, while the daily temperatures remained within the seasonal averages. The abundance of rainfall during this year would have provided an ample number of breeding sites for mosquitoes, which is likely the cause of the model's underestimation of trap counts for this year. The study by Wang et al. (2011) demonstrated a correlation of mosquito abundance and the previous 35 days of precipitation.

2.7 Discussion

We developed a temperature-driven model of mosquito population dynamics to track the stages and processes in the mosquito life cycle most influenced by temperature. Our model simulates mosquito surveillance data for a single-season and was applied to the Peel Region of Southern Ontario. Although the model was applied to a specific species in a certain geographical area, the structure of the model allows it to be adapted to other species of mosquitoes, since the biological processes across different mosquito species are similar. Tuning the model would only require that

parameter values and temperature-dependent response functions be adapted to fit the species being studied.

The model divides the mosquito life cycle into two separate and distinct compartments where all aquatic stages of development are grouped together in one compartment and the adult stage in another. In this way, the amount of accumulated temperature required to complete each stage of aquatic development from egg to pupa is untraceable. However, treating each stage as a separate compartment may provide improved model performance since each stage may have varying responses to temperature.

The use of a degree-day function to track the physiological development of aquatic mosquitoes is of primary importance, as it enables the model to capture important dynamics such as sudden increases in the mosquito population due to certain temperature patterns. Moreover, modelling development using degree-days allows for the addition of a mosquito control feature in the model to reduce the population of developing mosquitoes at specified times, which would allow for the study of mosquito control effectiveness on population dynamics. This could be a useful tool in determining the effectiveness and timing of mosquito control measures.

Our simulation results suggest that under certain environment conditions the mosquito population can be adequately predicted using temperature alone. However, the inability of the model to capture the observed dynamics of surveillance data in certain years indicates that additional variables need to be considered to account for the year to year variability in weather and other environmental factors. Since our model is focused solely on the effect of temperature on mosquito abundance, consideration of other factors such as precipitation and land use (spatial) may improve model performance and will be included in future work. Availability of more data on mosquito biology and its response to environmental factors would also improve accuracy.

Currently, the model is limited to forecasting mosquito abundance over a single-season. Extending the study to include a model describing the overwintering process would enable simulations to be run over multiple years with one set of initial conditions for the first year. Then, using short-term and long-term temperature forecasts as input in to the model, we could potentially forecast mosquito abundance for future years based on a range of climate projections.

3 Impact of temperature on the transmission dynamics of West Nile virus

3.1 Introduction

The objectives of this study were to 1) gain a better understanding of how mosquito biology and WNV transmission is influenced by temperature in order to develop reliable predictive models to forecast mosquito population abundance and WNV infection in the Peel Region, Southern Ontario, 2) identify and assess the temperature-dependent mechanisms involved in WNV transmission dynamics. To accomplish our objectives, we began by adapting our previously developed temperature-driven mosquito abundance model (Sec. 3.2.1) to work in tandem with the model for WNV transmission between mosquitoes and birds that we develop in this study (Sec. 3.2.3). In the transmission model, we employ the use of a degree-day (DD) function (Sec. 3.2.2) to track the progression of asymptomatic mosquitoes through the EIP. Then, under simplifying assumptions (Sec. 3.4), we study the existence and stability of equilibria and formulate an expression for the basic reproduction number (Sec. 3.5). In development of our model, we aimed to capture the within-season dynamics as well as the year-to-year variability in the reported number of mosquitoes testing positive for WNV. Moreover, we aimed to capture certain phenomena observed in surveillance data that were not captured in existing studies on the same region thereby allowing us to qualitatively assess the conditions that cause these phenomena based on simulation results (Sec. 3.6).

3.2 Model formulation (non-autonomous)

The model is constructed to track the temporal dynamics of adult female mosquitoes (vectors) and birds (reservoirs) over a single-season (spring to autumn). Since the model covers a relatively short period of several months, we only consider the vital dynamics for mosquitoes (Wonham et al. 2004). We ignore the vital dynamics of birds, since they are assumed to have offspring once per year during the spring and have an average lifespan of several years. Cross-infection between mosquitoes and birds is modeled with difference equations. Although there is more than one species of birds that are involved in the disease transmission cycle, we consider all birds as one family for simplicity (Fan et al. 2010). The bird population is categorized into susceptible S_b, infected I_b, recovered R_b, and dead D_b birds. The total living bird population calculate at time step t (day) is

$$N_b(t) = S_b(t) + I_b(t) + R_b(t). \tag{3.2.1}$$

The mosquito population is separated into two distinct stages: aquatic (eggs, larvae, and pupae), hereafter referred to as larva; and adults. As was done in our temperature-driven abundance model, mosquitoes are grouped into cohorts based on the day of their oviposition and are tracked throughout their lifetime from larva to adult. We consider five compartments representing susceptible larva $S_{l,k}$, infected larva $I_{l,k}$, susceptible adults $S_{m,k}$, asymptomatically infected adults $A_{m,k}$, and infected adults $I_{m,k}$, where the subscript k represents the day of oviposition and is used to track distinct cohorts. The total living population for a cohort k in the aquatic and adult stage, respectively, is given by

$$N_{l,k}(t) = S_{l,k}(t) + I_{l,k}(t) \quad and \quad N_{m,k}(t) = S_{m,k}(t) + A_{m,k}(t) + I_{m,k}(t) \tag{3.2.2}$$

The total living aquatic mosquito population across all cohorts is given by

$$N_l(t) = \sum_{k=t_0}^{t} \left[S_{l,k}(t) + I_{l,k}(t)\right]. \tag{3.2.3}$$

The total living adult mosquito population across all cohorts is given by

$$N_m(t) = \sum_{k=t_0}^{t} \left[S_{m,k}(t) + A_{m,k}(t) + I_{m,k}(t)\right], \tag{3.2.4}$$

where t_0 is the is first day of the mosquito season and is determined by temperature.

For this study, we assume mortality occurs at the beginning of each time step while birth, transfer between compartments, and infection occur at the end of each time step. A model diagram describing the mosquito bird interaction is depicted in Figure 3.1.

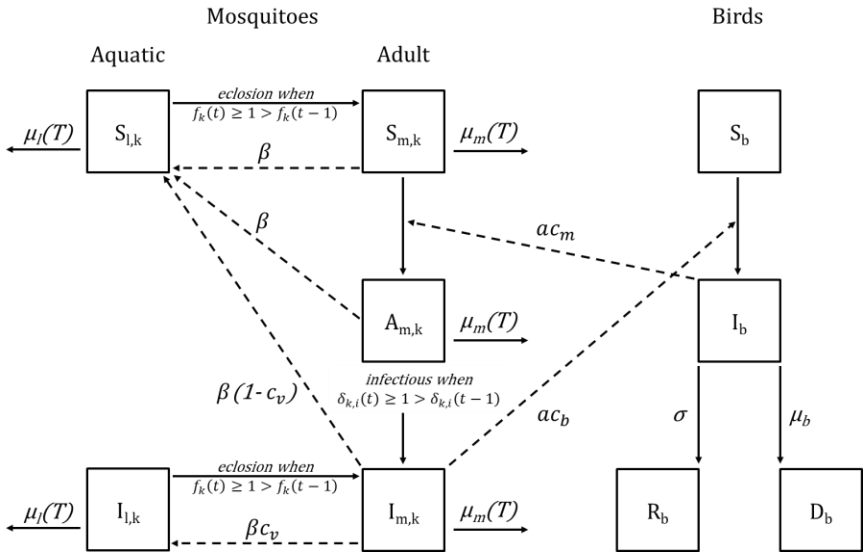

Figure 3.1: Model diagram of WNV transmission cycle between mosquitoes and birds. Parameter values and functions are given in Tables 1 and 2, respectively.

Model parameters and functions were based on the most relevant data from available literature. Definition, value, and dimension of model parameters and variables are given in Tables 1 and 2, respectively.

3.2.1 Extended mosquito abundance model

In the previous chapter, a temperature-driven mosquito abundance model was developed. In this chapter, we adapt the model equations for aquatic and adult stage mosquitoes of the abundance model to describe the susceptible, asymptomatic, and infected classes in the disease transmission cycle defined in equations (3.2.2) through (3.2.4). In this section, we give a description of the adaptations made to the abundance model to include the transmission cycle between mosquitoes and birds. Functions for aquatic development, mortality, and proportion of non-diapausing adult female mosquitoes used in the transmission model are the same as defined in Section 2.2 and are not restated here. Description of parameters and functions stated in this section can be found in Tables 1 and 2, respectively.

The adapted abundance model is composed of a system of multiple paired ODEs, calculated at discrete time steps (day), to track cohort populations throughout their lifetime in both the aquatic and adult stages. The ODE system for each cohort consists of five equations: two for susceptible and infected larva, and three for susceptible, asymptomatic, and infected adults. The instantaneous rate of survival for both aquatic and adult populations is modelled with an exponential function after Shaman et al. (2006). Survival of susceptible aquatic populations $S_{l,k}\ (t)$ at time $t > k > t_0$ is given by

$$\frac{dS_{l,k}(s)}{ds} = -\mu_l\big(T_l(t)\big)S_{l,k}(s) \qquad 0 \le f_k(t) < 1 \; and \; t+1 > s > t\,. \tag{3.2.5}$$

where the solution of (3.2.5) at time $t > k$ is $S_{l,k}(t) = S_{l,k}(k)e^{-\sum_{n=k+1}^{t}\mu_l(T_l(n))}$. The equation for infected larva $\frac{dI_{l,k}(t)}{dt}$ is defined in the same way. The susceptible adult mosquito population is given by

$$\frac{dS_{m,k}(s)}{ds} = -\mu_m\big(T(t)\big)S_{m,k}(s) \qquad f_k(t) > 1 \; and \; t+1 > s \ge t, \tag{3.2.6}$$

and similarly, for asymptomatic $\frac{dA_{m,k}(t)}{ds}$ and infected $\frac{dI_{m,k}(t)}{ds}$ adult mosquitoes. The functions $\mu_l\big(T_l(t)\big)$ and $\mu_m\big(T(t)\big)$ are the temperature-dependent mortality rates (day^{-1}) for aquatic and adult mosquitoes, respectively.

In the transmission model, we assume mortality, infection, and transfer between compartments occur at the beginning of each time step. Oviposition is assumed to occur at the end of each time step. Thus, on the day a cohort of adult mosquitoes reaches their maximum lifespan of ω days after eclosion, they die before they can reproduce.

Oviposition:

Vertical transmission in mosquitoes plays an important role in the persistence of WNV in regions that experience harsh winter climates (Swayne et al. 2000, Komar et al. 2003). We assumed that infectious females lay eggs that are infected with probability c_v. The total number of eggs oviposited on day t equals the total number of adults that are at least one day old since eclosion multiplied by the oviposition rate β. Adults that reach their maximum lifespan on that day die before oviposition. The number of susceptible and infected eggs oviposited on day t is given by

$$S_{l,k=t}(t) = \beta \sum_{k=t_0}^{t-2} \left[S_{m,k}(t) + A_{m,k}(t) + (1 - c_v) I_{m,k}(t) \right] \tag{3.2.7}$$

$$I_{l,k=t}(t) = \beta c_v \sum_{k=t_0}^{t-2} I_{m,k}(t). \tag{3.2.8}$$

Eclosion:

When a cohort accumulates enough DDs to complete development i.e., $f_k(t) \geq 1 > f_k(t-1)$, all individuals in the cohort will eclose into adults where a proportion of the new adult mosquitoes will enter diapause and the remaining individuals will enter the susceptible or infected classes of adult mosquitoes:

$$S_{l,k}(t) = I_{l,k}(t) = 0 \qquad if\ t < k\ or\ f_k(t) \geq 1 > f_k(t-1), \tag{3.2.9}$$

$$S_{m,k}(t) = S_{l,k}(t-1) e^{-\mu_l(T_l(t))} \gamma_k(T_k, P_k), \quad if\ f_k(t) \geq 1 > f_k(t-1) \tag{3.2.10}$$

$$I_{m,k}(t) = I_{l,k}(t-1) e^{-\mu_l(T_l(t))} \gamma_k(T_k, P_k), \quad if\ f_k(t) \geq 1 > f_k(t-1). \tag{3.2.11}$$

Adult Lifespan:

The maximum lifespan of an adult mosquito is ω days after eclosion:

$$S_{m,k}(t) = A_{m,k,i}(t) = I_{m,k}(t) = 0, \qquad if\ \ t = k + \tau_k + \omega, \tag{3.2.12}$$

where τ_k is the total number of days to complete development for a cohort born on day k.

Asymptomatic Infection:

The asymptomatic class of mosquitoes is divided into $\omega - 1$ subpopulations. Each subpopulation is identified by the subscript index i, which represents the day of asymptomatic infection. Each asymptomatically infected subpopulation is initiated when a susceptible mosquito contracts the virus after biting and infected bird.

$$A_{m,k,i=t}(t) = e^{-\mu_m(T(t-1))}\left(1-(1-c_m)^{\frac{a(1-\sigma-\mu_b)I_b(t-1)}{N_b(t-1)-\mu_b I_b(t-1)}}\right)S_{m,k}(t-1), \quad if\ t = t_k+1, t_k+2, \dots, t_k+\omega-1. \tag{3.2.13}$$

3.2.2 Transition rate from asymptomatic to infected class and EIP

The EIP has been reported in mosquitoes but not birds (Langevin et al. 2001, Turell et al. 2001). Thus, we only consider the EIP for mosquitoes and assume birds are immediately infectious once exposed to the virus. In compartmental models, the asymptomatic (or exposed) compartment is associated with the delay in virus transmission caused by the EIP. In a similar way as was done for mosquito development, we model the effect of the EIP with a linear degree-day function. Results from the study by Reisen et al. (2006) for the NY99 strain of WNV were used to estimate the minimum threshold temperature T_a, below which no thermal units are accumulated towards the completion of the EIP and the total DDs required to complete the EIP, denoted T_{DDa}. In their study, infected mosquitoes were reared at constant temperatures and then tested to determine the EIP associated with each temperature. The results were plotted as a function of temperature, and a linear relationship between temperature and the transition rate is clearly distinguishable (Figure 3.2).

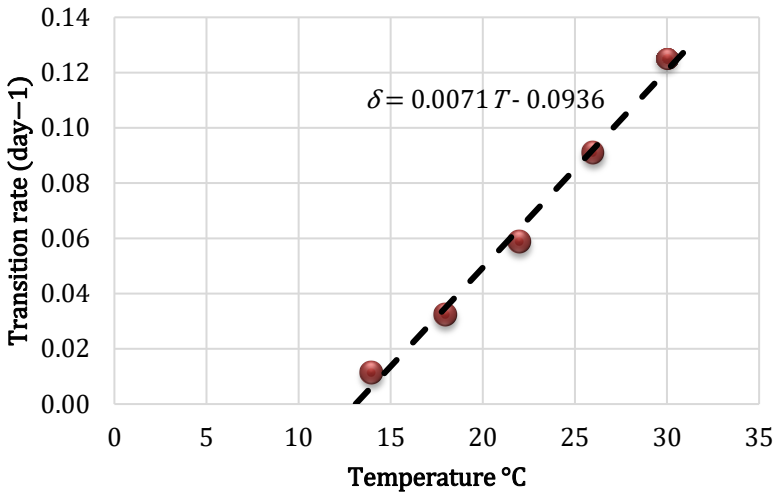

Figure 3.2: Transition rate as a function of temperature for NY99 strain of WNV (circles) (Reisen et al. 2006). Linear regression (dashed line) through data points estimated $T_a = 14$°C and $T_{DDa} = 139$°C.

A linear regression through the data points estimates the minimum temperature threshold and total degree-days to complete the virus incubation period as $T_a = 14$°C and $T_{DDa} = 139$°C, respectively. This estimate falls in line with similar values reported in existing studies (Goddard et al. 2003, Hartley et al. 2012, Brown 2015) for *Cx. pipiens*. The calculation for degree-days for the EIP is

$$DD_a(t) = \begin{cases} 0, & if\ T(t) \le T_a, \\ T(t) - T_a, & if\ T(t) > T_a, \end{cases} \tag{3.2.14}$$

and the daily proportion of accumulated T_{DDa} is

$$d\delta_{k,i}(t) = \frac{\max(0, T(t) - T_a)}{T_{DDa}} = \frac{DD_a(t)}{T_{DDa}}, \qquad i = t_k + 1, t_k + 2, \dots, t_k + \omega, \tag{3.2.15}$$

where the subscript i indicates the day a mosquito is exposed to the virus. The cumulative proportion of the EIP is tracked with the function

$$\delta_{k,i}(t) = \sum_{n=i}^{t} d\delta_{k,i}(n). \tag{3.2.16}$$

Once an asymptomatic mosquito accumulates enough degree-days to complete the EIP (i.e., when $\delta_{k,i}(t) \geq 1 > \delta_{k,i}(t-1)$), it will move to the infectious compartment for the cohort oviposited on day k.

3.2.3 Mosquito equations

In this section, we formulate equations describing the disease transmission dynamics between mosquitoes and birds based on the modelling assumptions in the previous sections. A susceptible aquatic cohort is initiated when adult mosquitoes, that are at least two days from reaching their maximum lifespan, lay eggs at rate β (by susceptible and asymptomatic adults) and $\beta(1-c_v)$ (by infected adults), where c_v is the probability of vertical infection from an infected mosquito. In a similar way, an infected aquatic cohort is initiated when infected adult mosquitoes lay eggs at rate βc_v. The equations for oviposition are given by (3.2.7) and (3.2.8). Aquatic populations are decreased by eclosion (3.2.9) to (3.2.11) and by natural death. The number of susceptible and infected mosquitoes surviving to the next time step $t+1$ is $S_{l,k}(t)e^{-\mu_l(T_l(t))}$ and $I_{l,k}(t)e^{-\mu_l(T_l(t))}$, respectively.

The susceptible adult mosquito population is increased when a cohort of immature mosquitoes in the aquatic stage accumulate enough DDs to complete development where a proportion $\gamma_k(T_k, P_k)$ of eclosing mosquitoes will become active host-seeking adults. Following the method of Lewis et al. (2006), the equation for susceptible adult mosquito cohorts $S_{m,k}(t+1)$ is derived as follows. The expected number of times a susceptible adult mosquito bites some infected bird in

one time step is $\frac{a(1-\sigma-\mu_b)I_b(t)}{N_b(t)-\mu_b I_b(t)}$. The probability a mosquito becomes infected after biting an infected bird is c_m, and the probability of avoiding infection is $(1-c_m)$. Hence, the probability of a susceptible adult mosquito avoiding infection in a single time step is $(1-c_m)^{\frac{a(1-\sigma-\mu_b)I_b(t)}{N_b(t)-\mu_b I_b(t)}}$. This term is commonly referred to as the force of infection; i.e., the per capita rate at which susceptible individuals become infected. The remaining number of susceptible mosquitoes in a cohort after a single time step is $e^{-\mu_m(T(t))}(1-c_m)^{\frac{a(1-\sigma-\mu_b)I_b(t)}{N_b(t)-\mu_b I_b(t)}}S_{m,k}(t)$, where $e^{-\mu_m(T(t))}$ is the proportion of mosquitoes that survive to the next time step. The asymptomatically infected mosquito population is increased when the virus is transmitted from an infected bird to a susceptible mosquito and is decreased by natural death and when they become infectious after completion of the EIP. The other equations for mosquitoes are derived using a similar approach. We assume infected mosquitoes do not recover from WNV infection and do not experience an increase in mortality caused by infection (Wonham et al. 2004). It is also assumed there is no horizontal transmission of the virus while in the aquatic stage of development (Turell et al. 2001).

Based on the assumptions of mosquito biology and vector-host interaction just described, the equations for mosquitoes are given by the following set of discrete-time equations for each cohort k where $t > k$:

$$S_{l,k}(t+1) = \left[S_{l,k}(t)e^{-\mu_l(T_l(t))}\right]H\left(1-f_k(t)\right) \tag{3.2.17}$$

$$I_{l,k}(t+1) = \left[I_{l,k}(t)e^{-\mu_l(T_l(t))}\right]H\left(1-f_k(t)\right) \tag{3.2.18}$$

$$S_{m,k}(t+1) = \left(\gamma_k(T_k, P_k) e^{-\mu_l(T_l(t))} S_{l,k}(t) + e^{-\mu_m(T)} (1 - c_m)^{\frac{a(1-\sigma-\mu_b) I_b(t)}{N_b(t) - \mu_b I_b(t)}} S_{m,k}(t) \right) \times \left(1 - H\left(1 - f_k(t)\right)\right) H\left(g_k(t)\right) \quad (3.2.19)$$

$$A_{m,k,i}(t+1) = e^{-\mu_m(T(t))} A_{m,k,i}(t) \left(1 - H\left(1 - f_k(t)\right)\right) H\left(g_k(t)\right) H\left(1 - \delta_{k,i}(t)\right), \quad (3.2.20)$$

$$where \;\; i = t_k + 1, t_k + 2, \ldots, t_k + \omega - 1$$

$$I_{m,k}(t+1) =$$

$$\left(\gamma_k(T_k, P_k) e^{-\mu_l(T_l(t))} I_{l,k}(t) + \left(I_{m,k}(t) + \sum_{i=t_k+1}^{t_k+\omega-1} \left(A_{m,k,i}(t) \left(1 - H\left(1 - \delta_{k,i}(t)\right)\right)\right)\right) e^{-\mu_m(T(t))} \right)$$

$$\times \left(1 - H\left(1 - f_k(t)\right)\right) H\left(g_k(t)\right). \quad (3.2.21)$$

where the asymptomatic class of mosquitoes $A_{m,k,i}(t)$ tracks ω distinct subpopulations of mosquitoes in cohort k that are exposed on day i after eclosion until reaching their maximum lifespan of ω days. $H(x)$ is the Heaviside function

$$H(x) = \begin{cases} 0, & x \leq 0 \\ 1, & x > 0. \end{cases} \quad (3.2.22)$$

The arguments $f_k(t) = \sum_{n=k}^{t} df_k(n)$, $\delta_{k,i}(t) = \sum_{n=i}^{t} d\delta_{k,i}(n)$ and $g_k(t) = k + \tau_k + \omega - t - 1$ are used to track the age or progression of aquatic, asymptomatic, and adult populations through their respective compartments.

3.2.4 Bird equations

The total bird population is assumed to be constant; i.e., no replenishment of the bird population via births since birds will mate and rear their offspring once a year during the spring. Since corvids have an average lifespan of 7–8 years depending on the species (Connecticut Department of Environmental Protection 2001), we assume birds do not die of natural causes during the study period. We also assume no migration of birds from other regions into the study area. In this study, we consider the horizontal transmission of the virus among birds to be negligible (Langevin et al. 2001). Infection from mosquitoes to birds was derived in the same way as was done for mosquitoes in Section 3.2.3. The probability of a susceptible bird avoiding infection in a one time step is $(1-c_b)^{\frac{ae^{-\mu_m(T(t))}\sum_{k=t_0}^{t-2} I_{m,k}(t)}{N_b(t)-\mu_b I_b(t)}}$ and the remaining number of susceptible birds after a single time step is $(1-c_b)^{\frac{ae^{-\mu_m(T(t))}\sum_{k=t_0}^{t-2} I_{m,k}(t)}{N_b(t)-\mu_b I_b(t)}} S_b(t)$. We note that mosquitoes reaching their maximum lifespan at each time step will die before being able to infect any birds. Thus, only mosquitoes that have at least two days to live at time t can transmit the virus to birds at time $t+1$. The infected bird population is increased by number of susceptible birds that become infected from the bite of infected mosquitoes and the number of newly infected birds is $\left(1-(1-c_b)^{\frac{ae^{-\mu_m(T(t))}\sum_{k=t_0}^{t-2} I_{m,k}(t)}{N_b(t)-\mu_b I_b(t)}}\right) S_b(t)$. The infected bird population decreases by death caused by infection at rate μ_b and by recovering from infection at rate σ. Recovered birds are assumed to

develop lifelong immunity and are no longer susceptible to the disease. Based on these assumptions, the model equations for the bird population are

$$S_b(t+1) = (1-c_b)^{\frac{ae^{-\mu_m(T(t))}\sum_{k=t_0}^{t-2} I_{m,k}(t)}{N_b(t)-\mu_b I_b(t)}} S_b(t) \tag{3.2.23}$$

$$I_b(t+1) = \left(1-(1-c_b)^{\frac{ae^{-\mu_m(T(t))}\sum_{k=t_0}^{t-2} I_{m,k}(t)}{N_b(t)-\mu_b I_b(t)}}\right) S_b(t) + (1-\sigma-\mu_b) I_b(t) \tag{3.2.24}$$

$$R_b(t+1) = R_b(t) + \sigma I_b(t) \tag{3.2.25}$$

$$D_b(t+1) = D_b(t) + \mu_b I_b(t). \tag{3.2.26}$$

3.3 Model properties (non-autonomous)

In the non-autonomous model described in (3.2.1) to (3.2.26), all model parameters (Table 1) and functions (Table 2) are assumed to be non-negative.

Proposition 3.3.1 *All solutions of model equations defined by* (3.2.17) *to* (3.2.26) *with* $S_{l,t_0}(t_0), I_{l,t_0}(t_0), S_{a,t_0}(t_0), A_{a,t_0}(t_0), I_{a,t_0,t_0}(t_0), S_b(t_0), I_b(t_0), N_l(t_0), N_m(t_0), N_b(t_0) \geq 0$ *remain non-negative for all time* $t_0 \leq t \leq t_{end}$ *under the condition* $\sigma + \mu_b \leq 1$.

Due to the range of values the parameters σ and μ_b can take, as defined in Table 1, the condition $\sigma + \mu_b \leq 1$ is naturally satisfied. Furthermore, it can be shown that all solutions of the system will remain non-negative in the feasible region

$$\Upsilon = \{(S_{l,k}, I_{l,k}, S_{a,k}, A_{a,k,i}, I_{a,k}, S_b, I_b, R_b, D_b) \in R^{(4+\omega)(t_{end}-t_0)+4}: S_{l,k}, I_{l,k}, S_{a,k}, A_{a,k,i}, I_{a,k}, S_b, I_b, R_b, D_b \geq 0\} \quad (3.3.27)$$

for all time $t_0 \leq t \leq t_{end}$. Thus, the region Υ is positively invariant. Since only adult female *Cx. pipiens* and *Cx. restuans* mosquitoes will enter a state of diapause, the initial number of aquatic mosquitoes $N_l(t_0)$ at the beginning of each season will be zero; i.e., $N_l(t_0) = 0$.

In the absence of disease, a balance in birth and death rates for mosquitoes does not necessarily guarantee the existence of a non-trivial disease-free equilibrium (DFE) in this model. Due to the temperature- and photoperiod-dependent function for the proportion of non-diapausing adults, all solutions of (3.2.17) to (3.2.21) with non-negative initial conditions will tend towards zero at the end of each season. Once the photoperiod falls below 14.75 daylight hours on day 211, which corresponds with the end of July, the proportion of non-diapausing adult female mosquitoes will continue to decrease as photoperiod decreases. For this reason, the non-autonomous model has only a trivial (mosquito-free) disease-free equilibrium, denoted by

$$E_* = ({S_l}^*, {I_l}^*, {S_m}^*, {A_m}^*, {I_m}^*, {S_b}^*, {I_b}^*, {R_b}^*, {D_b}^*) = (0, 0, 0, 0, 0, {N_b}^*, 0, 0, 0). \quad (3.3.28)$$

Figure 3.3 illustrates, in the absence of disease, the effect of diapause on the active host-seeking adult female mosquito population when temperature is held constant at low, optimal, and high temperatures over the study period.

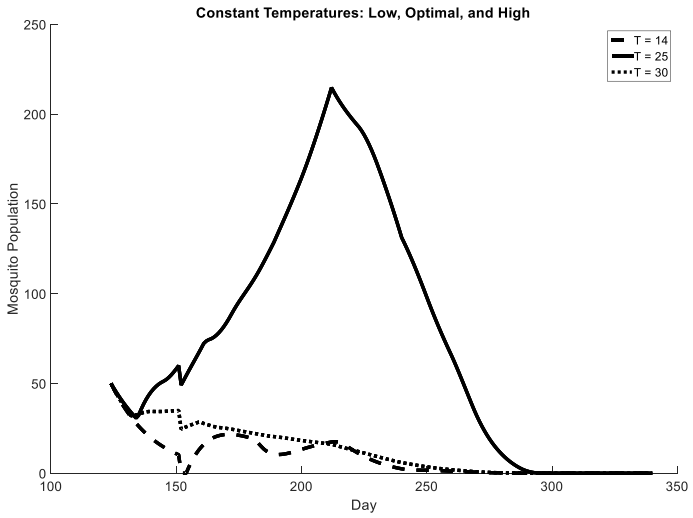

Figure 3.3: Numerical results for adult female mosquitoes at three constant temperatures in the absence of disease: $T = 14°\text{C}$ (dashed line), $T = 25°\text{C}$ (solid line), and $T = 30°\text{C}$ (dotted line).

Although the non-autonomous model in its current state only has the trivial (mosquito-free) disease-free equilibrium, we can make certain reasonable biological and environmental assumptions that simplifies the model structure to allow for the existence of the DFE where positive steady states exist in the mosquito population. In Section 3.4.1, we propose three simplifying assumptions that allow us to transform the model equations for mosquitoes (3.2.17) to (3.2.21) into a discrete-time linear age-structured population model. Then, in Section 3.5 we study the existence and stability of the DFE in the autonomous model.

3.4 Simplified model (autonomous)

Before further analysis of the qualitative dynamics of the non-autonomous model described in (3.2.1) to (3.2.26), we consider a simplified autonomous version of the model for comparison. The objective of analyzing the dynamics of the autonomous model is to determine if it has different qualitative dynamics with respect to the existence of steady-state solutions and their stability. We

begin by proposing modifications to model equations (3.2.1) to (3.2.26) by making simplifying assumptions about environmental conditions and mosquito biology that alter the structure of the model thereby allowing us to reduce the number of variables and equations. The first simplifying assumption removes the temporal dependence on temperature by holding the temperature at a constant for all time $t_0 \leq t \leq t_{end}$. The second assumption removes the effect of diapause on the developing mosquito population to allow for the existence of DFE. The third assumption removes the maximum lifespan constraint. We assume no vertical transmission in the fourth assumption. The fifth assumption changes the DD function used to track the progression of exposed mosquitoes through the EIP into an instantaneous rate function that is also dependent on temperature.

3.4.1 Simplifying assumptions

(S1) *Temperature is held constant:* $T(t) = T, \quad \forall t$

At constant temperatures, all cohorts will develop in the same amount of time regardless of the day on which they were oviposited. The total number of days to complete development for each cohort τ_k can now be denoted τ. Consequently, the model will be composed of $\tau + \omega$ paired equations to track cohorts of developing mosquitoes from the day of oviposition to the time they are τ days old. Then they will be tracked through their time as adults from the time of eclosion until they reach their maximum adult lifespan of ω days relative to the day of eclosion. Temperature-dependent functions for aquatic mortality ($\mu_l(T(t)) = \mu_l(T)$), adult mortality ($\mu_m\big(T(t)\big) = \mu_m(T)$), and transition rate from asymptotic to infected ($\delta\big(T(t)\big) = \delta(T)$), will become constant and will no longer change with time. This is a reasonable short-term assumption as natural weather patterns can sometimes exhibit periods of time where there is little variability in daily temperatures.

(S2) *Effect of diapause is removed:* $\gamma_k(T_k, P_k) = 1, \ \forall k$

To allow for the existence of a non-trivial disease-free equilibrium, the effect of diapause must be ignored. While this assumption enables us to simplify the model, it also tends to overestimate the mosquito population in the later part of the season after day 211. This assumption means that mosquitoes are no longer sensitive to the decreasing number of daylight hours, which induces a physiological response preparing them for diapause once the photoperiod falls below a lower threshold value. Hence, all new adults will enter the susceptible or infected classes upon eclosion.

(S3) *Maximum lifespan constraint removed:* $\omega \to \infty$

This assumption is made to simplify the model structure to allow for a more convenient calculation of the basic reproduction number R_0. To calculate R_0, which involves linearizing the model equations about the DFE, the equations for each compartment require consolidation (summation of all cohort equations in each compartment at each time step). A consequence of imposing a maximum lifespan constraint is that at each time step the number of adults remaining in a cohort that is ω days old must be removed from the total population. In the absence of disease, this is easy; however, due to the transfer of individuals between infected compartments at each time step, it is difficult to track the total number of adults remaining in a cohort for a specific compartment when trying to consolidate all the equations for each subpopulation.

(S4) *No vertical transmission in mosquitoes:* $I_l(t) = 0, \quad \forall t$

Vertical transmission plays an important role in the prevalence of WNV in regions with temperate climates like Southern Ontario where only non-parous adult female mosquitoes can survive harsh winter temperatures in a state of diapause. The impact of vertical transmission on the cross-infection between mosquitoes and birds within a single-season has been found negligible and can thus omitted from the autonomous model (Nasci et al. 2001, Turell et al. 2001).

(S5) *Asymptomatic mosquitoes become infectious at a temperature-dependent rate:*

$$\overline{\delta}(T) = \max(0, 0.00715T - 0.09359) \tag{3.4.29}$$

This assumes mosquitoes that become exposed to the virus after biting an infected bird will no longer experience a delay before becoming infectious due to the EIP. Instead, we model the transition between the asymptomatic and infectious compartments with a temperature-dependent rate $\overline{\delta}(T)$ that estimates the same instantaneous rate of transition as the DD function (3.2.15) using the same minimum temperature threshold T_a and total degree-days to complete the EIP, T_{DDa}. While this assumption simplifies the model, it tends to overestimate the progression of the disease, especially during the early part of the season, as exposed mosquitoes no longer must wait to accumulate enough degree-days before they become infectious. In Section 3.6.3, we analyze the effect of the EIP on disease transmission dynamics between mosquitoes and birds in the non-autonomous model. We use surveillance data to justify the use of a degree-day function to model the EIP.

Based on the assumptions (S1)–(S5), the model equations for mosquito discrete cohorts (3.2.17) to (3.2.21) can now be simplified and written as

$$S_{l,k}(t+1) = S_{l,k}(t)e^{-\mu_l(T)}H\big(1 - f_k(t)\big), \tag{3.4.30}$$

$$S_{m,k}(t+1) = \left(S_{l,k}(t)e^{-\mu_l(T)} + e^{-\mu_m(T)}(1-c_m)^{\frac{a(1-\sigma-\mu_b)I_b(t)}{N_b(t)-\mu_b I_b(t)}}S_{m,k}(t)\right)$$

$$\times\left(1 - H\big(1 - f_k(t)\big)\right) \tag{3.4.31}$$

$$A_{m,k}(t+1) = \left(\left(1-(1-c_m)^{\frac{a(1-\sigma-\mu_b)I_b(t)}{N_b(t)-\mu_b I_b(t)}}\right)S_{m,k}(t) + \left(1-\overline{\delta}(T)\right)A_{m,k}(t)\right)$$

$$\times\, e^{-\mu_m(T)}\left(1-H\left(1-f_k(t)\right)\right) \tag{3.4.32}$$

$$I_{m,k}(t+1) = \left(I_{m,k}(t) + \overline{\delta}(T)A_{m,k}(t)\right)e^{-\mu_m(T)}\left(1-H\left(1-f_k(t)\right)\right). \tag{3.4.33}$$

The consolidated equations for mosquitoes in terms of the total sub-populations in each compartment can now be expressed by

$$S_l(t+1) = \beta e^{-\mu_m(T)}\left(S_m(t)+A_m(t)+I_m(t)\right) + \left(1-\frac{e^{-\mu_l(T)(\tau-1)}}{1+\sum_{k=1}^{\tau-1}e^{-\mu_l k}}\right)e^{-\mu_l(T)}S_l(t) \tag{3.4.34}$$

$$S_m(t+1) = \frac{e^{-\mu_l(T)\tau}}{1+\sum_{k=1}^{\tau-1}e^{-\mu_l k}}S_l(t) + e^{-\mu_m(T)}(1-c_m)^{\frac{a(1-\sigma-\mu_b)I_b(t)}{N_b(t)-\mu_b I_b(t)}}S_m(t) \tag{3.4.35}$$

$$A_m(t+1) = e^{-\mu_m(T)}\left(1-(1-c_m)^{\frac{a(1-\sigma-\mu_b)I_b(t)}{N_b(t)-\mu_b I_b(t)}}\right)S_m(t) + e^{-\mu_m(T)}\left(1-\overline{\delta}(T)\right)A_m(t) \tag{3.4.36}$$

$$I_m(t+1) = e^{-\mu_m(T)}\overline{\delta}(T)A_m(t) + e^{-\mu_m(T)}I_m(t). \tag{3.4.37}$$

where the ratio $\frac{e^{-\mu_l(T)(\tau-1)}}{1+\sum_{k=1}^{\tau-1} e^{-\mu_l k}}$ represents the proportion of larvae at time t in the cohort that will eclose into adults at time $t+1$. The equations for birds based on the assumptions defined in (S1)-(S5) are now given by

$$S_b(t+1) = (1-c_b)^{\frac{ae^{-\mu_m(T)}I_m(t)}{N_b(t)-\mu_b I_b(t)}} S_b(t) \tag{3.4.38}$$

$$I_b(t+1) = \left(1-(1-c_b)^{\frac{ae^{-\mu_m(T)}I_m(t)}{N_b(t)-\mu_b I_b(t)}}\right) S_b(t) + (1-\sigma-\mu_b) I_b(t) \tag{3.4.39}$$

$$R_b(t+1) = R_b(t) + \sigma I_b(t) \tag{3.4.40}$$

$$D_b(t+1) = D_b(t) + \mu_b I_b(t). \tag{3.4.41}$$

3.4.2 Basic properties of autonomous model

We note that the function for diapause (2.2.5) does not influence mosquito population dynamics prior to day 211. Hence, when temperature is held constant, the non-autonomous model and simplified model produce nearly identical results up to that point. Thus, analysis of the simplified version of the model may still provide useful insight into the dynamics of disease transmission in the early part of the mosquito season.

The simplified model described in (3.4.34) to (3.4.41) assumes all model parameters are positive and model functions are non-negative. With non-negative initial data and the condition in

Proposition 3.3.1 satisfied, all solutions of the system for all time $t_0 \leq t \leq t_{end}$ will remain non-negative in the region

$$\Upsilon = \{(S_l, S_m, A_m, I_m, S_b, I_b, R_b, D_b) \in R^8 : S_l, S_m, A_m, I_m, S_b, I_b, R_b, D_b \geq 0\}. \quad (3.4.42)$$

Although the solutions of both the non-autonomous and simplified models are bounded on the closed interval $[t_0, t_{end}]$, we note that the trajectories of the solutions for each model at the end of the season under the same constant temperature scenario may differ. All solutions of the non-autonomous model will always tend to zero due to the effect of diapause; however, within a range of temperatures that are conducive to rapid aquatic development accompanied by low mortality, the solutions for the autonomous-model will appear to have an unbounded trajectory at time t_{end}. Within this range of temperatures, if simulations were to continue beyond t_{end} to infinity, the solutions for the mosquito equations would be unbounded due to the removal of the effect of diapause given in (S2).

3.5 Existence and stability of equilibria (autonomous)

3.5.1 Disease-free equilibrium E_0

It is assumed there is a balance in mosquito oviposition and mortality rates for the existence of a DFE. The parameter constraint for the existence of a DFE is obtained from equations (3.4.34) and (3.4.35) and is given by

$$\frac{(1 - e^{-\mu_m})}{e^{-\mu_m}} = \frac{\beta c_l e^{-\mu_l}}{\left(1 - e^{-\mu_l}(1 - c_l)\right)} \quad (3.5.43)$$

where and $c_l = \frac{e^{-\mu_l(\tau-1)}}{1+\sum_{k=1}^{\tau-1} e^{-\mu_l k}}$ for notational convenience.

The DFE is

$$E_0 = (S_l^*, S_m^*, A_m^*, I_m^*, S_b^*, I_b^*, R_b^*, D_b^*) = \left(\frac{\beta e^{-\mu_m}}{(1-(1-c_l)e^{-\mu_l})} N_m^*, N_m^*, 0, 0, N_b^*, 0, 0, 0\right) \quad (3.5.44)$$

where $S_m^* = N_m^*$ and $S_b^* = N_b^*$ in the absence of disease.

We observe the parameter constraint (3.5.43) includes temperature-dependent terms μ_l, μ_m, and τ. Thus, the existence of a DFE relies upon temperature being such that (3.5.43) is satisfied. It must be noted for a fixed oviposition rate β, there are only specific values of temperature that can generate the corresponding parameter values required by the constraint in (3.5.43). In the mosquito abundance model, when the oviposition rate and temperature are held constant, it was shown that there exist at least two temperatures below and above T_{op}, denoted T_1 and T_2 respectively, that can produce positive steady states in the mosquito population (Figure 3.4). Each temperature produces different parameter values; however, the DFE in both cases are given by E_0 in (3.5.44). We discuss the effect of T_1 and T_2 on the dynamics of disease transmission in further detail in Section 3.6.1.

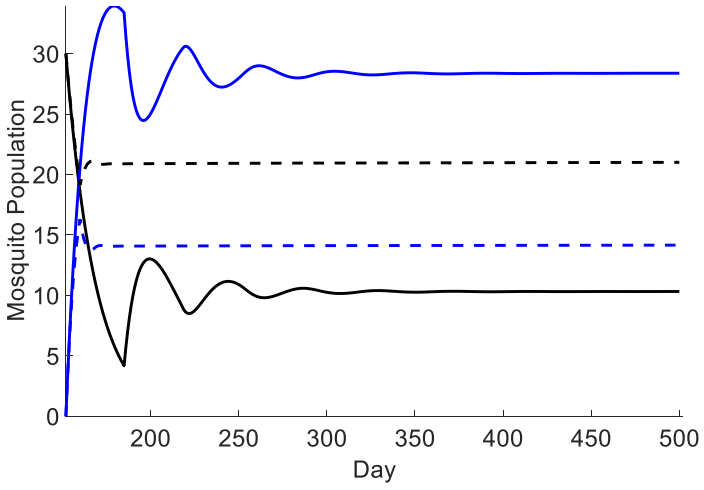

Figure 3.4: Numerical simulations for aquatic (blue) and adult female (black) mosquitoes demonstrating the existence of two positive steady states for mosquito populations about the DFE at temperatures $T_1 = 14$°C (solid lines) and $T_2 = 30$°C (dashed lines) with a fixed oviposition rate of $\beta = 0.12$. Parameter and function values are generated by each temperature and temperature-independent dependent parameter values are from Table 1.

3.5.2 Basic reproduction number R_0

Using Perron–Frobenious theory for non-negative matrices, the linear stability of the E_0 can be determined by the basic reproduction number R_0 (Cushing and Yicang 1994, Caswell 2001, Li and Schneider 2002). The basic reproduction number is defined as the number of new infections that arise out of an infected individual over the course of its lifetime in an otherwise susceptible population. For a discrete-time epidemic model, the expression for R_0 is the spectral radius (i.e. dominant eigenvalue), of the next-generation matrix constructed from the equations for compartments where the infection can reside (Caswell 2001, Li and Schneider 2002, Lewis et al. 2006). These equations can be written as $x(t+1) = Ax(t)$, where A is known as the projection matrix and $x(t)$ is the number of individuals in each infected compartment at time t (Caswell 2001, Lewis et al. 2006). The matrix A is then decomposed into two matrices such that $Ax(t) = (F + T\,)x(t)$, where the square matrices F and T represent the appearance of new infections and the transfer in and out of infected classes by other means, respectively. Both F and T are non-negative and T is non-singular with a spectral radius of less than 1. For the model equations given in (3.4.34) to (3.4.41), there are three compartments where the virus appears $A_m, I_m,$ and I_b; however, since we are only interested in new infections, we do not treat the progression from asymptomatic to infected adults as new infections. Linearization about E_0 yields

$$F = \begin{pmatrix} 0 & 0 & -e^{-\mu_m} a(1-\sigma-\mu_b)\ln(1-c_m)\dfrac{N_m^{\,*}}{N_b^{\,*}} \\ 0 & 0 & 0 \\ 0 & -e^{-\mu_m} a\ln(1-c_b) & 0 \end{pmatrix}, \tag{3.5.45}$$

$$T = \begin{pmatrix} e^{-\mu_m}(1-\overline{\delta}) & 0 & 0 \\ e^{-\mu_m}\overline{\delta} & e^{-\mu_m} & 0 \\ 0 & 0 & 1-\sigma-\mu_b \end{pmatrix} \tag{3.5.46}$$

and

$$A = F + T =$$

$$= \begin{pmatrix} e^{-\mu_m}\left(1-\overline{\delta}\right) & 0 & -e^{-\mu_m}a(1-\sigma-\mu_b)\ln(1-c_m)\dfrac{{N_m}^*}{{N_b}^*} \\ e^{-\mu_m}\overline{\delta} & e^{-\mu_m} & 0 \\ 0 & -e^{-\mu_m}a\ln(1-c_b) & 1-\sigma-\mu_b \end{pmatrix}. \tag{3.5.47}$$

The next-generation matrix takes the form $P = F(I-T)^{-1}$, where I denotes the Identity matrix (Cushing and Yicang 1994, Caswell 2001). The matrix P has elements p_{ij} which are the expected number of secondary infections of type i caused by a single infected individual of type j. The matrix $(I-T)^{-1}$ is

$$(I-T)^{-1} = \begin{pmatrix} \dfrac{1}{1-e^{-\mu_m}\left(1-\overline{\delta}\right)} & 0 & 0 \\ \dfrac{\overline{\delta}e^{-\mu_m}}{\left(1-e^{-\mu_m}\left(1-\overline{\delta}\right)\right)(1-e^{-\mu_m})} & \dfrac{1}{1-e^{-\mu_m}} & 0 \\ 0 & 0 & \dfrac{1}{\sigma+\mu_b} \end{pmatrix} \tag{3.5.48}$$

and

$$P = F(I-T)^{-1}$$

$$= \begin{pmatrix} 0 & 0 & \dfrac{a\tilde{C}_m(1-\sigma-\mu_b)e^{-\mu_m}{N_m}^*}{(\sigma+\mu_b){N_b}^*} \\ 0 & 0 & 0 \\ \dfrac{a\tilde{C}_b\overline{\delta}e^{-2\mu_m}}{\left(1-e^{-\mu_m}\left(1-\overline{\delta}\right)\right)(1-e^{-\mu_m})} & \dfrac{a\tilde{C}_b e^{-\mu_m}}{1-e^{-\mu_m}} & 0 \end{pmatrix}, \quad (3.5.49)$$

where $\tilde{C}_b = -\ln(1-c_b)$ and $\tilde{C}_m = -\ln(1-c_m)$ for convenience of notation. The basic reproduction number R_0 is the spectral radius of P, denoted $\rho(P)$, and is found by solving for the roots λ of its characteristic polynomial

$$\lambda\left(\lambda^2 - \frac{a^2(1-\sigma-\mu_b)\overline{\delta}e^{-3\mu_m}\tilde{C}_b\tilde{C}_m{N_m}^*}{\left(1-e^{-\mu_m}\left(1-\overline{\delta}\right)\right)(1-e^{-\mu_m})(\sigma+\mu_b){N_b}^*}\right) = 0 \quad (3.5.50)$$

By the Perron–Frobenius theory for non-negative matrices, the spectral radius of an irreducible non-negative matrix P has a unique, positive, and algebraically simple eigenvalue. Clearly, (3.5.50) has one eigenvalue equal to zero. Thus, the spectral radius of $\rho(P) = R_0$, is given by the positive root of (3.5.50).

$$R_0 = \sqrt{\frac{a\tilde{C}_b e^{-\mu_m}}{(1-e^{-\mu_m})}\frac{a\tilde{C}_m(1-\sigma-\mu_b)\overline{\delta}e^{-2\mu_m}{N_m}^*}{\left(1-e^{-\mu_m}\left(1-\overline{\delta}\right)\right)(\sigma+\mu_b){N_b}^*}} \quad (3.5.51)$$

The first term under the square root symbol $\frac{a\tilde{C}_b e^{-\mu_m}}{(1-e^{-\mu_m})}$ can be interpreted as the number of new birds infected by a single infectious mosquito over the course of its lifetime; (i.e. the R_0 of the virus from mosquitoes to birds). The second term $\frac{a\tilde{C}_m(1-\sigma-\mu_b)e^{-2\mu_m}\overline{\delta}{N_m}^*}{(\sigma+\mu_b)\left(1-e^{-\mu_m}\left(1-\overline{\delta}\right)\right){N_b}^*}$ can be interpreted as the R_0 of the virus from birds to mosquitoes and is expressed as the effective contact rate $a\tilde{C}_m$ multiplied

by the number of mosquitoes per bird $\frac{N_m{}^*}{N_b{}^*}$ that survive the period of exposure $\frac{e^{-2\mu m\overline{\delta}}}{\left(1-e^{-\mu m}\left(1-\overline{\delta}\right)\right)}$ multiplied by the average amount of time a bird is infectious $\frac{(1-\sigma-\mu_b)}{(\sigma+\mu_b)}$. The square root of the expression gives the geometric mean of the two terms and represents the average number of secondary infections produced by a single infectious mosquito or bird during its infectious lifespan.

At first inspection of (3.5.51), if parameter values are assumed to be constant, we observe that the ratio of mosquitoes to birds $\frac{N_m{}^*}{N_b{}^*}$ determines the invasiveness of virus transmission when introduced to a susceptible mosquito population of constant size. Setting $R_0 = 1$ and solving for mosquitoes yields the critical threshold value of susceptible mosquitoes $S_m{}^*$, below which the disease will die out and above which will cause an outbreak.

$$N_m{}^* = \frac{\left(1-e^{-\mu_m}\left(1-\overline{\delta}\right)\right)(1-e^{-\mu_m})(\sigma+\mu_b)}{\tilde{C}_b\tilde{C}_m a^2\overline{\delta}e^{-3\mu_m}(1-\sigma-\mu_b)}N_b{}^* = S_m{}^* \tag{3.5.52}$$

The exact value of $S_m{}^*$ depends on the parameter values. The parameters $e^{-\mu_l}$, $e^{-\mu_m}$ and $\overline{\delta}$ depend on temperature, implying the exact value of $S_m{}^*$ also depends implicitly on temperature.

The effect of each parameter on R_0 can be deduced from its expression in (3.5.51). The transition rate $\overline{\delta}$ has a positive correlation with R_0. This is consistent with the epidemiological interpretation that the longer a mosquito that is exposed to the virus remains in the asymptomatic class, the higher the probability that it will die before becoming infectious. Mortality rates, both natural (μ_l and μ_m) and disease induced (μ_b), have a negative impact on R_0. The higher the rate at which infectious individuals are removed from the transmission cycle decreases the number of infections it can cause during its infectious lifespan. Similarly, the recovery rate σ for birds also has a negative correlation with R_0 for the same reason, since it affects the rate of removal of

infectious individuals from the transmission cycle. The biting rate and probabilities of transmission (β, c_b, and c_m), clearly have a have a positive relationship with R_0.

In our model, due to the transient dynamics of the mosquito population prior to reaching its equilibrium state, the value of ${S_m}^*$ used in the calculation of R_0 is not readily obtained from the initial value of mosquitoes in the usual way. For a seasonally variable population, Wonham et al. (2004) showed that R_0 depends on the average susceptible mosquito population level over the entire mosquito season. Henceforth, we denote $\overline{S_m}$ to represent the average susceptible mosquito population on the interval $[t_0, t_{end}]$ and $\overline{R_0}$ to represent the mean of the individual reproduction numbers calculated daily over the same period. Both $\overline{S_m}$ and $\overline{R_0}$ depend on the initial conditions and must be computed numerically in our model due to the transient period at the start of each simulation. Using the same notation and a similar approach as Wonham et al. (2004), for a seasonally variable population we present the calculation of $\overline{S_m}$ and $\overline{R_0}$ using a graphical approach to find the critical level of the average mosquito population $\overline{{S_m}^*}$ that determines whether $\overline{R_0}$ will be less than or greater than 1 (Figure 3.5). We illustrate this approach with a simple example to calculate the mean population $\overline{S_m}$ and mean $\overline{R_0}$ over the season. In this example, we assume the mosquito population resides at a population level ${S_m}^a$ for t_a amount of time and at ${S_m}^b$ for the remaining amount of time t_b. Then

$$\overline{S_m} = \frac{t_a {S_m}^a + t_b {S_m}^b}{t_a + t_b} \tag{3.5.53}$$

and

$$\overline{R_0} = \frac{t_a {R_0}^a + t_b {R_0}^b}{t_a + t_b}. \tag{3.5.54}$$

where ${R_0}^a$ and ${R_0}^b$ are the basic reproduction numbers for population levels ${S_m}^a$ and ${S_m}^b$ relative to the initial bird population $N_b(t_0)$, respectively. Then, setting $\overline{R_0} = 1$ gives the critical threshold $\overline{{S_m}^*}$ that determines whether an outbreak will occur in a seasonally variable population of susceptible mosquitoes.

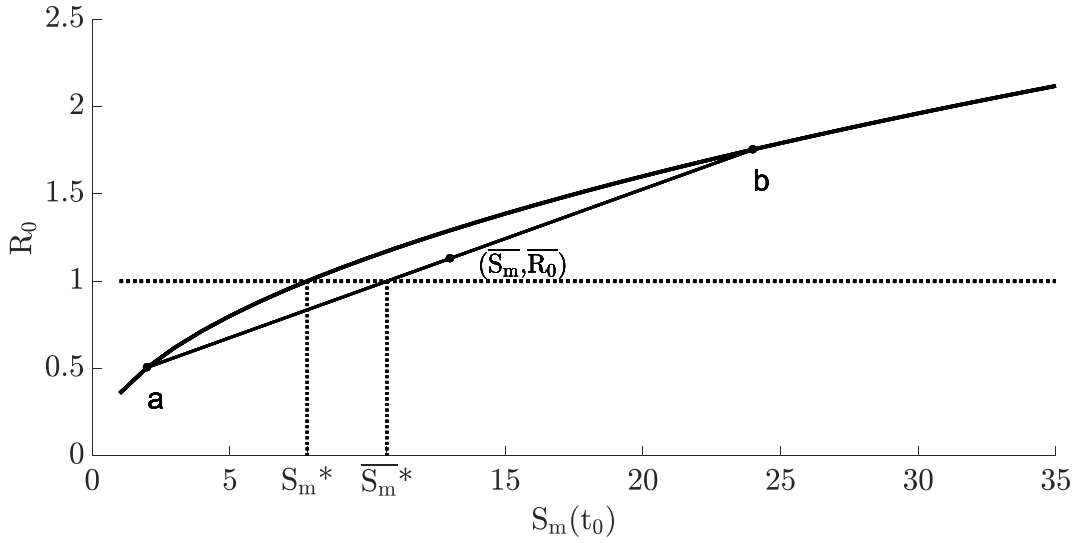

Figure 3.5: Graphical representation of calculating the critical threshold level $\overline{{S_m}^*}$ for a seasonally variable population.

From the example in Figure 3.5, we observe that if the average population $\overline{S_m}$ is reduced to a level such that $\overline{S_m} < \overline{{S_m}^*}$ then $\overline{R_0} < 1$ and an outbreak can be avoided. This could be accomplished by implementing mosquito control measures to reduce the higher population level ${S_m}^b$ for a long enough period such that $\overline{S_m} < \overline{{S_m}^*}$. This method can be extended to cover multiple population levels by applying equations (3.5.53) and (3.5.54) in the same way.

3.5.3 Linear stability of the disease-free equilibrium

The relationship between R_0 and the linear stability of the DFE is found by analyzing the spectral radius of the projection matrix A, otherwise known as the growth factor, denoted $r = \rho(A)$. It follows from Perron–Frobenius theory for non-negative matrices (Caswell 2001, Li and Schneider 2002), that the linear stability of E_0 can be determined by r and hence by R_0. The following theorem from Li and Schneider (2002) gives the relationship between r and R_0.

Theorem 4.2 *Suppose the $n \times n$ projection matrix $A = F + T$ is irreducible where F and T are non-negative, T is non-singular, and $\rho(T) < 1$. Let $P = F(I - T)^{-1}$. Suppose that $R_0 > 0$. Then*

i) $\rho\left(T + \frac{F}{R_0}\right) = 1$

and one of the following holds:

ii) $r = R_0 = 1$

iii) $1 < r < R_0$

iv) $0 < R_0 < r < 1$

To prove that the linear stability of E_0 can determined by R_0, we refer to Caswell (2001), where it is shown that if E_0 is an equilibrium solution of the matrix A, then E_0 is asymptotically stable if $r < 1$ and unstable if $r > 1$. It follows from Theorem 4.2 that E_0 is asymptotically stable if $R_0 < 1$ and unstable if $R_0 > 1$. It is easy to verify that matrices $A, F,$ and T in (3.5.45) to (3.5.47) satisfy the conditions given in Theorem 4.2. From (3.5.50), clearly P is non-negative and $\rho(P) > 0$. Thus, the linear stability of E_0 given in (3.5.44) is determined by R_0.

The stability results presented above are interpreted in the usual way regarding the asymptotic behavior of disease transmission for the system given in (3.4.34) to (3.4.41). However, these

results rely upon waiting for the system to reach its long-term regime, which is not feasible in practice (Li et al. 2011). The model in this study covers a single mosquito season which, in Southern Ontario, is relatively short and only lasts a few months (June through September). In the assessment of control strategies, the transient dynamics of disease transmission during this period cannot be ignored.

Using data from the literature on vector–host interaction and mosquito biology (Tables 1 and 2), we developed a WNV disease transmission model that relies on temperature as the driving force behind mosquito population abundance and disease transmission dynamics. In the following sections, we present numerical results and analysis of the effect of temperature on R_0 and on the dynamics of disease transmission over a single-season.

3.6 Results

3.6.1 The effect of temperature on R_0

Recall that R_0 is derived from the linearized system evaluated at the DFE and that for a fixed oviposition rate β, the DFE can only exist at temperatures that generate parameter values that satisfy the condition for the existence of a DFE given in (3.5.43). As previously mentioned in Sec. 3.5.1, there exists two such temperatures, T_1 and T_2, that satisfy this condition. Although the parameter values $\mu_l, \mu_m,$ and $\overline{\delta}$ generated by each of the two temperatures meet the conditions for the existence of a DFE given in (3.5.43), the critical threshold level for the number of mosquitoes per bird (3.5.52), which determines whether an outbreak will occur, can vary considerably between the two temperatures. It is worth noting that the parameters mentioned above cannot be selected independently from one another; i.e., each temperature generates a unique set of temperature-

dependent parameter values based on their respective functions. Examining the system in both temperature settings highlights the effect of temperature on mosquito biology and transmission dynamics when using the same initial conditions for both settings. In other words, initial population ratios of mosquitoes and birds that may lead to an outbreak at one temperature can be more or less severe at another temperature and in some cases no outbreak will occur at all (Figure 3.6). For instance, this would be an important factor to consider in the risk assessment of an outbreak in geographic locations where the mean temperature during the mosquito season is closer to one of the two temperatures. It should also be noted that the actual temperatures T_1 and T_2 also depend on the values of temperature-independent parameters.

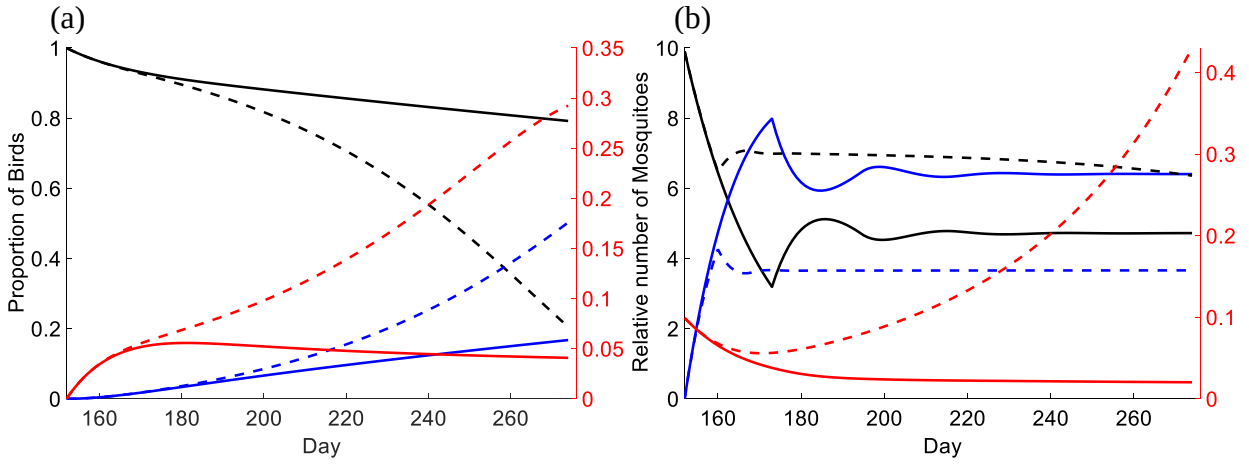

Figure 3.6: Numerical simulations of the autonomous model given in (3.4.34) through (3.4.41) for the proportion of birds (a) and the relative number of mosquitoes to initial birds (b) at temperatures $T_1 = 16.41°\text{C}$ and $T_2 = 28.34°\text{C}$ with initial values: $S_m(t_0) = 10, I_m(t_0) = 0.01, S_b(t_0) = 1,$ and $S_l(t_0) = A_m(t_0) = I_b(t_0) = R_b(t_0) = 0$. The threshold values of susceptible mosquitoes and average population size at each temperature were numerically computed to be $\overline{S_{m,T_1}}^* = 6.05$, $\overline{S_{m,T_1}} = 5$, $\overline{S_{m,T_2}}^* = 2.71$, and $\overline{S_{m,T_2}} = 7.17$. Simulations covered a single mosquito season from June through September (Days 152–274). Parameter values are from Tables 1 and 2. For birds (a), the left axis corresponds with the proportion of susceptible birds (black) and dead birds (blue). The right axis represents the proportion of infected birds (red). For mosquitoes (b), the relative numbers of susceptible aquatic (blue) and susceptible adult mosquitoes (black) are on the left axis while the infected adults (red) are on the right axis. At T_1 (solid lines), it takes 21 days for mosquitoes in the aquatic stage to complete development. Consequently, the average susceptible adult population during the season $\overline{S_{m,T_1}}$ drops significantly lower than its initial value. In this case, $R_{0,T_1} = 0.91$, and there is a mild outbreak in the bird population while the infected mosquito population monotonically tends to zero until the end of the simulation. At T_2 (dashed lines), the time to complete aquatic development is only 8 days, which produces a higher average mosquito population over the season compared with T_1 . Here, $R_{0,T_2} = 1.63$, and we

see the infected mosquito population begin to increase shortly after the start of the simulation. At T_2, the outbreak in birds is more severe, and the susceptible bird population almost goes extinct by the end of the season.

The numerical simulations depicted in Figure 3.6, highlight the importance of temperature in vector-borne disease transmission dynamics that is often overlooked in studies that do not consider the effect of temperature. These results demonstrate that the mosquito to bird ratio and temperature should be considered together when assessing the risk of an outbreak. Some studies on WNV transmission (Wonham et al. 2004, Jang 2007) attribute infection risk primarily to the ratio of initial mosquitoes to birds. While this is true in the context of their models, it is also important to understand how the mosquito to bird ratio is affected by changes in the environmental temperature it resides in. Temperature is the driving force behind mosquito population dynamics, and certain temperature patterns can cause an explosion in the mosquito population in a relatively short amount of time. Thus, if temperature is ignored in these scenarios, an outbreak is more likely to occur uninhibited by human intervention. On the other hand, with this understanding, local temperature forecasts could be used to the advantage of mosquito control programs in the timing of control measures. For example, if recent daily temperatures have been relatively low and local temperature forecasts predict that daily temperatures will rise dramatically in the near future, then implementing control measures at mosquito breeding sites while temperatures are still low could minimize the number of aquatic stage mosquitoes that would eclose into adults once the temperatures begin to rise.

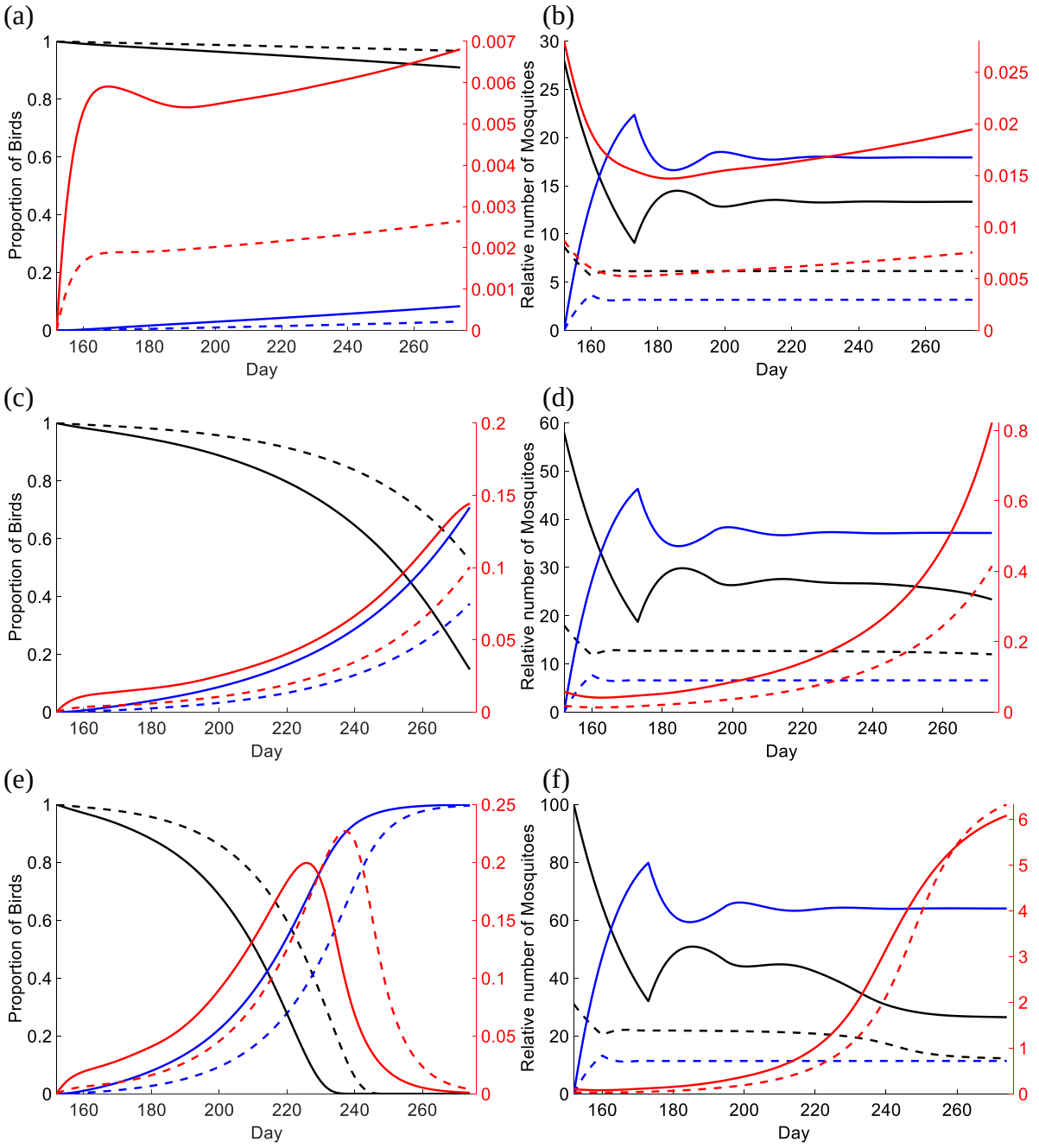

Figure 3.7: Comparisons of conditions required to generate the same value of R_0 at temperatures $T_1 = 16.41°C$ (solid lines) and $T_2 = 28.34°C$ (dashed lines) for the proportion of birds (a, c, e) and relative number of mosquitoes (b, d, f), respectively. For T_1 and T_2 the threshold values of susceptible mosquitoes are $\overline{S_{m,T_1}}^* = 12.36$ and $\overline{S_{m,T_2}}^* = 5.53$, respectively. In (a) and (b) $R_0 = 1.06, \overline{S_{m,T_1}} = 14.02$, and $\overline{S_{m,T_2}} = 6.22$. In (c) and (d) $R_0 = 1.53, \overline{S_{m,T_1}} = 29.03$, and $\overline{S_{m,T_2}} = 12.89$. In (e) and (f) $R_0 = 2, \overline{S_{m,T_1}} = 50.06$, and $\overline{S_{m,T_2}} = 22.23$. The description for the left and right axes and population type indicated by color is the same as in Figure 3.6.

In Figure 3.7, we compare the effect of temperature on the conditions required to produce the same R_0 value at both DFE temperatures T_1 and T_2. As expected, the transmission dynamics at both temperatures are very similar; however, at T_1, it takes approximately 2.25 times the average mosquito population required to generate the same R_0 value than at T_2 for all three cases. This is primarily due to the significantly longer amount of time required to complete aquatic development at T_1 (21 days) than at T_2 (8 days). Figure 3.8 illustrates the comparison of $\overline{R_0}$ as a function of $\overline{S_m}$ for $T_1 = 16.41$ and $T_2 = 28.34$ under the same model settings as Figure 3.7 using the approach described in (3.5.53) and (3.5.54).

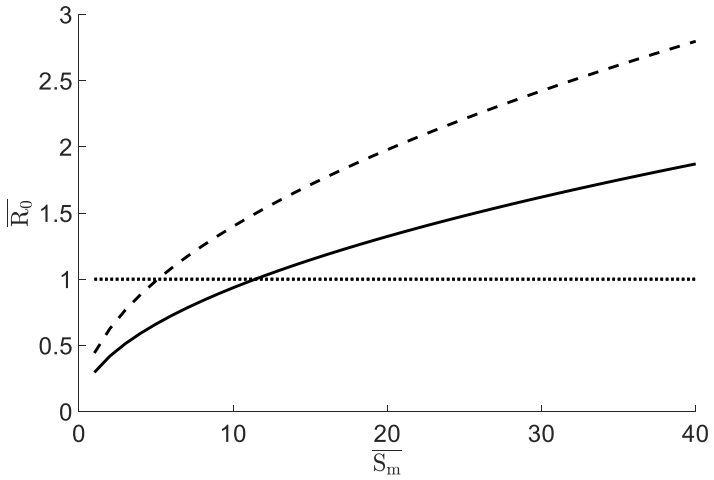

Figure 3.8: Comparison of $\overline{R_0}$ as a function of $\overline{S_m}$ at temperatures $T_1 = 16.41°C$ (solid line) and $T_2 = 28.34°C$ (dashed line).

3.6.2 MIR and SMIR

An important objective of modelling vector-borne diseases is to gain insight into the mechanisms that influence disease transmission. These insights help in the decision-making process regarding the timing and method of risk management strategies. The current method used to gauge the level of risk to humans in the Peel Region is the MIR. It uses WNV test results of weekly mosquito

surveillance data to indicate the current level of transmission intensity. The MIR is calculated as the number of pools of mosquitoes testing positive for WNV, denoted i_p, divided by the total number of mosquitoes tested, denoted M, expressed per 1,000 (Gu et al. 2003):

$$MIR = \frac{i_p}{M} * 1{,}000. \tag{3.6.55}$$

It is assumed that the proportion of infected mosquitoes is very small and that there is only one infected mosquito per pool that tests positive for WNV (actual number of positive mosquitoes per pool is unknown). Thus, the MIR can be thought of as a percentage of the sample that tests positive for WNV. In Figure 3.9, the number of reported human cases of WNV in the Peel Region (red bars, left axis) is depicted alongside the observed MIR for data (blue bars, right axis). Observe the MIR follows the trend in the reported number of human WNV cases well enough to be a good indicator for human infection risk.

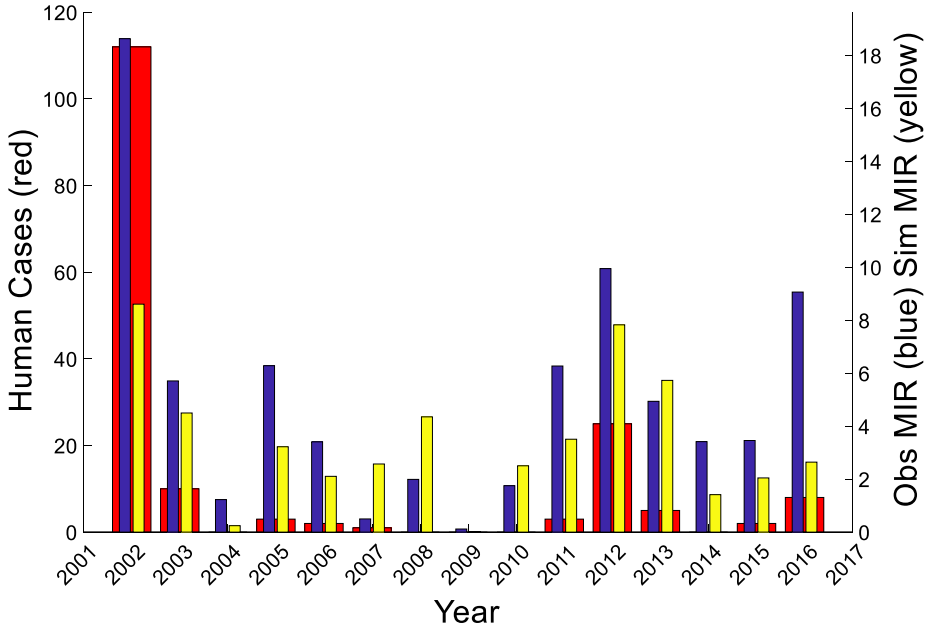

Figure 3.9: Reported number of humans testing positive for WNV (red bars, left axis), the observed MIR calculated annually (blue bars, right axis), and the simulated MIR calculated annually (yellow bars, right axis).

The MIR is not without its drawbacks. The calculation for the MIR does not take into consideration the environmental and weather conditions around the mosquito traps during the time they are set. Weather conditions between the time that traps are set and collected affects the actual number of mosquitoes that are captured. For instance, heavy rainfall or wind on the day a trap is set reduces the ability of the trap to capture mosquitoes during that session. The accuracy of the MIR also depends on the number of traps and the number of mosquitoes in each pool that is tested. Although it is assumed that there is only one infected mosquito per positive pool, this method could underestimate the MIR for a given week if the actual number of infected mosquito per positive pools is greater than one. This number is not actually known because mosquitoes are not individually tested due to the monetary and time cost of testing so many mosquitoes. The MIR also does not consider the number of amplifying reservoirs in its calculation. It is difficult to know the actual population of birds as there is no current surveillance of bird activity in the area.

Even with its drawbacks, the MIR is still a good indicator of risk to the human population. In this study, we use the assumption that infection rates are low in the mosquito population to calculate a simulated MIR (SMIR) based on the fraction of infected mosquitoes each day. We then compare the SMIR to the MIR for each year to assess the capacity of our model to predict the level of risk to humans. Similar to the MIR, the calculation for the SMIR is also expressed per 1,000 and is defined as

$$SMIR(t) = \frac{I_m(t)}{N_m(t)} * 1{,}000. \tag{3.6.56}$$

It should be noted that the MIR is calculated on a weekly basis whereas the SMIR is calculated daily when comparing the two indices. Thus, the MIR may not paint a full picture of the level of risk in-between the times mosquitoes are captured and tested each week. At the same time, it also

means we are unable to validate the SMIR estimates on days other than the dates of collection. We also note that the SMIR is not on the same scale as the MIR. Due to the lack of data on the actual number of birds and the proportion of infected mosquitoes at the beginning of each season, we assumed the same number of birds and proportion of infected mosquitoes at the beginning of each season. Thus, it is more important to compare the dynamics of each index rather than the magnitude. The availability of more data on this topic would improve SMIR estimates to be closer to the scale of the MIR. Numerical simulations of the SMIR compared to observed MIR values for each season is presented in Figure 3.10.

3.6.3 Numerical simulations

The model described in (3.2.1) to (3.2.26) was applied to the Peel Region, Southern Ontario, for years 2004–2016 using observed temperature data, mosquito surveillance data obtained from the Peel Public Health unit, and the parameter values and functions defined in Tables 1 and 2, respectively. Initial values of the total number of mosquitoes at the beginning of each season were selected using the method described in Section 2.6.2. The initial number of infected mosquitoes for each year was set at a proportion of 0.01 of the total number of initial mosquitoes (actual proportion is unknown). The remaining mosquitoes were assumed to be susceptible. The initial proportion of susceptible birds was set to 1 for each year (actual number unknown). We assumed no birds were infected with the virus at the beginning of each season as we assumed they have a disease-induced mortality rate and would have died prior to the start of the season.

Except for 2014, for years 2009-2016 we initially observed the SMIR followed the observed MIR in both trend and timing of peaks better than the preceding period from 2004 to 2008. A study by Koenig et al. (2010) found that WNV declined in virulence during its spread across North

America after its initial arrival in 1999. The study found that by Year 7 after introduction to an area, American crow populations began to stabilize. Thus, in numerical simulations (Figure 3.10) for years 2004–2008 we assumed a disease-induced mortality rate for birds that was double the rate used for simulations for years 2009–2016. Further investigation into the functional relationship of virulence over time will be pursued in future work to improve model accuracy.

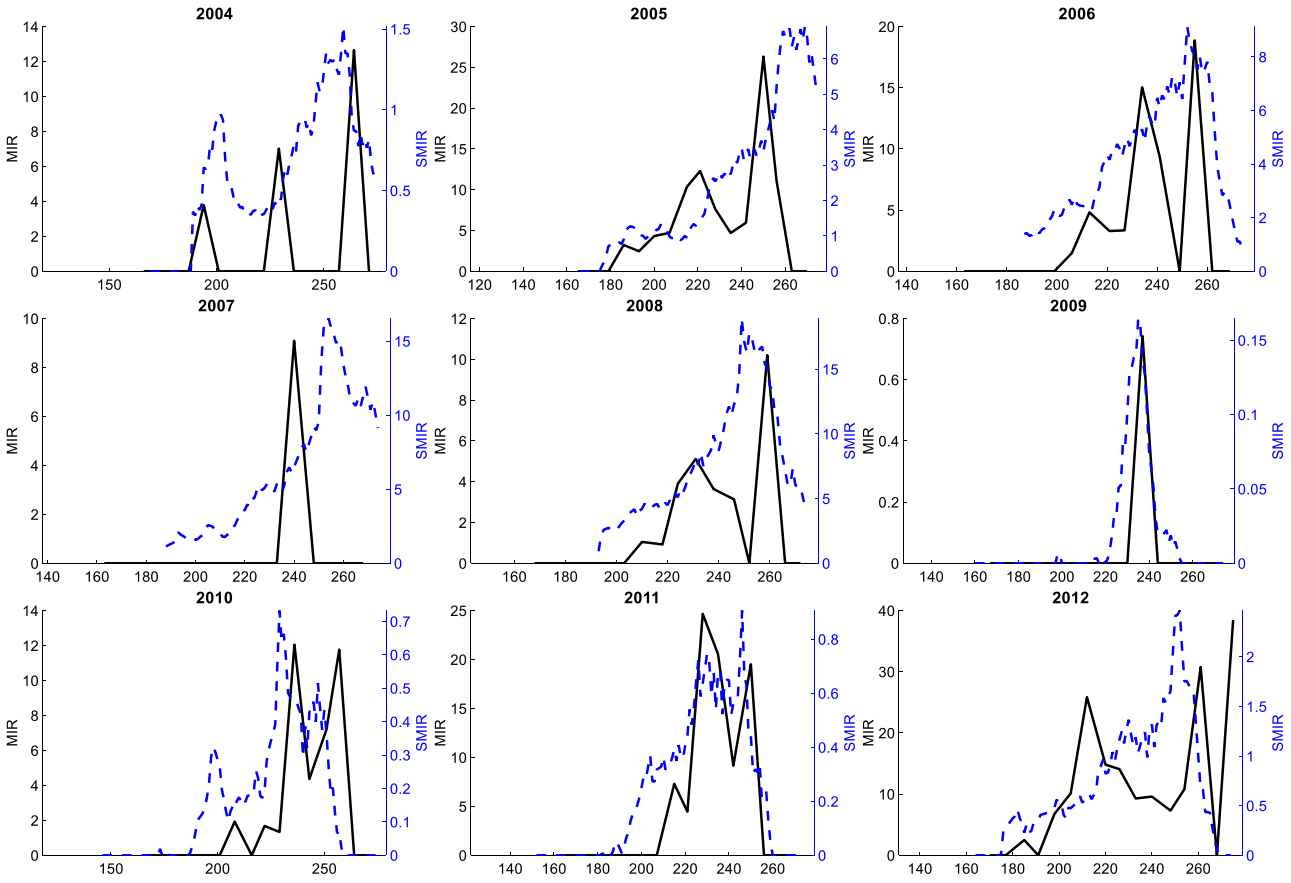

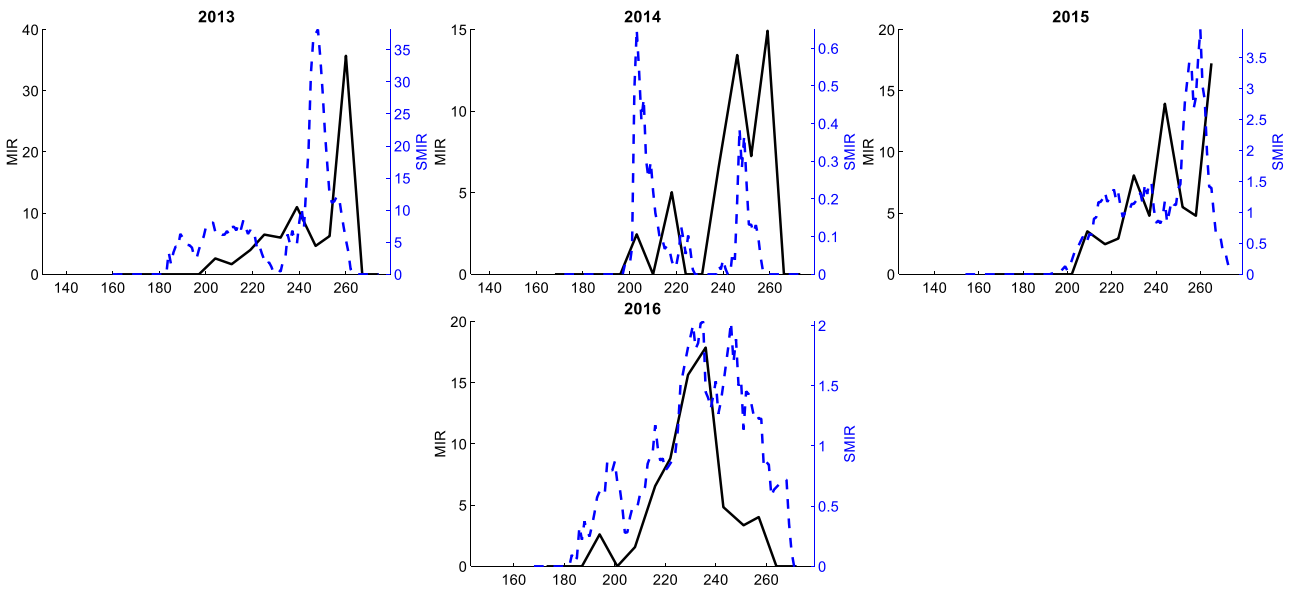

Figure 3.10**:** Numerical simulations for a single mosquito season (by day, bottom axis) comparing observed MIR (black lines, left axis) with numerical results for the SMIR (blue dashed lines, right axis) for years 2004–2016.

The simulated MIR (SMIR) compared well with both the number of human cases each year and the trend of the observed MIR within-season. We observed that the SMIR values calculated on an annual basis using the total positive pools divided by the total number of tested mosquitoes (x1,000) were proportional to the annual total number of confirmed human WNV cases (Figure 3.9, yellow bars). In 2007, the appearance of positive mosquitoes appeared significantly earlier in the SMIR than that indicated by MIR data. Among other factors, this could have been due in part to the transient dynamics of the model in the early part of the season. It could also be attributed to the maximum adult lifespan constraint we assumed in our mosquito abundance model. The study by Ciota et al. (2014) found that the longevity of adult mosquitoes was temperature-dependent both in laboratory and field experiments. Their results showed that longevity decreased as temperature increased. This variability in temperature-dependent longevity may also be the reason for differences between numerical results and observed MIR data for other years as well. The simulation for 2014 also seems to support this hypothesis. In 2014, the region experienced its

lowest average daily temperatures of the years considered in this study. The average daily temperature for the entire season was approximately 16.9°C. To test this hypothesis, we repeated the simulation for 2014 multiple times while increasing the maximum lifespan parameter in one-day increments. We found both the mosquito abundance model and transmission model produced the most accurate results when the maximum lifespan was set to 60 days. This value falls in line with the results from the study by Ciota et al. (2014).

We draw attention to the simulation for 2009, where there was only one week that mosquitoes tested positive for WNV in the surveillance data. Previous models on the same region were unable to capture this phenomena in their simulations. However, inspection of the data produced by our model simulations for this year gives a plausible explanation. The simulation data revealed that mosquitoes that became exposed to the virus up until the middle of the season were all dying before they could complete the EIP to become infectious and thus did not test positive for WNV when captured. The observed average daily temperature in the area during this mosquito season were relatively low compared to other years. These lower temperatures caused the EIP during the early part of the season to range between 29 to 50 days based on our simulations. In our model, we assumed a maximum lifespan of adult mosquitoes to be 28 days post eclosion. Then during a two-week window starting on day 220 until day 234 (August 7th–21st) temperatures rose to an average of 23.4°C which translated to an EIP of 18 days causing the appearance of infected mosquitoes in our simulations to corresponded with the date of capture on day 237 (August 25th). After this short window, temperatures once again fell to levels that inhibited mosquitoes from completing the EIP prior to reaching their maximum adult lifespan. Thus, there were no positive test results for the remainder of the season. Although this explanation was just one of many possible scenarios that could have led to the observed WNV surveillance activity for this year, it is supported by our

current understanding of mosquitoes' biological response to temperature and by our understanding of how the EIP affects transmission dynamics as evidenced in current literature (Reisen et al. 2006, Hartley et al. 2012). It should be noted that although the observed surveillance data for 2007 and 2009 appear almost identical in the timing of WNV appearance, the daily temperatures during 2009 may have been more conducive for mosquito longevity to be closer to the maximum lifespan we assumed in our model, thus causing the difference in model performance between the two years.

3.6.4 Forecasting WNV infection risk

An advantage of our model is that it can be applied as a real-time within-season forecasting tool in a straightforward and direct manner. The only requirements are that there have been at least three weeks of surveillance data, observed mean daily temperatures, and a temperature forecast. A minimum of three weeks of surveillance data is required as the model uses the first three observations to determine the initial value of susceptible mosquitoes (Section 2.6.2). Observed mean daily temperatures are required to determine the initial start day of the simulation as well as drive the mosquito population up to the current day the simulation is run. Appending the temperature forecast to the observed temperature data and running the model will produce simulation results up until the end of the forecasted date. It should be noted that the model is designed to cover a single-season and the temperature forecast cannot extend beyond the last day of the calendar year.

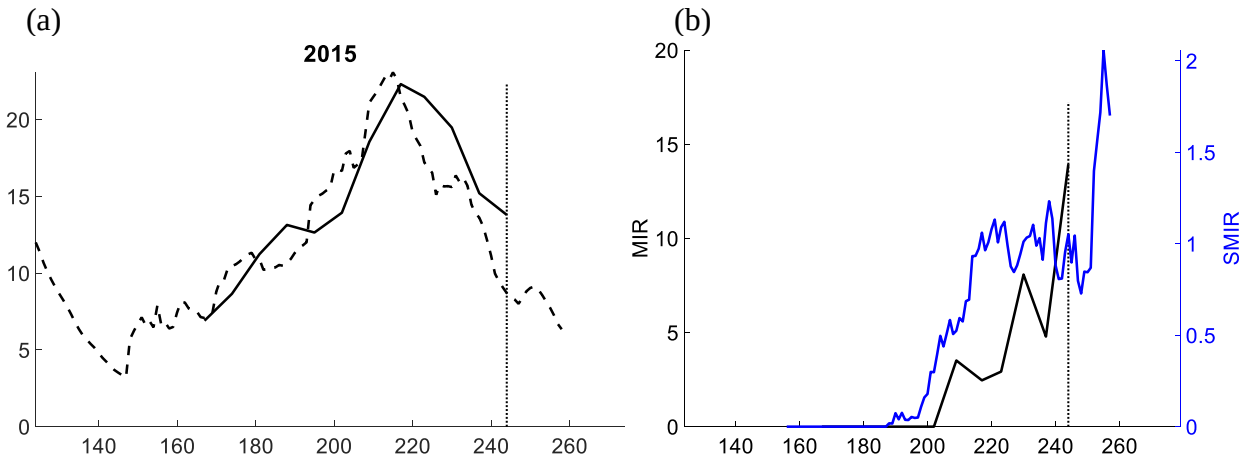

Figure 3.11: Two-week (Aug. 31st–Sept. 14th) simulated predictions based on forecasted mean daily temperatures for the Peel Region in 2015. Temperature forecast begins on day 243 (vertical dashed line). (a) Predicted mosquito trap counts (dashed line) and observed trap count data (solid line). (b) Predicted SMIR (blue line, right axis) compared with observed MIR data (black line, left axis).

An important characteristic of a model that is intended to be used as a predictive tool to inform public health policy is its ability to be applied in a user-friendly and straight forward manner. With this in mind, the framework of the model developed in this study was constructed to be easily adapted to be used as a forecasting tool for both mosquito trap counts and infection risk. Illustrated in Figure 3.11 is an example of applying the model to forecast two weeks of mosquito trap counts and infection risk using the observed mean daily temperatures and WNV surveillance data for 2015.

3.7 Discussion

Based on data available from existing literature on how temperature influences mosquito biology and the WNV transmission cycle (Tables 1 and 2), we developed a transmission dynamics model between mosquitoes and birds. Adapting the temperature-driven mosquito abundance model developed in chapter 2, the effect of temperature on mosquito development, mortality, and

diapause were explicitly accounted for in the WNV transmission model developed in Chapter 3. The effect of temperature on the EIP was also explicitly accounted for using a degree-day function to track the progression of the virus within exposed mosquitoes enabling the model to capture important transmission dynamics such as the timing of the first appearance of WNV in surveillance data.

We formulated an expression for the basic reproduction number R_0 based on a simplified version of the model evaluated about the disease-free equilibrium. The expression for R_0 contained temperature-dependent parameters that allowed us to quantitatively assess the invasiveness of the disease in different temperature settings. We showed that the ratio of mosquitoes to birds alone should not be the only factor considered in determining the conditions of disease outbreak. We found that, for a given set of initial conditions of mosquitoes and birds, temperature is the primary factor that drives the mosquito to bird ratio and thus transmission dynamics.

The model was then applied to the Peel Region, Ontario for validation. We assessed the capacity of the model to be used as a predictive risk-assessment tool by formulating a SMIR index based on the observed MIR calculation. The SMIR index fit the observed MIR data well for most years, especially in years after 2008, implying our model has potential to be used to complement existing risk assessment methods.

Existing studies on WNV transmission dynamics stress the importance of the mosquito to bird ratio in the assessment of methods to manage infection risk. Our study showed that the environmental temperature must also be considered in this assessment because temperature can either drive the level of infection to a major outbreak or, in some cases, force it to levels that are undetectable. This notion is supported by simulation results for the year 2009, where our model identified the likely mechanism responsible for the low frequency of positive test results to be a

temperature pattern that was not conducive for virus replication within exposed mosquitoes prior to natural death, thereby limiting the infectious period for mosquitoes that survived the EIP to only a few days that season.

Differences between model results and observation data suggest that both modelling methods and surveillance methods need improvement to gain better accuracy in forecasting WNV risk. The major limitation regarding improved model performance is the lack of available data on mosquito biology and related epidemiological processes. More research providing detailed data on the biological response of mosquitoes to environmental factors would improve model accuracy. Moreover, model validation is subject to the availability of surveillance data, both quality and quantity. Surveillance initiatives that increase the period of surveillance, sample size, and frequency of collection and testing would give a much broader base to which we could refine and tune our model for improved performance. Initiation of a surveillance program for WNV-related bird populations in the area could also significantly enhance model performance, as currently no such surveillance program exists in this region. With such data, initial conditions and parameter estimates could be refined to more closely match the conditions in a natural environment.

Although the model performed well in capturing within-season dynamics as measured by the MIR, simulation results for years 2004-2008 suggest our model needs to consider more factors than just temperature alone. Other environmental and entomological factors—such as land-use, precipitation, disease-induced mortality of reservoirs, and vector longevity—are important factors that affect disease transmission dynamics and should be considered in future work. Including land-use data can improve performance by adding a spatial dimension to the model so that population densities by location can be considered. The type of land (industrial, urban, or rural) around trap locations is important in that it can help determine the proximity to human populations and thus

influence estimates of the contact rate between vector, reservoir, and humans. Precipitation can have an amplifying effect on mosquito abundance by increasing the number of breeding sites and negatively affecting the population by 'washing out' mosquitoes in the aquatic stage if there is too much precipitation. We also did not include other transmission-related factors that have been shown to have a dependency on temperature, such as oviposition rate, biting preference, and mosquito biting rates, which also affect transmission dynamics.

4 Conclusions and future work

Mathematical models describing the relationship between environmental factors and WNV have advanced our understanding of key processes involved in transmission dynamics. The knowledge we have gained thus far has helped inform policies that have reduced the risk of infection to the human population. However, the complexities of disease transmission are vast and require further attention and modelling initiatives with the ultimate objective of eradicating WNV.

The findings in this dissertation contribute to the existing groundwork on WNV disease transmission dynamics by furthering our qualitative understanding of the relationship between temperature, mosquito biology, and the mechanisms that influence WNV transmission dynamics in the mosquito–bird transmission cycle. In Chapter 2, we developed a mosquito abundance model that used temperature as the driving force behind population dynamics. Using data obtained from laboratory studies on mosquito biology at constant temperatures, we formulated temperature-dependent response functions for key processes in the mosquito life cycle that have been shown to be heavily dependent on temperature: namely, mortality and diapause. Together with the use of a degree-day function to track the physiological age of developing mosquitoes, the resulting model could capture the variability in population dynamics observed in surveillance data. We showed how certain temperature patterns can cause a relatively small population of adult mosquitoes to suddenly increase or spike in a short amount of time. We also emphasized the importance of the effect of diapause, along with complementary research (Denlinger and Armbruster 2014, Zhang and Denlinger 2011) on population dynamics where other studies have tended to overestimate

mosquito populations at the end of the mosquito season. The model was then applied to the Peel Region, Southern Ontario, using observed temperature data to drive the population dynamics. Simulation results were then validated with annual surveillance data from 2004–2016. The model demonstrated an overall capacity to follow the observed within-season trend of mosquito trap counts.

In chapter 3, we extended the mosquito abundance model to describe the mosquito-bird WNV transmission cycle. While surveying various temperature-dependent processes involved in transmission dynamics, we found that the EIP is a key factor in determining the timing of WNV activity due to the delay caused by the time it takes to accumulate enough thermal units to become infectious. Thus, we opted to use a degree-day function to track the progression of exposed mosquitoes through the incubation period rather than using a simplified assumption of a constant transition rate or one that returned an instantaneous rate. Our choice in modelling the EIP in this way allowed us to qualitatively assess the factors that caused unusual behavior found in observed WNV surveillance data.

Based on the expression for R_0 that was formulated from a simplified version of the model, we proposed that the ratio of mosquitoes to birds should not be considered by itself in the assessment of risk reduction strategies. We showed that the mosquito to bird ratio must be considered in the context of environmental temperature. We demonstrated that a given set of initial values of mosquitoes and birds that could lead to an outbreak at one temperature setting may not necessarily lead to an outbreak at another temperature setting.

While the results of our study indicate promising potential for our transmission model to be used as a predictive tool to complement existing methods of measuring infection risk, we also acknowledge that further research is warranted to investigate factors not considered in our study.

Environmental factors—such as precipitation, land-use, and urban development as well as entomological factors such as biting rates, breeding habits, host preferences, the overwintering process, longevity, and host migration—all have an impact on transmission dynamics and will be considered in future work. As with many other studies, we also acknowledge that the biggest limitation of the accuracy of our model is the availability of reliable data. As more data becomes available, we will be able to improve model parameterization and thus its performance and reliability.

Currently, the model is limited to forecasting mosquito abundance over a single-season. Extending the study to describe the overwintering process would enable simulations to be run over multiple years with one set of initial conditions for the first year. Then, using short-term and long-term temperature forecasts as input in to the model, we could potentially forecast mosquito abundance and WNV infection risk for future years based on a range of climate projections. However, as previously mentioned, data on the overwintering process is limited. The goal of future work will be to improve model performance by incorporating other processes, mentioned above, that are influenced by temperature and considering the effect of other environmental factors on mosquito biology and disease transmission. The inherent design of our model's framework lends itself to be adaptable to other vector-borne diseases in different geographical settings. We plan to apply the framework of this model to other vector-borne diseases with a two-fold aim of further validating the strengths and weaknesses in the design of our model and to improve our understanding of transmission dynamics.

Bibliography

Abdelrazec, A., Cao, Y., Gao, X., Zhu, H., Proctor, P. and Zheng, H. (2014a). West Nile Virus Risk Assessment and Forecasting Using Statistical and Dynamical Models, in Analyzing and Modelling Spatial and Temporal Dynamics of Infectious Diseases (eds D. Chen, B. Moulin and J. Wu), John Wiley & Sons, Inc., Hoboken, NJ, USA. doi: 10.1002/9781118630013.ch4

Abdelrazec, A., Lenhart, S., Zhu, H. (2014b). Transmission dynamics of West Nile virus in mosquitoes and corvids and non-corvids. Journal of Mathematical Biology, 68(6): 1553–82.

Abiodun, G.J., Maharaj, R., Witbooi, P. (2016). Modelling the influence of temperature and rainfall on the population dynamics. *Malaria Journal*, *15*: 364.

Ahumada, J. A., Lapointe, D., Samuel, M. D. (2004). Modelling the population dynamics of Culex quinquefasciatus (Diptera: Culicidae), along an elevational gradient in Hawaii. *Journal of Medical Entomology*, *41*: 1157–70.

Anderson, J., and Main, A. (2006). Importance of vertical and horizontal transmission of West Nile virus by Culex pipiens in the Northeastern United States. *Journal of Infectious Diseases*, *194*(11): 1577–79.

Anderson, S. L., Richards, S. L., Tabachnick, W. J., and Smartt, C. T. (2010). Effects of West Nile Virus dose and extrinsic incubation temperature on temporal progression of vector competence in Culex pipiens quinquefasciatus. *Journal of American Mosquito Control Association*, *26*(1): 103–107.

Bayoh, M. N., Lindsay, S. W. (2003). Effect of temperature on the development of the aquatic stages of Anopheles gambiae sensu stricto (Diptera: Culicidae). *Bulletin of Entomological Research*. *93*: 375–381.

Bayoh, M. N., Lindsay, S. W. (2004). Temperature-related duration of aquatic stages of the Afrotropical malaria vector mosquito Anopheles gambiae in the laboratory. *Medical and Veterinary Entomology*. *18*: 174–179.

Blayneh, K. W., Gumel, A. B., Lenhart, S., and Clayton, T. (2010). Backward Bifurcation and Optimal Control in Transmission Dynamics of West Nile Virus. *Bulletin of Mathematical Biology*, *72*(4): 1006–28.

Bolling, B. G., Barker, C. M., Moore, C. G., and Pape, W. J. (2009). Modelling/GIS, risk assessment, economic impact: Seasonal patterns for entomological measures of risk for exposure to Culex vectors and West Nile virus in relation to human disease cases in Northeastern Colorado. *Journal of Medical Entomology*, *46*: 1519–31.

Bowman, C., Gumel, A. B., van den Driessche, P., Wu, J., and Zhu, H. (2005) A mathematical model for assessing control strategies against West Nile virus. *Bulletin of Mathematical Biology*, *67*: 1107–33.

Statistics Canada (2011). Census Profiles. http://www12.statcan.ca/census-recensement/2011/dp-pd/prof/details/page.cfm?Lang=E&Geo1=CD&Code1=3521&Geo2=PR&Code2=01&Data=Count&SearchText=peel&SearchType=Begins&SearchPR=35&B1=All&Custom=&TABID=1

Caraballo, H., and King, K. (2014). Emergency Department Management of Mosquito-Borne Illness: Malaria, Dengue, and West Nile Virus. *Emergency Medicine Practice*, *16*: 1–23.

Cailly, P., Tran, A., Balenghien, T., L'Ambert ,G., Toty, C., and Ezanno, P. (2012). A climate-driven abundance model to assess mosquito control strategies. *Ecological Modelling*, *227*: 7–17.

Caswell, H. (2001). *Matrix Population Models*. Sinauer, Sunderland, MA.

Centers for Disease Control and Prevention (1999a). Outbreak of west Nile-like viral encephalitis-New York. Morbidity and Mortality Weekly Report, *48*: 845–849, http://www.cdc.gov/mmwr/preview/mmwrhtml/mm4838a1.htm.

Centers for Disease Control and Prevention (1999b) Update: West Nile-like viral encephalitis-New York 1999. Morbidity and Mortality Weekly Report. *48*: 890–892, http://www.cdc.gov/mmwr/preview/mmwrhtml/mm4839a5.htm

Centers for Disease Control and Prevention (2014). West Nile virus: Fact sheet. http://www.cdc.gov/ncidod/dvbid/westnile/wnv_factSheet.htm

Chen, S., Blanford, J. I., Fleischer, S. J., Hutchinson, M., Saunders, M. C., and Thomas, M. B. (2013). Estimating West Nile Virus Transmission Period in Pennsylvania Using and Optimized Degree-Day Model. *Vector-Borne and Zoonotic Diseases*, *13*(7): 489–497.

Ciota, A. T., Matacchiero, A. C., Kilpatrick, A. M. (2014). The Effect of Temperature on Life History Traits of Culex Mosquitoes *Journal of Medical Entomology*, *51*(1): 55–62.

Cochran, J. M., & Xu, Y. (2012). A temperature-dependent age-structured mosquito life-cycle model. *Applicable Analysis*, *91*(2): 403–418.

Connecticut Department of Environmental Protection (2001). American Crow Fact Sheet. https://web.archive.org/web/20061105022804/http://www.mosquito.state.ct.us/fact/crowfact.htm

Craig, M. H., Snow, R. W., and le Sueur, D. (1999). A Climate-based Distribution Model of Malaria Transmission in Sub-Saharan Africa. *Parasitology Today*, *15*(3): 105–111.

Cruz-Pacheco, G., Esteva, L., Montano-Hirose, J., and Vargas, C. (2005). Modelling the Dynamics of West Nile Virus. *Bulletin of Mathematical Biology*, *67*(6): 1157–72.

Cummins, B., Cortez, R., Foppa, M., Walbeck, J., and Hyman, M. (2012). A spatial model of mosquito host-seeking behavior. *PLOS Computational Biology*, *8*(5): e1002500.

Cushing, J. M., and Yicang, Z. (1994). The net reproductive value and stability in matrix population models, *Natural Resource Modelling*, *8*: 297–333.

Denlinger, D. L., Armbruster, P. A. (2014). Mosquito Diapause. *Annual Review of Entomology*, *59*: 73–93.

Dohm, D., O'Guinn, M., and Turell, M. (2002). Effect of Environmental Temperature on the Ability of Culex pipiens (Diptera: Culicidae) to Transmit West Nile Virus. *Journal of Medical Entomology*, *39*(1): 221–225.

Edillo, F., Kiszewski, A., Manjourides, J., Pagano, M., Hutchinson, M., Kyle, A., Arias, J., Gaines, D., Lampman, R., Novak, R., Foppa, I., Lubelcyzk, C., Smith, R., Moncayo, A., and Spielman, A. (2009). Effects of Latitude and Longitude on the Population Structure of Culex pipiens s.l., Vectors of West Nile Virus in North America. *The American Journal of Tropical Medicine and Hygiene*, *81*(5): 842–848.

Eldridge, B. F. (1966). Environmental control of ovarian development in mosquitoes of the Culex pipiens complex. *Science*, *151*(3712): 826–828.

Eldridge, B. F., Johnson, M. D., and Bailey, C. L. (1976). Comparative studies of two North American mosquito species, Culex restuans and Culex salinarius: response to temperature and photoperiod in the laboratory. *Mosquito News*, *36*(4): 506–513.

Ewing, D. A., Cobbold, C. A., Purse, B. V., Nunn, M. A., and White, S. M. (2016). Modelling the effect of temperature on the seasonal population dynamics of temperate mosquitoes. *Journal of Theoretical Biology*, *400*: 65–79.

Ezanno, P., Aubry-Kientz, M., Arnoux, S., Cailly, P., L'Ambert, G., Toty, C., Balenghien, T., Tran A. (2015). A generic weather-driven model to predict mosquito population dynamics applied to species of Anopheles, Culex and Aedes genera of southern France. *Preventive Veterinary Medicine, 120*: 39–50.

Fan, G., Liu, J., van den Driessche, P., Wu, J., and Zhu, H. (2010). The impact of maturation delay of mosquitoes on the transmission of West Nile virus. *Mathematical Biosciences, 228*: 119–126.

Frobenius, G. (1912). Ueber Matrizen aus nicht negativen Elementen. *Sitzungsberichte der Königlich Preussischen Akademie der Wissenschaften*, 456–477.

Gantmacher, F. (1959). *Theory of matrices*, AMS Chelsea publishing.

Goddard, L. B., Roth, A. E., Reisen, W. K., and Scott, T. W. (2003). Vertical transmission of West Nile virus by three California Culex (Diptera: Culicidae) species. *Journal of Medical Entomology, 40*(6): 743–746.

Gong, H., DeGaetano, A., and Harrington, L. (2011). Climate-based models for West Nile Culex mosquito vectors in the Northeastern US. *International Journal of Biometeorology, 55*: 435–446.

Gu, W., Lampman, R., and Novak, R. (2003). Problems in Estimating Mosquito Infection Rates Using Minimum Infection Rate. *Journal of Medical Entomology*, *40*(5): 595–596.

Gu, W., and Novak, R. (2006). Statistical estimation of degree-days of mosquito development under fluctuating temperatures in the field. *Journal of Vector Ecology*, *31*: 107–112.

Gunaratne, C., Akbas, M. I., Garibay, I., and Ozmen, O. (2016). Evaluation of Zika Vector Control Strategies Using Agent-Based Modelling. Available at arXiv:1604.06121v2

Hartley, D. M., Barker, C. M., Le Menach, A., Niu, T., Gaff, H. D., and Reisen, W. K. (2012). Effects of Temperature on Emergence and Seasonality of West Nile Virus in California. *The American Journal of Tropical Medicine and Hygiene*, *86*(5): 884–894.

Hayes, C. G. (1988). *West Nile fever. In The arboviruses: epidemiology and ecology*, vol. 5 (ed. T. P. Monath), pp. 59–88. Boca Raton, FL: CRC Press.

Infection Prevention and Control Canada (2017). https://ipac-canada.org/west-nile-virus-resources.php

Jang, S. R.-J. (2007). On a discrete West Nile epidemic model. *Computational & Applied Mathematics*, *26*(3): 397–414.

Jetten, T. H., and Takken, W. (1994). *Anophelism Without Malaria in Europe: A Review of the Ecology and Distribution of the Genus Anopheles in Europe*. Wageningen Agricultural University Press, Wageningen.

Kilpatrick, A. M., Meola, M. A., Moudy, R. M., and Kramer, L. D. (2008). Temperature, Viral Genetics, and the Transmission of West Nile Virus by Culex pipiens Mosquitoes. *PLOS Pathogens*, *4*(6): e1000092.

Koenig, W. D., Hochachka, W. M., Zuckerberg, B., and Dickinson, J. L. (2010). Ecological determinants of American crow mortality due to West Nile virus during its North American sweep. *Oecologia*, *163*(4): 903–909.

Komar, N., Langevin, S., Hinten, S., Nemeth, N., and Edwards, E. (2003). Experimental Infection of North American Birds with the New York 1999 Strain of West Nile Virus. *Emerging Infectious Diseases*, *9*(3): 311–322.

Kunkel, K. E., Novak, R. J., Lampman, R. L., and Gu, W. (2006). Modelling the impact of variable climatic factors on the crossover of Culex restuans and Culex pipiens (Diptera: Culicidae), vectors of West Nile virus in Illinois. *The American Journal of Tropical Medicine and Hygiene*, *74*(1): 168–173.

Lana, R., Carneiro, T., Honório, N., and Codeço, C. (2011). Multiscale Analysis and Modelling of Aedes aegyti Population Spatial Dynamics. *Journal of Information and Data Management*, *2*(2): 211–220.

Langevin, S. A., Bunning, M., Davis, B., and Komar, N. (2001). Experimental Infection of Chickens as Candidate Sentinels for West Nile Virus. *Emerging Infectious Diseases*, *7*(4): 726–29.

Laperriere, V., Brugger, K., and Rubel, F. (2011). Simulation of the seasonal cycles of bird, equine and human West Nile virus cases. *Preventive Veterinary Medicine*, *99*: 99–110.

Leslie, P. H. (1945). "The use of matrices in certain population mathematics". *Biometrika*, *33*(3): 183–212.

Lewis, A., Renclawowicz, J., van den Driessche, P., and Wonham, M. (2006). A Comparison of Continuous and Discrete-Time West Nile Virus Models. *Bulletin of Mathematical Biology*, *68*: 491–509.

Li, C-K., and Schneider, H. (2002). Applications of Perron–Frobenius theory to population dynamics. *Journal of Mathematical Biology*, *44*: 450–462.

Loetti, V., Schweigmanna, N., and Burroni, N. (2011). Development rates, larval survivorship and wing length of Culex pipiens (Diptera: Culicidae) at constant temperatures. *Journal of Natural History*, *45*: 2207–17.

Lounibos, L. P., Suarez, S., Menendez, Z., Nishimura, N., et al. (2002). Does temperature affect the outcome of larval competition between Aedes aegypti and Aedes albopictus? *Journal of Vector Ecology*, *27*: 86–95.

Madder, D. J., Surgeoner, G. A., and Helson, B. V. (1983). Number of generations, egg production and development time of Culex pipiens L. and Culex restuans Theo. (Diptera: Culicidae) in Southern Ontario. *Journal of Medical Entomology*, *20*: 269–281.

Meillon, B., De Sebastian, A., and Khan, Z. H. (1967). The duration of egg, larval and pupal stages of Culex pipiens fatigans in Rangoon, Burma. *Bulletin of the World Health Organization*, *36*: 7–14.

Nasci, R. S., Savage, H. M., White, D. J., Miller, J. R., Cropp, B. C., Godsey, M. S., Kerst, A. J., Bennett, P., Gottfried, K., and Lanciotti, R. S. (2001). West Nile virus in Overwintering Culex mosquitoes, New York City, 2000. *Emerging Infectious Diseases*, *7*(4): 742–744.

Otero, M., Solari, H., and Schweigmann, N. (2006). A Stochastic Population Dynamics Model for Aedes Aegypti: Formulation and Application to a City with Temperate Climate. *Bulletin of Mathematical Biology*, *68*: 1945–74.

Paz, S., and Semenza, J. C. (2013). Environmental drivers of West Nile fever epidemiology in Europe and Eurasia-review. *International Journal of Environmental Research and Public Health*, *10*: 3543–62.

Paz, S. (2015). Climate change impacts on West Nile virus transmission in a global context. Philosophical Transactions of the Royal Society B, *370*: 20130561.

Perron, O. (1907). Zur Theorie der Matrices. *Mathematische Annalen*, *64*(2): 248–263.

Reisen, W. K. (2013). Ecology of West Nile Virus in North America. *Viruses*, *5*: 2079–2105.

Reisen, W. K., Fang, Y., and Martinez, V. M. (2006). Effects of Temperature on the Transmission of West Nile Virus by Culex tarsalis (Diptera: Culicidae). *Journal of Medical Entomology*, *43*(2): 309–317.

Rueda, L. M., Patel, K. J., Axtell, R. C., and Skinner, R. E. (1990). Temperature-dependent development and survival rates of Culex quinquefasciatus and Aedes aegypti (Diptera: Culicidae). *Journal of Medical Entomology*, *27*: 892–898.

Ruiz, M. O., Chaves, L. F., Hamer, G. L., Sun, T., Brown, W. M., Walker, E.D., et al. (2010). Local impact of temperature and precipitation on West Nile virus infection in Culex species mosquitoes in northeast Illinois, USA. *Parasites & Vectors*, *3*: 19.

Sejvar, J. J., MD. (2003). West Nile Virus: An Historical Overview. *The Ochsner Journal*, *5*(3): 6–10.

Service, M. W. (1993). *Mosquito Ecology: Field Sampling Methods, 2nd ed*. Chapman & Hall, London, United Kingdom.

Shaman, J., Spiegelman, M., Cane, M., and Stieglitz, M. (2006). A hydrologically driven model of swamp water mosquito population dynamics. *Ecological Modelling*, *194*: 395–404.

Shelton, R.M., (1973). The effect of temperatures on development of eight mosquito species. *Mosquito News*, *33*: 1–12.

Spielman, A. (2001). Structure and seasonality of nearctic Culex pipiens populations. *Annals of the New York Academy of Sciences*, *951*: 220–234.

Swayne, D., Beck, R., and Zaki, S. (2000). Pathogenicity of West Nile virus for turkeys. *Avian Diseases*, *44*: 932–7.

Sykes, Z. M. (1969). On Discrete Stable Population Theory. *Biometrics, 25*(2): 285–293.

Tachiiri, K., Klinkenberg, B., Mak, S., and Kazmi, J. (2006). Predicting outbreaks: a spatial risk assessment of West Nile virus in British Columbia. *International Journal of Health Geographics, 5*: 21.

Thomas, D. M., and Urena, B. (2001). A model describing the Evolution of West Nile-like Encephalitis in New York City. *Mathematical and Computer Modelling*, *34*: 771–781.

Tran, A., L'Ambert, G., Lacour, G., Benot, R., Demarchi, M., Cros, M., Cailly, P., Aubry-Kientz M., Balenghien, T., Ezanno, P. (2013). A rainfall- and temperature-driven abundance model for Aedesal bopictus populations. *International Journal of Environmental Research and Public Health, 10*: 1698–1719.

Turell, M. J., O'Guinn, M. L., Dohm, D. J., and Jones, J. W. (2001). Vector competence of North American mosquitoes (Diptera: Culicidae) for West Nile virus. *Journal of Medical Entomology, 38*: 130–134.

United States Environmental Protection Agency (2017). Mosquito Life Cycle https://www.epa.gov/mosquitocontrol/mosquito-life-cycle

United States Naval Observatory (2017). http://aa.usno.navy.mil/data/docs/RS_OneYear.php

Wang, J., Ogden, N. H., and Zhu, H. (2011). The impact of Weather Conditions of Culex pipiens and Culex restuans (Diptera: Culicidae) Abundance: A Case study in the Peel Region. *Journal of Medical Entomology*, *48*(2): 468–475.

Wonham, M. J., De-Camino-Beck, T., and Lewis, M. A. (2004). An epidemiological model for West Nile virus: invasion analysis and control applications. *Proceedings of the Royal Society of London. Series B, 271*: 501–507

World Health Organization (2017). Mosquito-borne diseases: Fact sheet. http://www.who.int/neglected_diseases/vector_ecology/mosquito-borne-diseases/en/

Yoo, E.-H., Chen, D., Diao, C., and Russell, C. (2016). The effects of weather and environmental factors on West Nile virus mosquito abundance in Greater Toronto Area. *Earth Interactions*, *20* (3): 1–22.

Zhang, Q., and Denlinger, D. L. (2011). Molecular structure of the prothoracicotropic hormone gene in the northern house mosquito, Culex *pipiens*, and its expression analysis in association with diapause and blood feeding. *Insect Molecular Biology*, *20*: 201–13.